



## 저작자표시-비영리-변경금지 2.0 대한민국

이용자는 아래의 조건을 따르는 경우에 한하여 자유롭게

- 이 저작물을 복제, 배포, 전송, 전시, 공연 및 방송할 수 있습니다.

다음과 같은 조건을 따라야 합니다:



저작자표시. 귀하는 원저작자를 표시하여야 합니다.



비영리. 귀하는 이 저작물을 영리 목적으로 이용할 수 없습니다.



변경금지. 귀하는 이 저작물을 개작, 변형 또는 가공할 수 없습니다.

- 귀하는, 이 저작물의 재이용이나 배포의 경우, 이 저작물에 적용된 이용허락조건을 명확하게 나타내어야 합니다.
- 저작권자로부터 별도의 허가를 받으면 이러한 조건들은 적용되지 않습니다.

저작권법에 따른 이용자의 권리는 위의 내용에 의하여 영향을 받지 않습니다.

이것은 [이용허락규약\(Legal Code\)](#)을 이해하기 쉽게 요약한 것입니다.

[Disclaimer](#)

공학박사 학위논문

# High-Quality Video Streaming over Wireless Networks

무선 통신 네트워크 환경에서의 효과적인  
비디오 스트리밍 기법 연구

2013년 8월

서울대학교 대학원

전기정보공학부

최 문 환

공학박사 학위논문

# High-Quality Video Streaming over Wireless Networks

무선 통신 네트워크 환경에서의 효과적인  
비디오 스트리밍 기법 연구

2013년 8월

서울대학교 대학원

전기정보공학부

최 문 환

# High-Quality Video Streaming over Wireless Networks

지도교수 최 성 현

이 논문을 공학박사 학위논문으로 제출함

2013년 4월

서울대학교 대학원

전기정보공학부

최 문 환

최문환의 공학박사 학위 논문을 인준함

2013년 6월

위 원 장: 박 세 응 (인)

부위원장: 최 성 현 (인)

위 원: Kang G. Shin (인)

위 원: 서 승 우 (인)

위 원: 오 성 준 (인)

# Abstract

## High-Quality Video Streaming over Wireless Networks

Today, along with the rapid growth of the network performance, the demand for high-quality video streaming services has greatly increased. The emerging 60 GHz multi-Gbps wireless technology enables the streaming of high-quality uncompressed video, which was not possible with other existing wireless technologies. To support such high quality video with limited wireless resources, an efficient link adaptation policy, which selects the proper Modulation and Coding Scheme (MCS) for a given channel environment, is essential. We introduce a new metric, called *expected Peak Signal-to-Noise Ratio (ePSNR)*, to numerically estimate the video streaming quality, and additionally adopt Unequal Error Protection (UEP) schemes that enable flexible link adaptation. Using the ePSNR as a criterion, we propose two link adaptation policies with different objectives. The proposed link adaptation policies attempt to (1) maximize the video quality for given wireless resources, or (2) minimize the required wireless resources while meeting the video quality. Our extensive simulation results demonstrate that the introduced variable, i.e., ePSNR, well represents the level of video quality. It is also shown that the proposed link adaptation policies can enhance the resource efficiency while achieving acceptable quality of the video streaming.

Meanwhile, Forward Error Correction (FEC) can be exploited to realize reliable video multicast over Wi-Fi with high video quality. We propose reliable video multi-

cast over Wi-Fi networks with coordinated multiple Access Points (APs) to enhance video quality. By coordinating multiple APs, each AP can transmit (1) entirely different or (2) partially different FEC-encoded packets so that a multicast receiver can benefit from both spatial and time diversities. The proposed scheme can enlarge the satisfactory video multicast region by exploiting the multi-AP diversity, thus serving more multicast receivers located at cell edge with satisfactory video quality. We propose a resource-allocation algorithm for FEC code rate adaptation, utilizing the limited wireless resource more efficiently while enhancing video quality. We also introduce the method for estimating the video packet delivery ratio after FEC decoding. The effectiveness of the proposed schemes is evaluated via extensive simulation and experimentation. The proposed schemes are observed to enhance the ratio of satisfied users by up to 37.1% compared with the conventional single AP multicast scheme.

The multicast transmission is inherently unreliable due to the transmission failures caused by wireless channel errors, however, the error control with Automatic Repeat reQuest (ARQ) is not provided for the multicast transmission in legacy IEEE 802.11 standard. To overcome the unreliability of multicast transmission, finally, we propose the reliable multicast protocols considering both ARQ and packet-level FEC together. For the proposed reliable multicast protocol, to reduce the overheads of feedback messages while providing the reliable multicast service, the multiple efficient feedback protocols, i.e., Idle-time-based feedback, Slot-based feedback, Flash-based feedback, and Busy-time-based feedback, are proposed. The proposed feedback protocols let the AP know easily the number of requiring parity frames of the worst user(s) for the recovery of the lost packets. The feedback overheads can be reduced by intending the concurrent transmissions, which makes the collisions, between feedback messages. In addition, utilizing the efficient feedback protocols, we propose the PHY rate adaptation based on the close-loop MCS feedback in multicast transmissions. From the

performance evaluations, the proposed protocols can efficiently reduce the feedback overheads, while the reliable multicast transmissions are guaranteed.

**Keywords:** Video streaming, link adaptation, uncompressed video, expected PSNR, 60 GHz networks, Unequal Error Protection (UEP), video multicast, Forward Error Correction (FEC), Raptor FEC, Wi-Fi, coordinated multi-APs, Automatic Repeat reQuest (ARQ), and efficient feedback

**Student Number:** 2007-30842

# Contents

<b>Abstract</b>	<b>i</b>
<b>Contents</b>	<b>iv</b>
<b>List of Tables</b>	<b>viii</b>
<b>List of Figures</b>	<b>ix</b>
<b>1 Introduction</b>	<b>1</b>
1.1 Video Streaming over Wireless Networks . . . . .	1
1.1.1 Uncompressed Video Streaming over 60 GHz band . . . . .	2
1.1.2 Video Multicast over IEEE 802.11 WLAN . . . . .	3
1.2 Overview of Existing Approaches . . . . .	5
1.2.1 Link Adaptation over Wireless Networks . . . . .	5
1.2.2 Video Streaming over IEEE 802.11 WLAN . . . . .	6
1.2.3 Reliable Multicast over IEEE 802.11 WLAN . . . . .	8
1.3 Main Contributions . . . . .	9
1.4 Organization of the Dissertation . . . . .	11
<b>2 Link Adaptation for High-Quality Uncompressed Video Streaming in 60</b>	



<b>GHz Wireless Networks</b>	<b>12</b>
2.1 Introduction . . . . .	12
2.2 ECMA-387 and Wireless HDMI . . . . .	17
2.2.1 ECMA-387 . . . . .	18
2.2.2 Wireless HDMI (HDMI PAL) . . . . .	21
2.2.3 UEP Operations . . . . .	22
2.2.4 ACK Transmissions for Video Streaming . . . . .	23
2.2.5 Latency of compressed and uncompressed video streaming . .	24
2.3 ePSNR-Based Link Adaptation Policies . . . . .	25
2.3.1 ePSNR . . . . .	28
2.3.2 PSNR-based Link Adaptation . . . . .	30
2.4 Performance Evaluation . . . . .	33
2.4.1 Evaluation of ePSNR . . . . .	34
2.4.2 Performance of Link Adaptation . . . . .	40
2.5 Summary . . . . .	45
<b>3 Reliable Video Multicast over Wi-Fi Networks with Coordinated Multiple APs</b>	<b>47</b>
3.1 Introduction . . . . .	47
3.2 System Environments . . . . .	50
3.2.1 Time-Slotted Multicast . . . . .	50
3.2.2 FEC Coding Schemes . . . . .	52
3.3 Reliable Video Multicast with Coordinated Multiple APs . . . . .	52
3.3.1 Proposed Video Multicast . . . . .	52
3.3.2 Video Multicast Procedure . . . . .	55
3.4 FEC Code Rate Adaptation . . . . .	58
3.4.1 Estimation of Delivery Ratio . . . . .	59

3.4.2	Greedy FEC Code Rate Adaptation . . . . .	61
3.5	Performance Evaluation . . . . .	63
3.5.1	Raptor Code Performance . . . . .	64
3.5.2	Simulation Results: No Fading . . . . .	66
3.5.3	Simulation Results: Fading Channel . . . . .	69
3.5.4	Simulation Results: Code Rate Adaptation . . . . .	70
3.5.5	Experimental Results . . . . .	74
3.5.6	Prototype Implementation . . . . .	76
3.6	Summary . . . . .	79
<b>4</b>	<b>Reliable Video Multicast with Efficient Feedback over Wi-Fi</b>	<b>81</b>
4.1	Introduction . . . . .	81
4.2	Motivation . . . . .	85
4.3	Proposed Feedback Protocols for Reliable Multicast . . . . .	87
4.3.1	Idle-time-based Feedback . . . . .	88
4.3.2	Slot-based Feedback . . . . .	89
4.3.3	Flash-based Feedback . . . . .	91
4.3.4	Busy-time-based Feedback . . . . .	92
4.4	PHY Rate Adaptation in Multicast Transmission . . . . .	93
4.5	Performance Evaluation . . . . .	96
4.5.1	Performance evaluation considering feedback error . . . . .	104
4.6	Summary . . . . .	109
<b>5</b>	<b>Conclusion and Future Work</b>	<b>110</b>
5.1	Research Contributions . . . . .	110
5.2	Future Research Directions . . . . .	111

<b>Abstract (In Korean)</b>	<b>121</b>
감사의 글	123

# List of Tables

2.1	MCSs for Type A Devices in ECMA-387 . . . . .	35
2.2	Relationship between PSNR and MOS [20] . . . . .	42
3.1	Satisfied users and average PSNR . . . . .	70

# List of Figures

2.1	Spectrum allocation map at 60 GHz band. . . . .	15
2.2	Superframe structure of ECMA-387. . . . .	19
2.3	An example of a DRP negotiation procedure. . . . .	20
2.4	Operation of S-UEP in ECMA-387. . . . .	24
2.5	Latency of compressed and uncompressed video streaming. . . . .	26
2.6	The formats of beacon frame and channel state information element. .	27
2.7	BER of MCSs in ECMA-387. . . . .	34
2.8	Comparison of ePSNR from analysis and PSNR from simulations. . .	36
2.9	Effectiveness of UEP. . . . .	38
2.10	Measured PSNR values when $\text{SNR} = -2.5$ dB. . . . .	39
2.11	Amount of required resources per superframe for 720p30 video stream- ing. . . . .	40
2.12	PSNR performance for various link adaptation policies. . . . .	41
2.13	Minimum resource allocation for $\text{Min AR}(-E)$ . . . . .	44
2.14	Snapshots at $\text{SNR} = 5$ dB and $T_{\text{allocate}} = 8$ ms. . . . .	45
3.1	Illustration of time-slotted video multicast by multiple APs. . . . .	50
3.2	Illustration of the proposed reliable video multicast schemes. . . . .	53
3.3	The procedure of proposed video multicast with application-layer FEC. .	56

3.4	Video packet delivery ratio $P(n, r)$ with Raptor code ( $N_O = 44$ ). . .	64
3.5	Delivery ratio when there are two APs (no fading, $N = 50$ , $N_O = 44$ ). . .	65
3.6	PSNR vs. delivery ratio. . . . .	67
3.7	PSNR when there are two APs (no fading, $N = 50$ , $N_O = 44$ ). . . . .	68
3.8	Performance when there are two APs. . . . .	69
3.9	Four APs at (90,90), (270,90), (90,270), (270,270), and 2,000 users. . .	71
3.10	Four APs at random locations and 500 users. . . . .	72
3.11	Four APs and 500 users at the random locations in 300 m $\times$ 300 m area. .	73
3.12	Experimental environment. . . . .	74
3.13	Experimental results ( $N_O = 44$ ). . . . .	75
3.14	Implementation of demonstrable video multicast. . . . .	76
3.15	A snapshot of the demonstration. . . . .	77
3.16	Average PSNR. . . . .	78
4.1	An example of GCR procedure. . . . .	82
4.2	An example of GCR w/ FEC. . . . .	85
4.3	An example of ARQ w/ FEC procedure. . . . .	86
4.4	An example of reliable multicast with idle-time-based feedback. . . . .	88
4.5	An example of reliable multicast with slot-based feedback. . . . .	90
4.6	An example of reliable multicast with flash-based feedback. . . . .	91
4.7	An example of reliable multicast with busy-time-based feedback. . . . .	92
4.8	An example of reliable multicast with busy-time-based feedback and PHY rate adaptation. . . . .	94
4.9	Performance comparison for the different frame error rate (MCS: 6.5 Mbps, # multicast users= 10). . . . .	96
4.10	Performance comparison for the different number of multicast users (MCS: 6.5 Mbps, frame error rate= 0.1). . . . .	98

4.11	Performance comparison for the different number of multicast users (MCS: 65.0 Mbps, frame error rate= 0.1). . . . .	100
4.12	Performance comparison between w/ ARQ and w/o ARQ (MCS: 6.5 Mbps, # multicast users= 10). . . . .	101
4.13	The average airtime for the various MCSs (Busy-time-based FB, # multicast users= 10). . . . .	102
4.14	The average airtime for the different frame error rates and $N_{init}$ (MCS: 6.5 Mbps, # multicast users= 10). . . . .	103
4.15	Empirical model based on the experiments. . . . .	104
4.16	Assumed feedback error model. . . . .	106
4.17	Performance comparison for the different detection error models (MCS: 6.5 Mbps). . . . .	107
4.18	Performance comparison for the different detection error models (MCS: 6.5 Mbps, # multicast users= 10). . . . .	108
5.1	The summary of this dissertation. . . . .	112

# **Chapter 1**

## **Introduction**

### **1.1 Video Streaming over Wireless Networks**

Today, along with the rapid growth of the network performance, the demand for high-quality video streaming services has greatly increased. The emergence of high-speed Wi-Fi, such as IEEE 802.11n [28] and IEEE 802.11ac [29], has enabled high-quality and bandwidth-hungry applications such as video streaming to/from smartphones. In addition, recent improvements in wireless technologies have revealed the availability of communications at 60 GHz band, referred to as the millimeter-wave (mmWave) band. 60 GHz band is characterized by the wide bandwidth, the limited transmission range, which allows high spatial reuse of the frequency, and finally, high degree of directivity due to the wavelet of the high frequency. Accordingly, a directional antenna technology is generally employed so that the 60 GHz band inherently assumes Line-of-Sight (LoS) communications.

The most attractive feature of the 60 GHz band is that it enables multi-Gbps wireless links. Therefore, 60 GHz technologies are able to support various applications such as data bus, file transferring, and (uncompressed) video streaming, where many of



them were not possible with other existing wireless technologies. In particular, thanks to the high-speed transmissions at 60 GHz band, a high-quality video streaming with an uncompressed source can be supported so as to reduce the overhead of encoding and decoding as well as to enhance the video quality.

### **1.1.1 Uncompressed Video Streaming over 60 GHz band**

Due to the limited bandwidth in wireless communications, it has been impossible to provide high-quality uncompressed video streaming services that require Gigabits per second (Gbps) bandwidth, e.g., full High Definition Television (HDTV) streams with a few Gbps data rate. Note that even in an up-to-date Wi-Fi system supporting the newly developed IEEE 802.11n [1] standard, which is designed for the high throughput performance in Wireless Local Area Networks (WLANs), the theoretical maximum achievable throughput is known to be up to 600 Mbps.

To cope with the lack of available bandwidth, video compression schemes have been widely adopted. That is, the required bandwidth of a high-quality video stream is reduced by compressing the video data. Even for the real-time video transmission, e.g., wireless monitor, wireless TV, and wireless projector, Wi-Fi-based commercial wireless real-time display products based on the compressed streaming have been introduced, e.g., Wireless Display (WiDi) [2].

For the high-quality real-time video transmissions requiring ultra low latency, e.g., wireless monitor and wireless projector which require close interaction, the uncompressed video streaming without complicated video coding schemes might be preferred, as long as the bandwidth is allowed, due to the limitation of computing resources and possible delay of encoding/decoding process during the video compression. Actually, it is reported that some commercial wireless real-time display solutions based on the compressed streaming sometimes experience a significant latency as

much as users can recognize depending on the hardware resources. Moreover, widely-employed lossy video coding schemes, e.g., MPEG-4 and H.264, may deteriorate the quality of video through the encoding/decoding process and cause error propagation problem in erroneous video transmission environments [7]. In addition, for the compressed video streaming, it requires that the transmitter and the receiver have the same compression technique or some transcodec to convert the compression format.

Uncompressed video streaming consequently can resolve these problems, and it also has other additional merits. For example, it supports the universal standard formats, better audio/video synchronization, reduced operational complexity and risk, and so on [8]. Considering the real-time video streaming, e.g., wireless monitor, wireless TV, and wireless projector, as the main application, uncompressed video streaming is more suitable than the compressed video streaming, while the limitation of bandwidth is the most critical issue. For these reasons, most of the recently-developed standard specifications for 60 GHz communications, e.g., 802.11ad [17], ECMA-387 [14], 802.15.3c [13], and Wi-Gig [19], mainly assume uncompressed video applications rather than the compressed video applications.

### **1.1.2 Video Multicast over IEEE 802.11 WLAN**

There have been increasing R&D efforts in utilizing smartphones' Wi-Fi as smartphone user population and applications rapidly expand. When the same video data needs to be delivered to multiple receivers, multicast that transmits the data to multiple receivers only once is more efficient than unicasting the same data to each receiver individually. IEEE 802.11 [28] standard supports multicast transmission, in which a transmitter sends a packet to multiple receivers with a single transmission. This efficiency of multicast triggered a wide investigation of video multicast in Wi-Fi systems, in which the video data is delivered to multiple receivers via multicast transmissions.

However, error control with Automatic Repeat reQuest (ARQ) is not feasible in multicast, since there is no acknowledgement of requesting packet-retransmission. Therefore, multicast is inherently vulnerable to the transmission failures caused by wireless channel errors. To overcome this deficiency, application-layer packet-level FEC (AL-FEC) has been proposed widely [30, 31, 50]. In AL-FEC, the FEC encoding and decoding are performed in the application layer, which can help the receiver recover the erased data packets by exploiting the additional parity packets that are generated from data packets by FEC encoder. AL-FEC is helpful, especially in multicast scenarios, since the additional parity packets can compensate the unreliable nature of multicast. Moreover, in most cases, although the lost packets of different users could be different, by utilizing AL-FEC, all such different lost packets can be recovered by the same parity packets.

To overcome the unreliability of multicast transmission, two emerging standards define new ARQ features for the reliable video multicast service, i.e., Directed Multicast Service (DMS) in 802.11v [46], and GroupCast with Retries (GCR) in 802.11aa [47].

DMS allows a multicast user to request its serving AP to transmit multicast frames destined to itself as unicast frames. This conversion from multicast to unicast may have advantages in terms of reliability and efficiency, in that unicast transmission can utilize MAC-layer ARQ, RTS/CTS exchange, and higher PHY rate. However, the same multicast frame is transmitted multiple times with the different destination address whenever DMS service is requested by the multiple users. This reduces the benefit of the multicast transmission.

On the other hand, in order to provide reliable multicast service, GCR defines two additional retransmission schemes, namely, GCR unsolicited retry (GCR-UR) and GCR Block Ack (GCR-BA). GCR-UR makes the AP retransmit multicast frames without receiving any retry request from receivers. In order to utilize the time diversity

gain, an original frame and its retransmitted frame should be transmitted in different transmit opportunities (TXOPs). However, GCR-UR might make the meaningless retransmission of the multicast frames even though all the multicast users already receive the multicast frames.

GCR-BA enables multicast receivers to use the block acknowledgement (Block Ack) for multicast frames. After sending a number of multicast frames, the AP regularly requests a user to transmit the Block Ack frame by sending an individual Block Ack reQuest (BAQ) frame, then the receiving user sends a Block Ack (BA) frame to indicate which MAC protocol data units (MPDUs) are correctly received. After gathering the Block Acks from one or more of GCR group members, the AP decides which MPDUs should be retransmitted. The choice of users to whom the AP requests the Block Ack is implementation-dependent. However, GCR-BA cannot guarantee the reliability of the multicast transmission as long as all the users do not send BA frames. On the contrary, collecting all the users' information of the received frames makes a huge overhead. To guarantee the reliability of the multicast users which send BA frames, the AP retransmits the MPDUs which are not received by all the users.

## **1.2 Overview of Existing Approaches**

### **1.2.1 Link Adaptation over Wireless Networks**

There have been many link adaptation policies proposed for IEEE 802.11 and cellular networks, e.g., [23, 24]. The typical goal of the existing link adaptation policies has been the maximization of the throughput. However, the goal should depend on the application requirement. For example, the video streaming quality cannot be met by using such existing link adaptation algorithms.

Some papers consider link adaptation regarding video quality [21, 25] in WLAN

environments. The authors, however, consider compressed video streaming instead of uncompressed video, and propose link adaptation policies that use the feedback of predefined video frame's Peak Signal-to-Noise Ratio (PSNR) [21], or minimize the mean square error (MSE) [25]. These policies cannot directly improve video quality.

There are many researches on 60 GHz networks [9,26,27]. These papers mainly focus on physical and MAC layers, such as neighbor discovery problems or coexistence problems in 60 GHz networks, but not closely related with guaranteeing the quality of video streams.

There also have been efforts which consider Unequal Error Protection (UEP) for the compressed video streaming [12] or uncompressed video streaming [10, 11] in 60 GHz networks. These papers measure the video quality in various UEP environments. However, these papers do not propose any link adaptation policies based on the UEP.

### **1.2.2 Video Streaming over IEEE 802.11 WLAN**

Most of the research efforts on improving the performance of video transmission over IEEE 802.11 WLAN are focused on single AP environments. In [39], an adaptive cross layer protection strategy for enhancing the robustness and efficiency of scalable video unicast transmission in a single AP environment is proposed, in which various protection strategies existing in the protocol stack, e.g., AL-FEC, maximum MAC retransmission limit, and packet size adaptation, are jointly optimized for a given channel condition. In [30], Raptor code-based schemes for video multicast are presented. In order to achieve the reliability and efficiency of video multicast, Raptor code rate is dynamically determined based on the given channel condition in a single AP environment.

M. Santos *et al.* [40] introduce a novel QoE-aware multicast mechanism for video

transmission. The mechanism is developed by integrating a structured set of collision prevention, feedback and rate adaptation control mechanisms without FEC in a single AP environment. In [41], for enhancing the reliability of video multicast, the authors propose a Wi-Fi multicast system named DirCast, in which an AP converts multicast packets to targeted unicast transmissions and most of the stations operate in promiscuous mode to overhear the unicast transmissions. To minimize the amount of consumed air time, DirCast uses greedy algorithm-based destination control and association control, which is inherently applied to a single AP environment without FEC. Another MAC-level video multicast protocol named REMP is proposed in [42], in which AP selectively retransmits erroneous multicast frames and adjusts MCS under varying channel conditions. The authors also propose an extended version of REMP for efficient delivery of scalable video over IEEE 802.11n WLANs, in which different layers of scalable video can be transmitted with different MCSs to guarantee the minimal satisfactory video quality to all users while providing a higher video quality to users exhibiting better channel conditions. Nevertheless, the proposed scheme is developed in a single AP environment without FEC.

On the other hand, there are some works exploiting multi-AP diversity. In [43], Y. Zhu *et al.* propose a multi-AP architecture and compare its performance in terms of throughput with the traditional WLANs from a network perspective. Herein, multi-AP means that each user is capable of maintaining multiple associations. However, they consider performance improvements of uplink only and have not incorporated FEC scheme across multiple associations. In [44], J. Vella *et al.* propose a multi-AP infrastructure that multiple transmit sources such as APs can be placed at the edge of a coverage area so as to aid the stations which are suffering from severe signal attenuation. They call the AP placed at the edge as slave AP and the AP placed at the center of the coverage area as master AP. The slave AP and master AP share a common

frequency channel and transmit during non-overlap time durations so that stations can receive video multicast packets from both slave AP and master AP. Whereas, they just consider packet repetition between master AP and slave AP as a diversity scheme and leave the evaluation of other FEC schemes for future work.

### **1.2.3 Reliable Multicast over IEEE 802.11 WLAN**

Most of the research efforts for the reliable multicast over IEEE 802.11 WLAN are focused on the ARQ of a single multicast packet. In [53], the defined group ACK request makes each multicast receiver transmit its ACK frame in a different time slot without the collision. It can prevent the collision between ACK frames, however, the ACK overhead linearly increases as the number of multicast receivers increases. In [49, 51, 54], Negative ACK (NACK) signal is used for requesting the retransmission of the failed packet. By utilizing the collisions between NACK frames, the sender can know one or more reception failures among the multicast receivers. However, since the ARQ protocols are focused on a single multicast packet' retransmission, the packet needs to be retransmitted, even if all the receivers except one receiver correctly receives the packet. Another reliable multicast with ARQ is proposed in [52]. each receiver sends ACK signal on a corresponding OFDMA subcarrier to indicate the correct reception of the multicast packet. However, the proposed protocols are focused on only a single multicast packet' retransmission, too.

On the other hand, there are lots of the research efforts utilizing Packet-level Forward Error Correction (FEC) in the multicast transmissions. In [30], the reliable multicast protocols are proposed with cross-layer FEC code rate and PHY rate adaptations by collecting the feedback from the multicast receivers before sending the multicast packets. Another reliable multicast protocol with FEC code is proposed in [?]. FEC code rate is adaptively selected from the time-slot based feedback from the multicast

receivers. However, these protocols do not consider ARQ protocols, and hence, 100 % reliability can not be guaranteed.

## 1.3 Main Contributions

The objective of this dissertation is to provide high-quality reliable video streaming over wireless networks. The main contributions of this dissertation are as follows.

- **Link Adaptation for High-Quality Uncompressed Video Streaming in 60 GHz Wireless Networks:** we introduce a new metric, called *expected Peak Signal-to-Noise Ratio (ePSNR)*, to numerically estimate the video streaming quality, and additionally adopt Unequal Error Protection (UEP) schemes that enable flexible link adaptation by offering a variety of MCS selection. Using the ePSNR as a criterion, we propose two link adaptation policies with different objectives. The proposed link adaptation policies attempt to (1) maximize the video quality for given wireless resources, or (2) minimize the required wireless resources while meeting the video quality. With the use of ePSNR, the proposed link adaptation policies tend to select the most efficient MCS out of the MCSs that achieve the acceptable video quality considering the required resources. Our work is the first research on the link adaptation policy for the uncompressed video streaming. Our extensive simulation results demonstrate that the introduced variable, i.e., ePSNR, well represents the level of video quality. It is also shown that the proposed link adaptation policies can enhance the resource efficiency while achieving acceptable quality of the video streaming.
- **Reliable Video Multicast over Wi-Fi Networks with Coordinated Multiple APs:** we propose reliable video multicast over Wi-Fi networks with coordinated multiple Access Points (APs) to enhance video quality. By coordinating mul-



multiple APs, each AP can transmit (1) entirely different or (2) partially different FEC-encoded packets so that a multicast receiver can benefit from both spatial and time diversities. The proposed scheme can enlarge the satisfactory video multicast region by exploiting the multi-AP diversity, thus serving more multicast receivers located at cell edge with satisfactory video quality. To our best knowledge, this is the first work to extend AL-FEC based reliable video multicast to multiple AP environments, thus exploiting spatial and time diversities. We propose a resource-allocation algorithm for FEC code rate adaptation, utilizing the limited wireless resource more efficiently while enhancing video quality. The proposed FEC code rate adaptation algorithm makes more multicast users be served with satisfactory video quality. We also introduce the method for estimating the video packet delivery ratio after FEC decoding. The effectiveness of the proposed schemes is evaluated via extensive simulation and experimentation. The proposed schemes are observed to enhance the ratio of satisfied users by up to 37.1% compared with the conventional single AP multicast scheme.

- **Reliable Video Multicast with Efficient Feedback over Wi-Fi:** we propose the reliable multicast protocols considering both ARQ and packet-level FEC together, to overcome the unreliability of multicast transmission. For the proposed reliable multicast protocol, the multiple efficient feedback protocols reducing the overheads of feedback messages while providing the reliable multicast service are proposed. The feedback overheads can be reduced by intending the concurrent transmissions, which makes the collisions, between feedback messages, while the AP easily knows the number of requiring parity frames of the worst user(s) for the recovery of all the lost packets. In addition, utilizing the efficient feedback protocols, we propose the PHY rate adaptation based on the close-loop MCS feedback in multicast transmissions. From the performance evaluations,

the proposed protocols can efficiently reduce the feedback overheads, while the reliable multicast transmissions are guaranteed.

## **1.4 Organization of the Dissertation**

The remainder of this dissertation is organized as follows. Chapter 2 presents the proposed link adaptation policies for high-quality uncompressed video streaming over 60 GHz wireless networks. We first introduce the uncompressed video streaming and Giga-bps communications over 60 GHz band. We propose link adaptation policies using ePSNR, and the performance evaluation is presented.

Chapter 3 introduces the proposed reliable video multicast over Wi-Fi networks with coordinated multiple APs to enhance video quality. The system environments of video multicast with AL-FEC code over multiple APs are introduced. We present a new reliable video multicast protocol with coordinated multiple APs, and introduces its detailed procedure with AL-FEC. An FEC code rate adaptation algorithm is proposed, and we evaluate the performance of the proposed video multicast protocol.

Chapter 4 presents the reliable video multicast with the efficient feedback protocols over Wi-Fi. The unreliability issues on the multicast over Wi-Fi are introduced. The motivation of the proposed reliable multicast protocols with ARQ and packet-level FEC is presented. We propose new feedback protocols for the reliable multicast. In addition, the PHY rate adaptation utilizing the efficient feedback protocols is proposed and the performance of the proposed multicast protocols is evaluated.

Finally, Chapter 5 concludes this dissertation with a summary of the main contributions and describe possible future research directions.

## **Chapter 2**

# **Link Adaptation for High-Quality Uncompressed Video Streaming in 60 GHz Wireless Networks**

## **2.1 Introduction**

Today, along with the rapid growth of the network performance, the demand for high-quality video streaming services has greatly increased. Due to the limited bandwidth in wireless communications, however, it has been impossible to provide high-quality uncompressed video streaming services that require Gigabits per second (Gbps) bandwidth, e.g., full High Definition Television (HDTV) streams with a few Gbps data rate. Note that even in an up-to-date Wi-Fi system supporting the newly developed IEEE 802.11n [1] standard, which is designed for the high throughput performance in Wireless Local Area Networks (WLANs), the theoretical maximum achievable throughput is known to be up to 600 Mbps.

To cope with the lack of available bandwidth, video compression schemes have been widely adopted. That is, the required bandwidth of a high-quality video stream is reduced by compressing the video data. Even for the real-time video transmission,

e.g., wireless monitor, wireless TV, and wireless projector, Wi-Fi-based commercial wireless real-time display products based on the compressed streaming have been introduced, e.g., Wireless Display (WiDi) [2], Apple Airplay mirroring [3], and Miracast [4].

However, for the high-quality real-time video transmissions requiring ultra low latency, e.g., wireless monitor and wireless projector which require close interaction, the uncompressed video streaming without complicated video coding schemes might be preferred, as long as the bandwidth is allowed, due to the limitation of computing resources and possible delay of encoding/decoding process during the video compression.

Actually, it is reported that some commercial wireless real-time display solutions based on the compressed streaming sometimes experience a significant latency as much as users can recognize depending on the hardware resources [5]. We also measure the latency of a commercial wireless real-time display solution by comparing the screens of the transmitter (Samsung Galaxy Note 10.1 [6]) and the receiver (Samsung AllShare Cast dongle [6]) which are connected by Miracast. In the results, it is shown that the mean latency is about 170 ms with a standard deviation of 140 ms, and thus a human can recognize the latency especially in the interactive and/or dynamic video environments.

Moreover, widely-employed lossy video coding schemes, e.g., MPEG-4 and H.264, may deteriorate the quality of video through the encoding/decoding process and cause error propagation problem in erroneous video transmission environments [7]. In addition, for the compressed video streaming, it requires that the transmitter and the receiver have the same compression technique or some transcodec to convert the compression format.

Uncompressed video streaming consequently can resolve these problems, and it

also has other additional merits. For example, it supports the universal standard formats, better audio/video synchronization, reduced operational complexity and risk, and so on [8]. Considering the real-time video streaming, e.g., wireless monitor, wireless TV, and wireless projector, as the main application, uncompressed video streaming is more suitable than the compressed video streaming, while the limitation of bandwidth is the most critical issue. For these reasons, most of the recently-developed standard specifications for 60 GHz communications, e.g., 802.11ad [17], ECMA-387 [14], 802.15.3c [13], and Wi-Gig [19], mainly assume uncompressed video applications rather than the compressed video applications. Thus, we consider the uncompressed video streaming in this chapter.

Recent improvements in wireless technologies have revealed the availability of communications at 60 GHz band, referred to as the millimeter-wave (mmWave) band. 60 GHz band is characterized by the wide bandwidth, the limited transmission range, which allows high spatial reuse of the frequency, and finally, high degree of directivity due to the wavelet of the high frequency. Accordingly, a directional antenna technology is generally employed so that the 60 GHz band inherently assumes Line-of-Sight (LoS) communications. Fig. 2.1 shows the worldwide spectrum allocation at 60 GHz band [9]. Note that 3.5 GHz bandwidth between 59.4 GHz and 62.9 GHz is allocated as a common unlicensed band among these countries.

The most attractive feature of the 60 GHz band is that it enables multi-Gbps wireless links. Therefore, 60 GHz technologies are able to support various applications such as data bus, file transferring, and (uncompressed) video streaming, where many of them were not possible with other existing wireless technologies. In particular, thanks to the high-speed transmissions at 60 GHz band, a high-quality video streaming with an uncompressed source can be supported so as to reduce the overhead of encoding and decoding as well as to enhance the video quality.

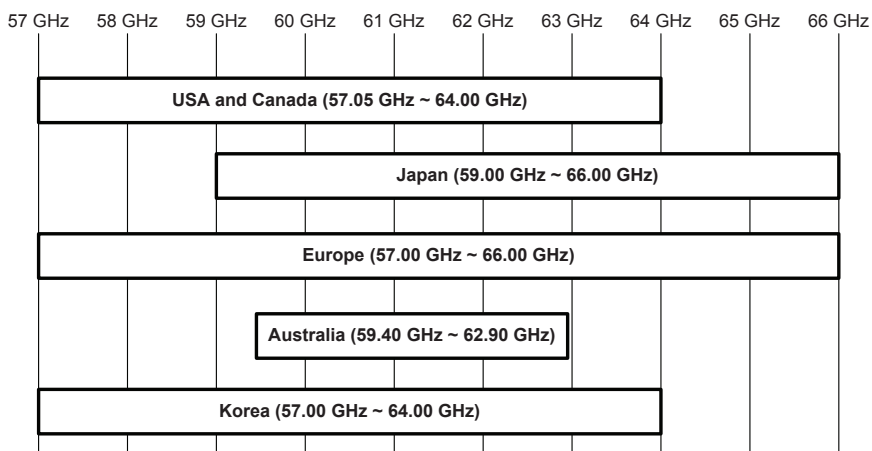


Figure 2.1: Spectrum allocation map at 60 GHz band.

In the 60 GHz system, multiple Modulation and Coding Schemes (MCSs) are supported. In a general sense, the selection of a more robust MCS can provide a better video streaming service while requiring more wireless bandwidth. Even in such a high bandwidth environment of 60 GHz band, the possible wireless resource might be limited for the multiple reasons, e.g., sharing it with other devices and avoiding the interference, since the 60 GHz band is the unlicensed band. On the other hand, the selection of a higher MCS can provide the better resource efficiency while the video quality might become worse due to the potential wireless channel error. Therefore, the link adaptation algorithm for the selection of MCS is necessary for both the video quality and the resource efficiency.

In order to further improve the quality of the video streaming service, we consider Unequal Error Protection (UEP) [10–12]. It should be noted that in the video data, some data bits are more important than others; for example, in the data bits that represent the color information of a video pixel, Most Significant Bits (MSBs) are more important than Least Significant Bits (LSBs) in terms of the color representation. If

protecting all the data bits in a video frame is not possible due to some constraints,<sup>1</sup> using UEP, i.e., better protecting more important data (e.g., MSBs in a video pixel), is a good solution for providing the acceptable quality for the video streaming service in a more resource efficient manner.

In this chapter, we propose two Medium Access Control (MAC) layer link adaptation policies that incorporate two different objectives, namely, (1) maximizing the video quality for given wireless resources, and (2) minimizing the required resources while meeting the video quality. To supplement the proposed link adaptation policies, we introduce a new metric, i.e., *expected Peak Signal-to-Noise Ratio (ePSNR)*, which estimates the quality of a video stream in a given wireless channel environment. The ePSNR is used as a criterion for the proposed link adaptation to find the most proper Modulation and Coding Scheme (MCS) and the amount of required wireless resources. Considering UEP in the proposed link adaptation yields a detailed link adaptation by offering a variety of MCS selection. With the use of ePSNR, the proposed link adaptation policies tend to select the most efficient MCS out of the MCSs that achieve the acceptable video quality considering the required resources.

The rest of this chapter is organized as follows. Section 2.2 presents ECMA-387 standard and wireless HDMI PAL. In Section 2.3, we propose link adaptation policies using ePSNR, and Section 2.4 presents the performance evaluation. Finally, Section 2.5 summarizes the chapter.

---

<sup>1</sup>Note that the protection of a data bit requires additional redundant bits for error detections and/or corrections, which increases the amount of total data to be transmitted. We deal with this problem in detail in Section 2.3.

## 2.2 ECMA-387 and Wireless HDMI

There are several standard groups that have been developing 60 GHz wireless technologies. IEEE 802.15.3c, which specifies Wireless Personal Area Network (WPAN) targeting at the throughput of 1–5 Gbps at 60 GHz band, was published in 2009 [13]. ECMA-387 [14] published in 2010 is another standard for 60 GHz wireless communication. The target system and the applications of ECMA-387, which employs ECMA-368<sup>2</sup> [15] MAC and 60 GHz Physical layer (PHY) technology, are similar to those of IEEE 802.15.3c. ECMA-387 also defines wireless High-Definition Multimedia Interface (HDMI) [16] Protocol Adaptation Layer (PAL) mainly for the support of high-quality uncompressed video streaming. IEEE 802.11ad [17] is currently being developed for a WLAN operating at 60 GHz. It aims at various applications such as data transferring, video streaming, and so on, in WLAN environments.

The common characteristic of these standard-based MAC protocols for the high-quality video streaming is to allocate resources in advance for the reliable video streaming. Since the systems that adopt these MAC protocols use predetermined resource blocks without contentions, high-quality video streams with a huge amount of data can be effectively transmitted. Furthermore, there are other standard organizations, such as Wireless High Definition (WirelessHD) [18] and Wireless Gigabit Alliance (WiGig) [19], for high speed communication at 60 GHz band. WirelessHD and WiGig have been organized for HD video streaming and high speed communication, respectively. These standard groups assume uncompressed video applications as the main applications which can utilize huge bandwidth effectively.

In this chapter, we focus on ECMA-387, which is a promising technology based a distributed MAC, and also defines HDMI PAL, thus making this standard suitable

---

<sup>2</sup>ECMA-368 is the standard for UWB band, and ECMA-387 inherits the main MAC protocol from ECMA 368.



for uncompressed video streaming. In fact, many other 60 GHz standards are not open to public at this time. Note that the proposed link adaptation policies can be readily adopted for other wireless technologies supporting uncompressed video streaming.

### 2.2.1 ECMA-387

ECMA-387 defines three different types of devices (i.e., types A, B, and C) which employ different PHYs, and also have different capabilities. Out of these, type A device is particularly designed for data transferring and video streaming, both uncompressed and lightly compressed. As we consider uncompressed video streaming as our target application, type A devices are considered in this work.

Fig. 2.2 depicts the superframe structure of ECMA-387 MAC, where the durations of one superframe and the minimum resource allocation unit, referred to as Medium Allocation Slot (MAS), are fixed as 16.384 ms and 64  $\mu$ s, respectively. A superframe consists of a beacon period for beacon transmissions and a data communication period for data packet transmissions. In the beacon period, each device independently selects a time slot that is mutually exclusive with each other, and then transmits its own beacon message in a sequential manner. In the beacon period, neighboring devices overhear the transmitted beacon messages. Beacon frames include not only neighbor information but also the time slot information which is exploited for data transmissions.

Through the Distributed Reservation Protocol (DRP) negotiation procedure during the beacon period, the MASs in the data transmission period are allocated for data communications.<sup>3</sup> Once a group of MASs are reserved to a device for data transmissions, those MASs are periodically used by this device in every superframe, until the reserved MASs are rescheduled by a subsequent DRP negotiation procedure. The reserved MASs might need to be changed due to the time-varying channel condition

---

<sup>3</sup>The reserved MASs can be composed of multiple non-contiguous MASs.

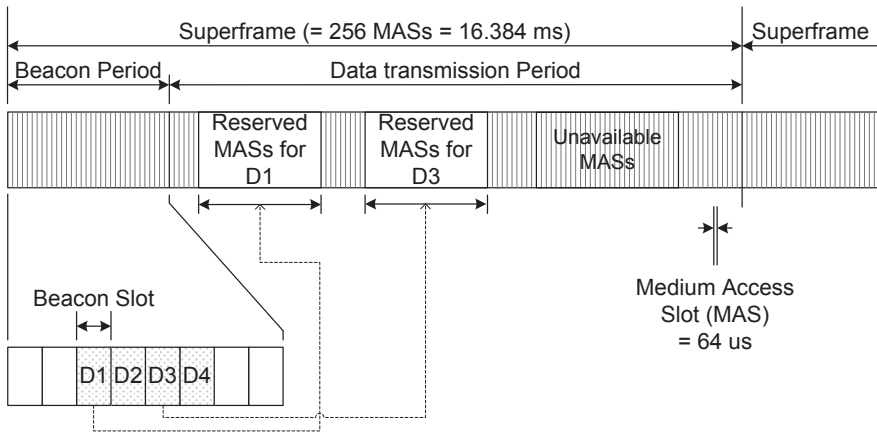


Figure 2.2: Superframe structure of ECMA-387.

and/or the changed load of application traffic.

Fig. 2.3 shows an example of a DRP negotiation procedure. There are two types of negotiation mechanisms, i.e., implicit negotiation and explicit negotiation. The implicit negotiation is executed through the exchange of the information elements in the beacon frames and the explicit negotiation is executed through the exchange of DRP reservation request command frame and DRP reservation response command frame with some information elements.

Each device maintains the information of its available MASs which are not occupied by neighboring devices and are not interfered by unknown devices through the interference detection procedures, e.g., sensing the channel on the specific MASs. The transmitter, i.e., the owner of DRP, checks its available MASs and it selects the MASs to transmit its data to the receiver, i.e., the target of DRP, periodically considering the load of application traffic.

The DRP reservation request is transmitted with a DRP Information Element (IE), which includes reservation status, reservation reason code, reservation type, DRP al-

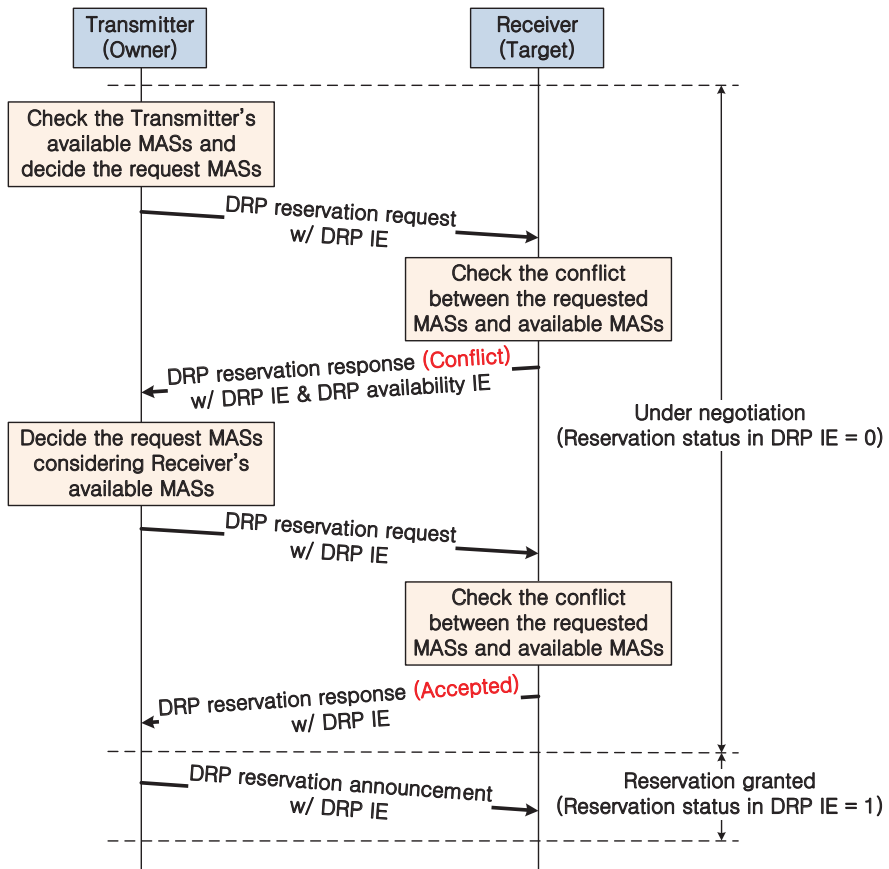


Figure 2.3: An example of a DRP negotiation procedure.

location bitmap fields, and so on. The receiver, which receives the DRP reservation request, checks the conflict between the requested MASs of the DRP allocation bitmap fields and its available MASs. If the conflict is detected, that is, its unavailable MASs are requested by the transmitter, the receiver transmits a DRP reservation response with DRP IE, where its reason code indicates *conflict* and with a DRP availability IE which represents its available MASs as the bitmap. The transmitter transmits a DRP reservation request again with modified DRP allocation bitmaps considering both its

available MASs and the receiver's available MASs of the DRP availability IE.

If the transmitter receives a DRP reservation response which indicates *accepted*, the DRP reservation is granted and the transmitter announces the granted DRP reservation via the beacon frame. To let the neighboring devices know the information of the occupied MASs, the transmitter broadcasts the information of the reserved MASs through DRP IE in every beacon frame until the DRP reservation is terminated.

Through this negotiation procedure, each device can reserve the MASs, which are available for both the transmitter and the receiver, while avoiding the overlapped allocation and the periodic interference from the neighboring devices and unknown devices. In general, most of wireless systems working at 60 GHz band mainly support the MAC protocols based on the periodic resource allocation. Thus, the interference from unknown devices is also likely to be periodic.

Fig. 2.2 shows an example where Device 1 (D1) and Device 3 (D3) reserve the MASs in the data transmission period. After this DRP negotiation procedure, D1 and D3 can periodically access the reserved MASs without any interference since these MASs are exclusively dedicated to these two devices. Some MASs might become unavailable due to the possible interference or being occupied by neighbor devices. If a device detects the reservation conflicts, e.g., interference from neighbor devices and unknown devices, which makes bad communication environments, the device can relocate its reserved MASs through the DRP modification procedure. If the interference is detected even in the beacon period, the start timing of the superframe, i.e., Beacon Period Start Time (BPST), can be also changed.

### **2.2.2 Wireless HDMI (HDMI PAL)**

HDMI PAL is defined as a part of the ECMA-387 standard, and this aims at replacing the original wireline cable of HDMI [16] with the ECMA-387 wireless link with-

out modifying the original HDMI protocol by using wireless converters between the HDMI source and sink devices. Since the original HDMI utilizes uncompressed video transmission, HDMI PAL also basically supports uncompressed video streaming and optionally adopts Reed Solomon (RS) coding for reliable communication.

HDMI is designed as a compact audio/video interface for transmitting uncompressed digital data. HDMI has three separate communication channels, namely, Display Data Channel (DDC), Transition Minimized Differential Signaling (TMDS), and the optional Consumer Electronics Control (CEC). DDC and CEC are used for control and management, and TMDS carries video, audio, and auxiliary data. HDMI supports multiple video formats, e.g., Standard-Definition Television (SDTV), Enhanced-Definition Television (EDTV), and High-Definition Television (HDTV), with multiple color models, e.g., RGB and YCbCr, encoded with a color depth<sup>4</sup> up to 48 bits/pixel. In wired HDMI, the data of these channels are transmitted in parallel through multiple ports. In wireless HDMI of ECMA-387, however, the data bits of these channels are aggregated and are transmitted through a single wireless channel. This accordingly mandates packetization/multiplexing and depacketization/demultiplexing functionalities at the transmitter and receiver, respectively.

### **2.2.3 UEP Operations**

As part of HDMI PAL, two different types of UEPs are defined where these schemes basically try to provide better error protection to more important data than less important data. A UEP can be used to minimize the waste of wireless resources due to channel errors by strongly protecting important data bits while meeting the overall video quality requirement. However, the use of UEP slightly increases the packet header overhead compared with the non-UEP case, i.e., Equal Error Protection (EEP). The

---

<sup>4</sup>The color depth is the number of bits used to represent a video pixel.

first type of UEP, referred to as Parallelized Bit based UEP (P-UEP), uses UEP MCSs, that are specifically defined for the UEP purpose at the PHY, and the second type, referred to as Sequential Packet Based UEP (S-UEP), utilizes the existing non-UEP MCSs, and applies different MCSs to MSBs and LSBs, respectively. Note that when a video pixel is represented by a number of bits, the errors in MSBs more severely distort the color of the pixel compared with those in LSBs, and hence, S-UEP better protects MSBs by applying more reliable MCS. In the case of P-UEP, the number of UEP MCSs is quite limited, while S-UEP can support a wide range of protection levels via various combinations of existing non-UEP MCSs. For this reason, we consider the S-UEP scheme in this work.

Fig. 2.4 shows the operation of S-UEP in ECMA-387 when the RGB color model and the color depth of  $3n_R$  bits/pixel are used. Note that a video frame is composed of a number of pixels, where each pixel is represented by red, green, and blue colors when the RGB video color model is used. In Fig. 2.4,  $R_k$ ,  $G_k$ , and  $B_k$  indicate red, green, and blue color data of the  $k$ -th pixel, respectively. Each of  $R_k$ ,  $G_k$ , and  $B_k$ , represented by  $n_R$  bits, is divided into  $n_M$  MSBs and  $n_L$  LSBs. That is,  $n_R = n_M + n_L$ , where  $n_M$  and  $n_L$  are configurable values as addressed below. After this division, MSBs and LSBs are separately packetized with headers including the UEP information, and then are transmitted with two different MCSs. Note that the MCS used for MSBs (LSBs) should be for a lower (higher) rate to support more (less) reliable transmission.

## 2.2.4 ACK Transmissions for Video Streaming

In most MAC protocols, a receiver acknowledges the successful reception of a data packet by responding with an Acknowledgement (ACK) packet. If a transmitter does not receive the corresponding ACK in time, the transmitter retransmits the previous data packet assuming that the receiver failed to receive the data packet due to channel

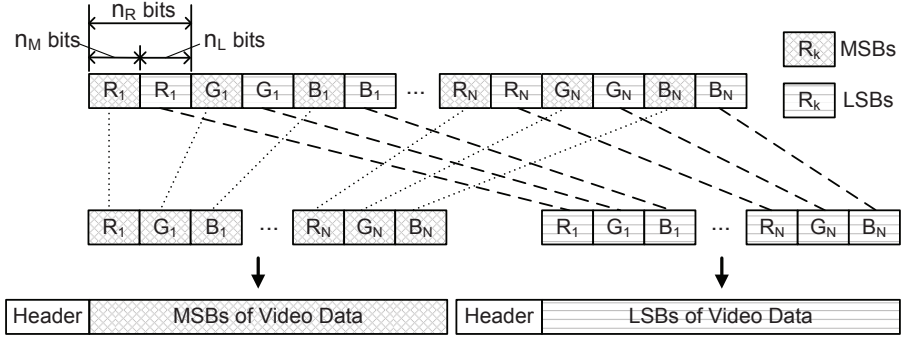


Figure 2.4: Operation of S-UEP in ECMA-387.

errors.

In video data transmissions, however, short-term video distortion due to packet errors might be more desirable than extended delay caused by retransmissions. Note that retransmissions of video data packets may also result in a short-term video distortion due to the delayed delivery of the video packets. Moreover, the overhead of ACK transmissions might significantly deteriorate the system performance. Accordingly, No Acknowledge (no-ACK) mode is typically employed for video streaming in ECMA-387, and we also consider no-ACK mode in our work.

### 2.2.5 Latency of compressed and uncompressed video streaming

As we have mentioned above, lots of Wi-Fi-based commercial wireless real-time display products based on the compressed streaming have been introduced and it is reported that some of solutions sometimes experience a significant latency as much as users can recognize depending on the hardware resources [5]. We measure the latency of a commercial wireless real-time display solution by comparing the screens of the transmitter (Samsung Galaxy Note 10.1 [6]) and the receiver (Samsung AllShare Cast

dongle [6]) which are connected by Miracast [4]. The resolution of the screen is  $1280 \times 800$  (WXGA). To measure the latency, the stopwatch application is used. By comparing the time difference between the screens of the transmitter and receiver which display the time of stopwatch at the same time, we measure the latency between the transmitter and the receiver. In the results, it is shown that the mean latency is about 170 ms with a standard deviation of 140 ms, and the maximum latency is about 600 ms. Actually, a human can recognize the latency especially in the interactive and/or dynamic screen environments.

To compare the latency between compressed and uncompressed video streaming, we evaluate the latency of uncompressed video by the simulation. The resolution of video is assumed as  $1280 \times 720$  p30, and we assume that the display latency is about 10 ms. Fig. 2.5 shows the latency of compressed and uncompressed video streaming. In the case of *Efficiently allocated* scheme which indicates that the resource is allocated considering the video source rate and the used MCS (e.g., A1 or A9 in Table 2.1), the higher MCS has longer latency since the size of the allocated resource of higher MCS is smaller than that of lower MCS. Meanwhile, in the case of *Fully allocated* scheme which indicates that the resource is fully allocated, the higher MCS has shorter latency since the video data can be transmitted faster with higher MCS. As a result, uncompressed video streaming achieves significantly lower latency ( $< 50$  ms) than the compressed video streaming.

## 2.3 ePSNR-Based Link Adaptation Policies

Peak Signal-to-Noise Ratio (PSNR) is a widely-accepted metric to evaluate the quality of video streaming [20] by measuring the distortion factor of the received data compared with the original data. Using PSNR for the link adaptation of video streaming,



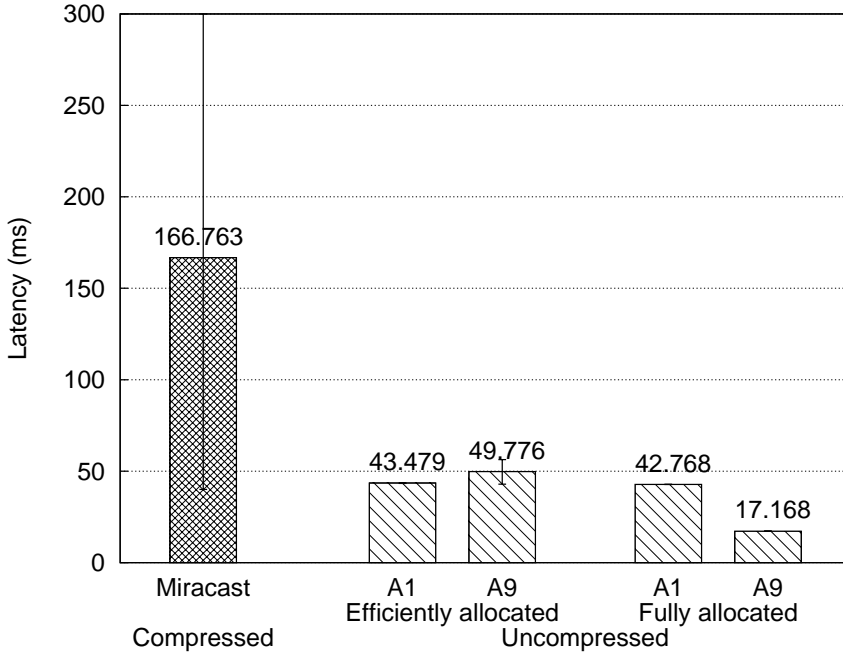


Figure 2.5: Latency of compressed and uncompressed video streaming.

one can provide high-quality video by keeping the PSNR threshold [21]. However, it is difficult for both transmitter and receiver to calculate the PSNR value since the evaluation of PSNR requires both original and received video data. Especially the transmitter cannot assess the PSNR value prior to the video frame transmission because it cannot know the possible distortion due to the channel error on the video data during the transmission. Thus, PSNR can be hardly used by the transmitter for the link adaptation. Of course, the receiver also cannot assess how much the received video data are damaged either because it has no knowledge about the original video data.

Since the transmitter cannot assess the actual PSNR value, in this chapter we introduce a variable, called *expected Peak Signal-to-Noise Ratio (ePSNR)*, to estimate the received quality of the video streaming at the transmitter side in a given wireless

10 octets	9 octets	$L_1$ octets	...	$L_N$ octets
MAC header	Beacon parameters	Information Element 1	...	Information Element N

(a) Beacon frame format

1 octet	1 octet	2 octets	2 octets
Element ID	Length(=4)	Transmitter Address	Channel State Information (SNR)

(b) Proposed channel state information element format

Figure 2.6: The formats of beacon frame and channel state information element.

channel environment. ePSNR utilizes the channel state information, i.e., the average Signal-to-Noise Ratio (SNR), fed back by the receiver in order to approximate the PSNR value experienced at the receiver side. The wireless channel of 60 GHz band is generally known to be quasi-static, i.e., the state of the wireless channel does not vary within a superframe duration, due to the frequency characteristics of 60 GHz band [22]. Under this assumption, the receiver sends the channel state information via a beacon frame per superframe. If the channel state information is not changed from the previous value, the receiver can skip sending the channel state information.

Fig. 2.6 shows the formats of a beacon frame and the proposed channel state information element (IE). The channel state information element consists of 6 bytes, including the information element ID, the length of IE, the transmitter's address, and the SNR value for representing the quantized value of the average SNR (in dB) with 65536 levels. The length of a beacon slot is fixed as  $21.3 \mu s$  and the transmission time of a beacon frame cannot exceed  $mMaxBeaconLength$ , i.e.,  $16.59 \mu s$ , considering the guard time between the beacon slots [14]. This  $mMaxBeaconLength$  allows the transmission of a beacon frame with the length up to about 440 bytes. The length of

a beacon frame could be variable depending on the conveyed information elements. The most of information elements, e.g., DRP IE and DRP availability IE, are selectively included in the beacon frame and the length of each information element can be also variable. Basically, the maximum length of a beacon frame is large enough to include the additional information, i.e., channel state information, and hence, carrying the channel state information in the beacon frame is not a significant overhead. Moreover, this channel state information does not need to be in every beacon frame.

The transmitter, which overhears the beacon frame of the receiver, then uses this channel information feedback in order to estimate the ePSNR of the receiver. From the channel state information, i.e., the average SNR, the transmitter first estimates bit error rate (BER) values due to the channel error for each MCS. From these BER values, the transmitter can estimate the ePSNR values for each MCS, and then decides the transmission rate (i.e., MCS) based on the estimated ePSNR. This MCS selection procedure based on the channel state information is done every superframe period and the transmitter transmits all the video packets via the selected MCS. If the fed-back channel state information is not changed from the previous channel state information, the MCS selection procedure can be skipped.

### 2.3.1 ePSNR

The PSNR of a received video frame can be represented as the following equation when the RGB video color model is used.<sup>5</sup>

$$PSNR = 20 \log_{10} \left( \frac{MAX}{\sqrt{MSE}} \right), \quad (2.1)$$

---

<sup>5</sup>Note that HDMI also supports the RGB video color model.

where  $MAX$  and  $MSE$  are the maximum possible pixel value and the mean squared error of one video frame, respectively.  $MAX$  can be determined by

$$MAX = 2^{n_R} - 1, \quad (2.2)$$

where  $n_R$  is the number of bits to represent each color in the RGB model, so the color depth is  $3n_R$  (in number of bits). When  $N$  is the number of pixels per video frame,  $MSE$  is defined by

$$MSE = \frac{1}{N} \sum_{i=1}^N \frac{(R_i - R'_i)^2 + (G_i - G'_i)^2 + (B_i - B'_i)^2}{3}, \quad (2.3)$$

where  $R_i$ ,  $G_i$ , and  $B_i$  are the data of the original red, green, and blue colors of the  $i$ -th video pixel, respectively, and  $R'_i$ ,  $G'_i$ , and  $B'_i$  are the data of the received red, green, and blue colors of the  $i$ -th video pixel, respectively.

A high PSNR value implies that errors rarely occur in video transmission, and a low PSNR value implies that the distortion of the received video is substantial. If no error occurs in a video transmission, the PSNR value should be infinity, as  $MSE = 0$  in Eq. (2.1).

Assuming that the original video data pattern follows the uniform distribution and  $N$  is large enough,  $MSE$  of the color data can be approximated as

$$MSE \approx E[(I - K)^2], \quad (2.4)$$

where  $I$  and  $K$  are the original data of a pixel's color, which is uniformly distributed over  $[0, 2^{n_R} - 1]$ , and the distorted data from the original data, respectively.

MSBs and LSBs of a video pixel are transmitted by different MCSs with UEP, and hence, the Bit Error Rates (BERs) of MSBs and LSBs are also dependent on the adopted MCSs. To calculate  $E[(I - K)^2]$ , we define  $I_k$  and  $K_k$ , which represent the original and received data of  $k$  bits, respectively. That is,  $I_k$  has a uniform distribution over  $[0, 2^k - 1]$ .

If the MSB, i.e., the  $k$ -th bit of  $I_k$ , is erroneous,  $(I_k - K_k)^2$  is equal to either  $(-2^{k-1} + I_{k-1} - K_{k-1})^2$  or  $(2^{k-1} + I_{k-1} - K_{k-1})^2$  with probability  $1/2$ . On the other hand, if the MSB, i.e., the  $k$ -th bit of  $I_k$ , has no error,  $(I_k - K_k)^2$  is equal to  $(I_{k-1} - K_{k-1})^2$ . Therefore,  $E[(I_k - K_k)^2]$  is represented as

$$\begin{aligned}
E[(I_k - K_k)^2] &= \frac{1}{2}E[(2^{k-1} + I_{k-1} - K_{k-1})^2] \cdot BER_k \\
&\quad + \frac{1}{2}E[(-2^{k-1} + I_{k-1} - K_{k-1})^2] \cdot BER_k \\
&\quad + E[(I_{k-1} - K_{k-1})^2] \cdot (1 - BER_k) \\
&= (2^{k-1})^2 \cdot BER_k + E[(I_{k-1} - K_{k-1})^2] \\
&= \sum_{i=0}^{k-1} (2^{2i} \cdot BER_{i+1}),
\end{aligned} \tag{2.5}$$

where  $BER_i$  is the BER of the  $i$ -th bit.

Now, since the length of  $I$  is  $n_R$  in Eq. (2.4), ePSNR can be represented as follows:

$$ePSNR = 20 \log_{10} \left( \frac{2^{n_R} - 1}{\sqrt{\sum_{i=0}^{n_R-1} (2^{2i} \cdot BER_{i+1})}} \right). \tag{2.6}$$

### 2.3.2 PSNR-based Link Adaptation

For the stable video streaming service in ECMA-387 MAC, a transmitter reserves the MASs that can be periodically used without interference. Note that the low-rate MCS can provide reliable transmission at the cost of long transmission time, while the high-rate MCS can shorten the packet transmission time while being prone to channel errors. If the size of reserved MASs is unlimited, the best option for the transmitter to guarantee the reliability of the video stream is using the most reliable MCS that consumes the longest transmission time. However, it is not the case in reality; the size of reserved MASs is limited by the network environments, e.g., the number of users

sharing the wireless medium and unusable MASs due to the interference. Moreover, even in the case that a device can use all the MASs exclusively, sometimes, the higher MCS might be required due to the amount of video data. This requires the transmitter to find the most appropriate MCS at a given channel condition and the length of reserved MASs via an efficient link adaptation.

It should be noted that the 60 GHz wireless channel is relatively static, i.e., the channel variation is not severe [22], and most of the MAC standards at the 60 GHz band support protocols for the channel state feedback under the assumption that the receiver can intelligently estimate the channel state. The UEP operation is also helpful for the transmitter since the transmitter has more candidates for the MCS selection using the UEP MCSs—to this end, we assume that the operation of UEP in Fig. 2.4 is adopted in the MAC layer. We further assume that the employed video format of the application traffic is known at the MAC layer. In this chapter, we propose two link adaptation policies to ensure acceptable video quality by finding the proper MCS for MSBs and LSBs through the estimated ePSNR parameter. In the following, the amount of reserved MASs within a single superframe is referred to as the *allocated resources* (in seconds).

### **Link Adaptation for Maximizing PSNR**

Under this link adaptation policy, the transmitter finds the MCS that provides the maximum ePSNR value with given allocated resources. The objective function can be represented as

$$\arg \max_{\text{MCS}_{\text{UEP}}} \text{ePSNR}(\text{MCS}_{\text{UEP}}). \quad (2.7)$$

Here,  $\text{MCS}_{\text{UEP}}$  includes both possible EEP MCSs and MCS combinations for UEP with different  $n_M$ 's (i.e., the number of MSBs).

Because the required resources for the selected MCS should not exceed the allocated resources, the MCS should satisfy the following constraint:

$$d_u(\text{MCS}_{\text{UEP}}) < T_{\text{allocate}}, \quad (2.8)$$

where  $d_u(\text{MCS}_{\text{UEP}})$  is the required resources per superframe using  $\text{MCS}_{\text{UEP}}$ , and  $T_{\text{allocate}}$  is the length of the allocated resources per superframe.  $d_u(\text{MCS}_{\text{UEP}})$  can be derived as follows.

$$d_u = \begin{cases} \left(T_O + \frac{L_H + X}{\text{MCS}_{\text{EEP}}}\right) \cdot Y, & \text{for EEP,} \\ \left(2 \cdot T_O + \frac{L_H + \frac{X \cdot n_L}{n/3}}{\text{MCS}_{\text{LSB}}} + \frac{L_H + \frac{X \cdot n_M}{n/3}}{\text{MCS}_{\text{MSB}}}\right) \cdot Y, & \text{for UEP,} \end{cases} \quad (2.9)$$

where  $T_O$ ,  $L_H$ ,  $X$ , and  $Y$  are the time overheads for transmitting a single packet, the aggregated length of HDMI PAL, MAC, and PHY layer headers, the length of a single packet, and the number of packets transmitted within a single superframe, respectively. Here,  $X \times Y$  represents the size of video data transmitted per superframe.

The objective of this link adaptation policy is to maximize the estimated average PSNR by selecting the optimal MCS that (1) achieves the maximum PSNR value; and (2) satisfies the constraint given in Eq. (2.8). As the number of available MCSs is limited and the number of MSBs (i.e., bits 1 to  $n_R$ ) is also finite, finding the optimal MCS via exhaustive searching is not a computationally challenging problem. However, it is also possible to make a table of the optimal MCS versus SNR at the given allocated resources by using the exhaustive search, and then use the table during the run time to reduce the computational complexity. After finding the optimal MCS, the device will update the  $T_{\text{allocate}}$  value with  $d_u(\text{selectedMCS}_{\text{UEP}})$  to reduce the unused resources.

### Link Adaptation for Minimizing Allocated Resources

Minimizing the wireless resource that is consumed by each device is an important issue for improving the system capacity in multi-user networks, since the remaining wireless

resources provide a chance to accommodate additional devices in the network. In this subsection, we propose a link adaptation policy that minimizes the amount of allocated resources, while maintaining a certain level of PSNR.

The objective function for this link adaptation policy is given by

$$\arg \min_{\text{MCS}_{\text{UEP}}} d_u(\text{MCS}_{\text{UEP}}), \quad (2.10)$$

with the following constraints:

$$d_u(\text{MCS}_{\text{UEP}}) < T_{\text{allocate}}, \quad (2.11)$$

and

$$\text{ePSNR}(\text{MCS}_{\text{UEP}}) > \text{PSNR}_{\text{Threshold}}. \quad (2.12)$$

In order to minimize the required resources per superframe,  $d_u$ , the transmitter selects the highest-rate MCS with the smallest  $d_u$ , while maintaining the PSNR under the threshold. Hence, the transmitter attempts to find the MCS that minimizes  $d_u$ , among the MCSs that achieve the target PSNR. If such an MCS is not available due to the bad channel condition, the transmitter selects the MCS achieving the highest PSNR value out of the MCSs that satisfy  $d_u < T_{\text{allocate}}$ . This approach yields the PSNR values that exceed the threshold in most cases, while minimizing the amount of the wireless resources that are used by the transmitters. Here, by updating the  $T_{\text{allocate}}$  value with  $d_u(\text{selectedMCS}_{\text{UEP}})$ , the allocated resources are minimized.

## 2.4 Performance Evaluation

In this section, we evaluate the performance of ePSNR via the comparison with the measured PSNR value of the simulation. Through this evaluation, we confirm that the derived ePSNR value is very closely matched with the measured PSNR. Using this



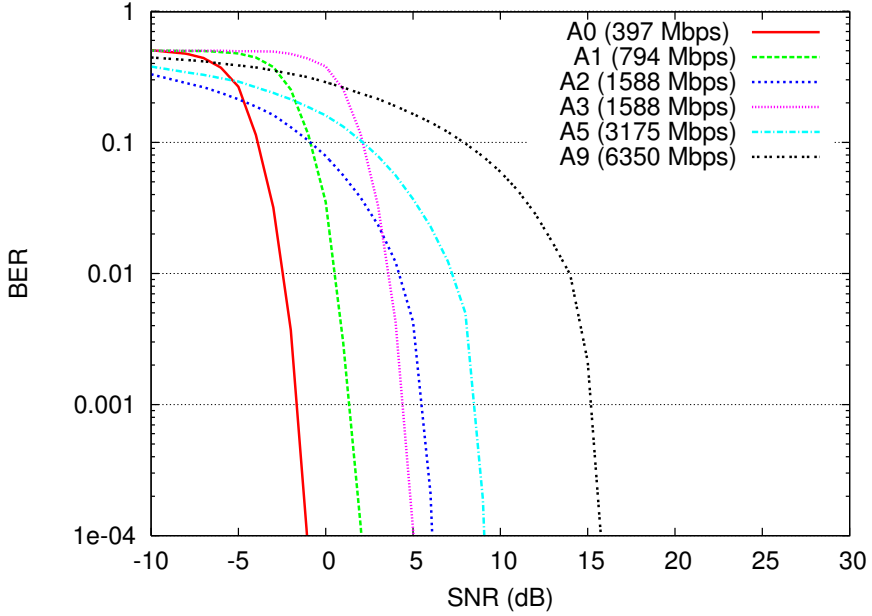


Figure 2.7: BER of MCSs in ECMA-387.

ePSNR, we evaluate the performance of our link adaptation policies by comparing them with other conventional link adaptation policies.

### 2.4.1 Evaluation of ePSNR

We first verify the validity of the proposed ePSNR by comparing with the measured PSNR from simulations using real video traces. For the evaluation of ePSNR with a measured PSNR value, we consider the MCSs for type A devices of ECMA-387 standard in Table 2.1, and their BER curves in Fig. 2.7. Six different MCSs are considered, which are based on mandatory Single Carrier Block Transmission (SCBT) modulation schemes. MCS A0 is the lowest and the most robust transmission rate, which uses Time Domain Spreading Factor (TDSF) of 2, and MCS A9 is the highest and the least

Table 2.1: MCSs for Type A Devices in ECMA-387

Type	Data Rate (Gbps)	Modulation	Coding	CC Code Rate	TDSF
A0	0.397	BPSK	RS&CC	1/2	2
A1	0.794	BPSK	RS&CC	1/2	1
A2	1.588	BPSK	RS	1	1
A3	1.588	QPSK	RS&CC	1/2	1
A5	3.175	QPSK	RS	1	1
A9	6.350	16-QAM	RS	1	1

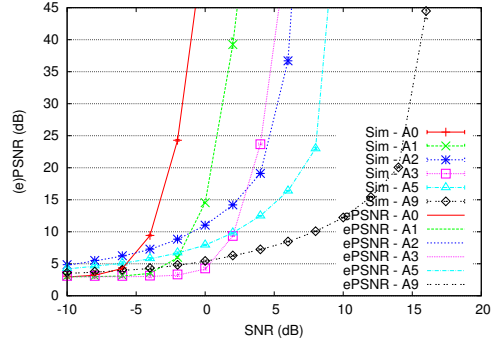
robust transmission rate among the MCSs defined in ECMA-387.

In Fig. 2.7, we observe that the BER patterns of MCSs A0, A1, and A3 with rate 1/2 Convolutional Code (CC) are different from those of MCSs A2, A5, and A9 that do not adopt CC. For the simulation, a 30 second video clip with video format of  $1280 \times 720$  p30 (referred to as 720p30), one of EDTV/HDTV video formats, is used.<sup>6</sup> We use the RGB color model and the color depth is assumed to be  $(3n_R) = 24$  (bits/pixel). That is, the data length of each color, i.e., Red, Green, and Blue, is 8 bits, and the number of MSBs (i.e.,  $n_M$ ) for UEP is between 1 and 7. We generate random error patterns according to the BER of each MCS, and measure the PSNR by comparing the original data and distorted data of each video frame (900 video frames in total).

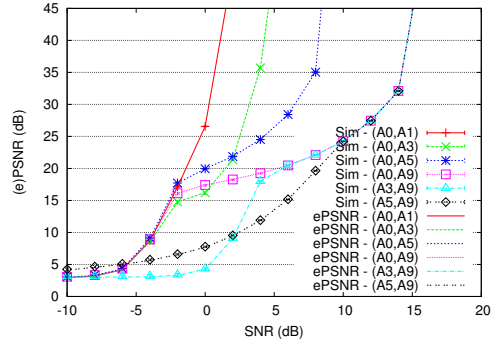
Fig. 2.8 shows the results of ePSNR that is calculated from Eq. (2.6) and the simulation results of the measured PSNR of EEP and UEP MCSs together. Fig. 2.8(a) shows the results of EEP MCSs, and Figs. 2.8(b) and 2.8(c) show the results of UEP MCSs when the numbers bits in MSBs are 2 and 4, respectively. In the legend of Figs. 2.8(b) and 2.8(c), the first and the second MCSs indicate the MCSs used for

---

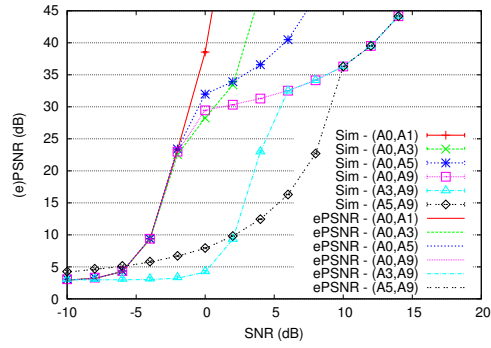
<sup>6</sup>p30 stands for the video frame rate of 30 frames per second with progressive scanning.



(a) EEP



(b) UEP with the number of MSBs ( $n_M$ ) = 2



(c) UEP with the number of MSBs ( $n_M$ ) = 4

Figure 2.8: Comparison of ePSNR from analysis and PSNR from simulations.

MSBs and LSBs, respectively. The ePSNR values derived from Eq. (2.6) are presented in solid lines, and the measured PSNR values obtained from the simulations are presented by dots. In fact, for a given SNR, the minimum, maximum, and average PSNR values measured out of 900 video frames are shown while these three values are almost the same. This is due to the fact that a video frame is composed of 921600 ( $= 1280 \times 720$ ) pixels, which is enough for representing the randomness of the pixels. It is shown that the derived ePSNR values well match with the average PSNR values, and this validates the accuracy of our formulation of ePSNR. Accordingly, we can use this ePSNR as a metric for the MCS selection based on this observation.

From Figs. 2.8(b) and 2.8(c), it is also found that the MCS of MSBs determines the PSNR performance in the low SNR region, and the MCS of LSBs does in the high SNR region. For example, in Fig. 2.8(b), (A0,A1), (A0,A3), (A0,A5) and (A0,A9) perform almost the same when SNR is under  $-2$  dB, and (A0,A9), (A3, A9) and (A5,A9) perform almost the same when SNR is above 10 dB. This is due to the fact that at least MSBs need to be successfully delivered in order to provide nominal video quality in the low SNR region, and selecting an appropriate MCS of LSBs can further enhance the PSNR performance in the high SNR region.

Figs. 2.8(b) and Fig. 2.8(c) show that the PSNR performance is getting better in the high SNR region while the PSNR performances are almost the same in the low SNR region, when the number of MSBs increases. For example, in the case of (A3,A9), the PSNR performances of  $n_M = 2$  and  $n_M = 4$  when SNR is under 2 dB are almost the same. However, the case of  $n_M = 4$  achieves over 10 dB better PSNR performance compared with the case of  $n_M = 2$  when SNR is above 5 dB. Fig. 2.8(b) and Fig. 2.8(c) also show that the derived ePSNR values well match with the average PSNR values.

Fig. 2.9 demonstrates the measured PSNR values depending on the BER of MSBs (i.e.,  $BER_{MSB}$ ), BER of LSBs (i.e.,  $BER_{LSB}$ ), and the number of MSBs (i.e.,  $n_M$ ).

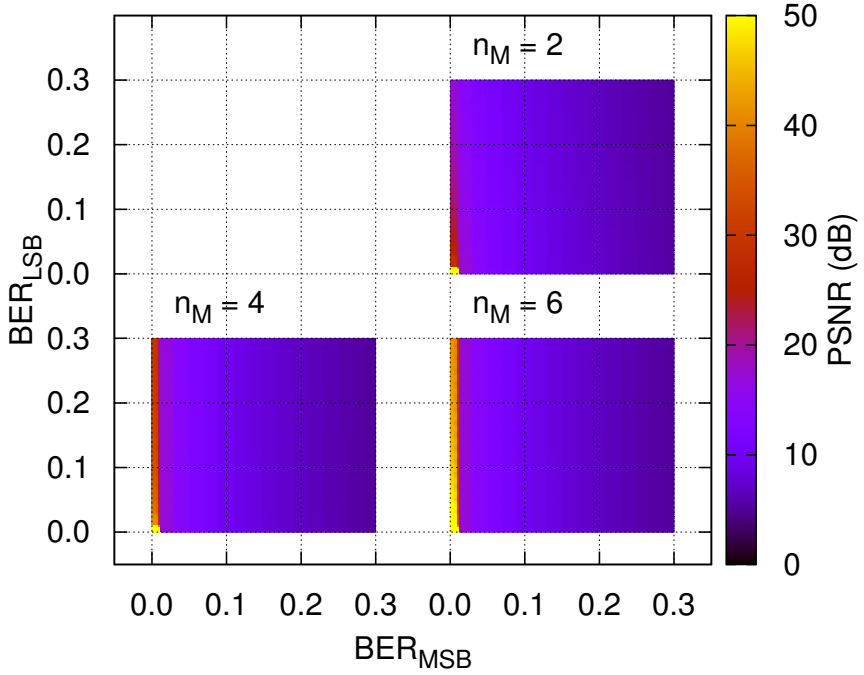


Figure 2.9: Effectiveness of UEP.

The video quality is mainly decided by  $BER_{MSB}$  rather than  $BER_{LSB}$ .  $BER_{LSB}$  affects the video quality only in the very low  $BER_{MSB}$  region. As  $n_M$  increases, the overall video quality can increase in the low  $BER_{MSB}$  region regardless of  $BER_{LSB}$ . Therefore, The UEP which applies different MCSs to MSBs and LSBs can maintain the video quality in the sense of reducing the error rate of MSBs. However, for the stronger protection, more resource is required with the larger  $n_M$  and the more robust MCS of MSBs.

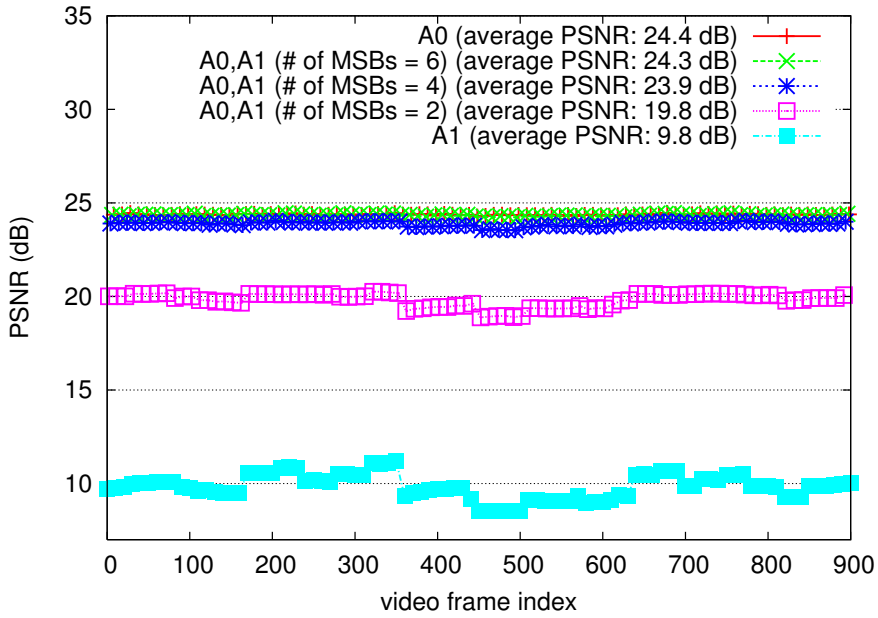


Figure 2.10: Measured PSNR values when  $\text{SNR} = -2.5$  dB.

Fig. 2.10 demonstrates the measured PSNR values of all 900 video frames for MCSs A0, A1, and UEP MCS combination (A0,A1) with various numbers of MSBs when SNR is  $-2.5$  dB. Obviously, MCS A0, which has the best BER performance, presents the highest PSNR values, while MCS A1 shows lower PSNR values. In case of UEP, as the number of MSBs increases, the PSNR gets closer to the PSNR of MCS A0. In case when the number of MSBs is 2 or 4 in UEP, the PSNR value is almost the same as the value of MCS A0. Accordingly, UEP makes more efficient video streaming with the quite similar video quality in a given environment.

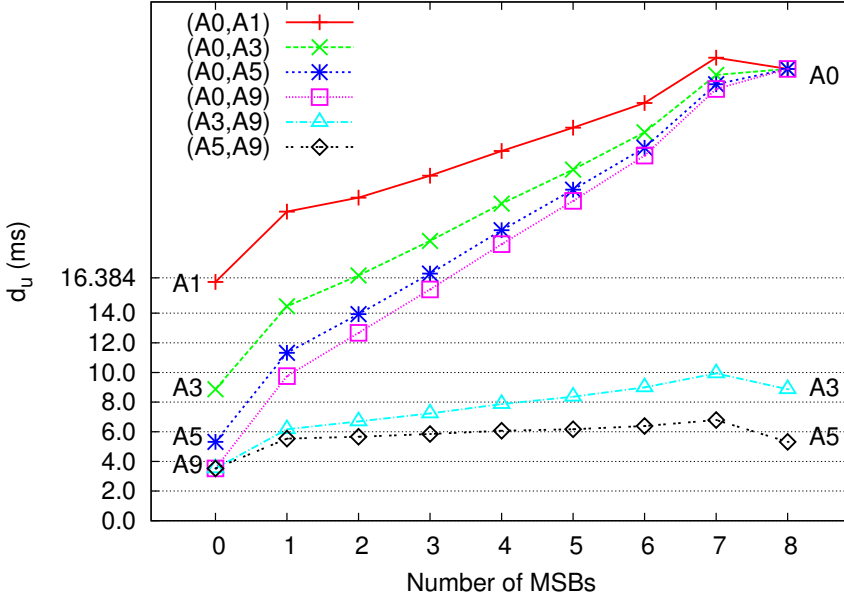


Figure 2.11: Amount of required resources per superframe for 720p30 video streaming.

## 2.4.2 Performance of Link Adaptation

Fig. 2.11 shows the amount of allocated resources per superframe (i.e.,  $d_u$ ), for 720p30 video streaming as the number of MSBs increases for 6 different MCS combinations. Here, we assume that one horizontal line of a video frame is packetized into a single packet. In case of 720p30 video, each packet length is 3840 bytes ( $= 1280 \times 24$  bits) since there are 1280 pixels along a horizontal line of a video frame, and 720 packets are transmitted for a video frame since there are 720 pixels along a vertical line of a video frame. Two extreme cases, i.e., the number of MSBs equal to 0 and 8, represent EEP cases. That is, when the number of MSBs is zero, all the data is transmitted by using the MCS of LSBs, and when the number of MSBs is 8, all the data is transmitted

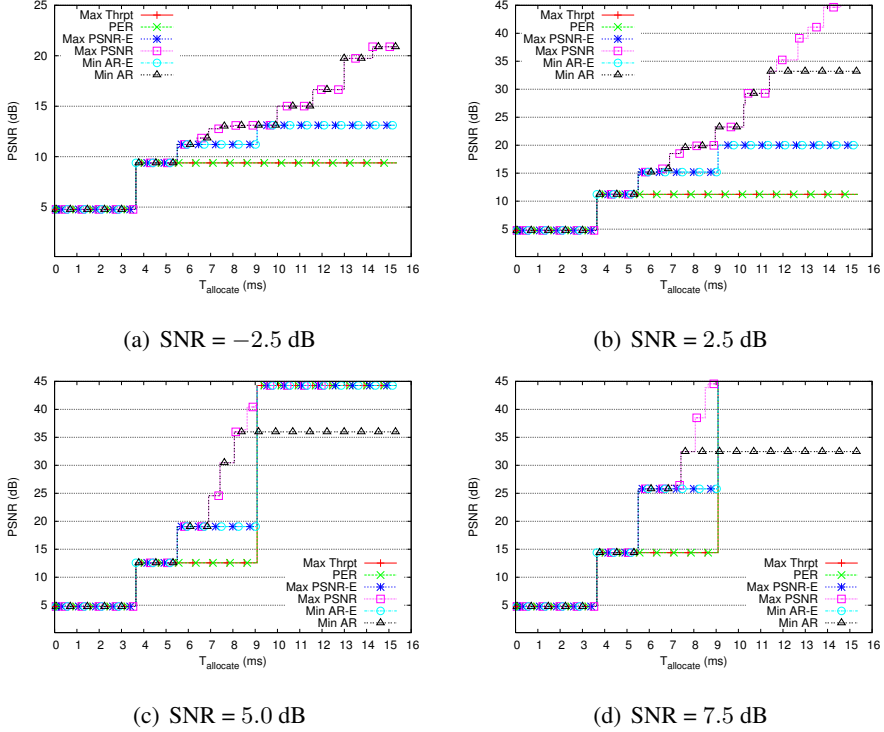


Figure 2.12: PSNR performance for various link adaptation policies.

by using the MCS of MSBs.

We observe that as the number of MSBs increases, the amount of required resources increases because the MCS of MSBs requires more resources than the MCS of LSBs. However, we see that EEP cases require relatively smaller resources compared with UEP cases because UEP requires extra protocol overheads, e.g.,  $2T_O$  instead of  $T_O$  in Eq. (2.9). Note that the maximum  $d_u$  value is 16.384 ms, which is the super-frame duration. This implies that the MCS combinations corresponding to the points above the 16.384 ms line cannot be actually used for the link adaptation at all. For example, MCS A0 cannot be used for 720p30 video streaming, even though the device can occupy all the resource (i.e., MASs) exclusively.



Table 2.2: Relationship between PSNR and MOS [20]

PSNR (dB)	MOS
$> 37$	5 (Excellent)
$31 - 37$	4 (Good)
$25 - 31$	3 (Fair)
$20 - 25$	2 (Poor)
$< 20$	1 (Bad)

From Fig. 2.8 and Fig. 2.11, we find that the video quality can be enhanced through the proper MCS selection in a given channel environment. For example, when SNR is equal to  $-2$  dB, the case of UEP MCS (A0,A9) with  $n_M = 2$  shows the better video quality (i.e., PSNR) with the smaller  $d_u$  than the case of EEP MCS A1. Therefore, the link adaptation for the proper MCS selection is important for both video quality and resource efficiency.

We now compare the PSNR performance of the proposed and other conventional link adaptation policies. In the link adaptation policies with UEP, all the possible MCS combinations are considered. That is, we consider 6 EEP MCSs and 30 UEP MCSs for the MCS selection. Fig. 2.12 shows the results of PSNR for the different link adaptation policies in different SNR environments. The following six link adaptation policies are compared.<sup>7</sup>

- *Max Thrpt*: a link adaptation policy for maximizing the throughput performance as many other conventional link adaptation policies do, for given allocated re-

---

<sup>7</sup>Based on our survey, our work is the first research on the link adaptation policy of the uncompressed video streaming. The link adaptation of the compressed video streaming is not considered for the comparison, because the video quality of compressed video heavily depends on the video coding parameters, e.g., coding rate, coding type, and codec.

sources,  $T_{\text{allocate}}$ .

- *PER*: a link adaptation policy, which selects the highest-rate MCS which achieves Packet Error Rate (PER) less than 0.1 for given allocated resources,  $T_{\text{allocate}}$ .
- *Max PSNR*: our proposed link adaptation policy for maximizing PSNR for given allocated resources,  $T_{\text{allocate}}$ , as presented in Section 2.3.2.
- *Max PSNR-E*: *Max PSNR* considering only EEP MCSs.
- *Min AR*: our proposed link adaptation policy for minimizing the allocated resources with a given upper bound of the allocated resources  $T_{\text{allocate}}$  and the PSNR threshold  $\text{PSNR}_{\text{Threshold}}$ , as presented in Section 2.3.2. Based on the relationship between PSNR and Mean Opinion Score (MOS) [20] in Table 2.2, and assuming MOS of 4 as acceptable video quality, we adopt  $\text{PSNR}_{\text{Threshold}} = 31$  dB.
- *Min AR-E*: *Min AR* considering only EEP MCSs.

In Fig. 2.12, the PSNR performance increases as the size of  $T_{\text{allocate}}$  increases in all SNR ranges, because more robust MCSs can be used with more allocated resources. However, *Max Thrpt* and *PER* policies have worse PSNR performance than the proposed policies because those do not care about the received PSNR. *Max PSNR-E* and *Min AR-E* perform worse than *Max PSNR* and *Min AR* since the number of available MCSs is limited. Figs. 2.12(b), 2.12(c), and 2.12(d) show that *Min AR* performs worse than *Max PSNR* in case of high allocated resources while *Min AR* still supports acceptable video quality.

Fig. 2.13 shows the minimum of allocated resources with different  $\text{PSNR}_{\text{Threshold}}$  values for *Min AR(-E)* policies. Each device requires less amount of allocated resources for video transmission as the SNR increases, since higher-rate MCSs become

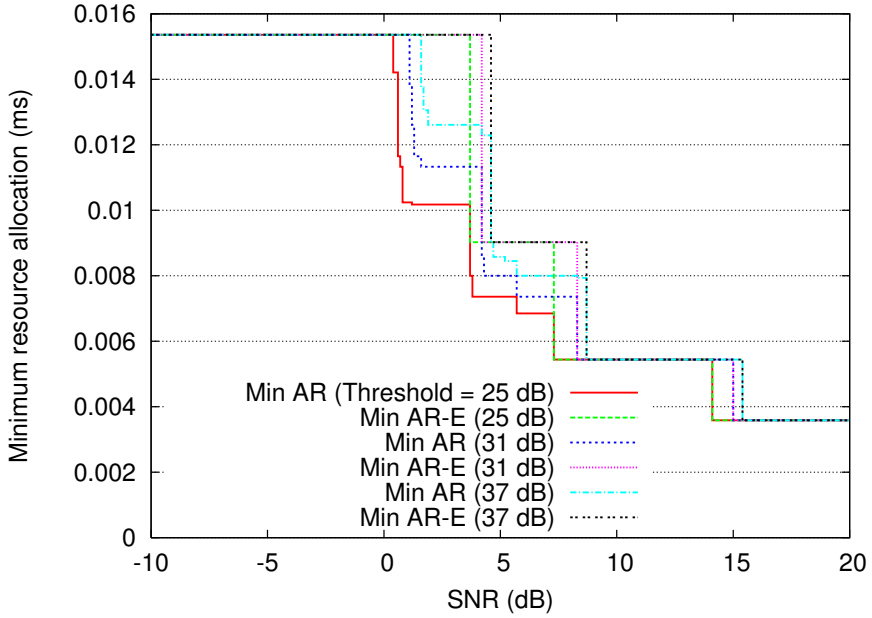


Figure 2.13: Minimum resource allocation for *Min AR(-E)*.

available. Also low  $\text{PSNR}_{\text{Threshold}}$  values moderate the requirements for the reliable video streaming, and hence, can further reduce the allocated resources. *Min AR* policy has more chances to reduce the allocated resources than *Min AR-E* policy since the set of available MCSs is extended by including UEP MCSs.

Fig. 2.14 compares the snapshots of the video clip for two different link adaptation policies, i.e., *Max Thrpt* policy in Fig. 2.14(a) and *Max PSNR* policy in Fig. 2.14(b), when SNR is equal to 5 dB and  $T_{\text{allocate}}$  is equal to 8 ms. By selecting appropriate MCSs, as demonstrated in Fig. 2.14(a), the proposed link adaptation policy achieves good video quality while the snapshot in Fig. 2.14(b) is distorted enough to distinguish the distortion by the eye.



(a) *Max Thrpt* policy (PSNR = 12.6 dB)



(b) *Max PSNR* policy (PSNR = 30.5 dB)

Figure 2.14: Snapshots at SNR = 5 dB and  $T_{\text{allocate}} = 8$  ms.

## 2.5 Summary

In this chapter, we propose new link adaptation policies for high-quality uncompressed video streaming at 60 GHz band. For the better link adaptation, we adopt UEP schemes

and develop a new parameter, i.e., ePSNR. ePSNR estimates the video quality in the error-prone wireless channel environments, and the proposed link adaptation policies select the appropriate MCSs using this ePSNR value. Through the proposed link adaptation policies, we can provide high video quality and efficient resource allocation at the same time.

Though we in this chapter consider uncompressed video, the size of video source is still a big constraint for reliable video streaming. Adaptation of video source format is worth considering for the future work in order to resolve this problem. By adapting both video source format and MCS, more efficient resource allocation with acceptable video quality is expected.

Nowadays, the uncompressed video streaming is considered even in Wi-Fi network, via the emerging Wi-Fi system, i.e., 802.11ac [29], which can provide very high throughput (up to nearly 7 Gbps). We plan to extend our work to this emerging Wi-Fi system and other 60 GHz systems, too.

## **Chapter 3**

# **Reliable Video Multicast over Wi-Fi Networks with Co-ordinated Multiple APs**

### **3.1 Introduction**

There have been increasing R&D efforts in utilizing smartphones' Wi-Fi as smartphone user population and applications rapidly expand. In particular, the emergence of high-speed Wi-Fi, such as IEEE 802.11n [28] and IEEE 802.11ac [29], has enabled high-quality and bandwidth-hungry applications such as video streaming to/from smartphones. Moreover, there exist applications, such as screen-sharing and TV broadcast, in which multiple users need the same video. When the same video data needs to be delivered to multiple receivers, multicast that transmits the data to multiple receivers only once is more efficient than unicasting the same data to each receiver individually. IEEE 802.11 [28] standard supports multicast transmission, in which a transmitter sends a packet to multiple receivers with a single transmission. This efficiency of multicast triggered a wide investigation of video multicast in Wi-Fi systems, in which the video data is delivered to multiple receivers via multicast transmissions.

However, error control with Automatic Repeat reQuest (ARQ) is not feasible in multicast, since there is no acknowledgement of requesting packet-retransmission. Therefore, multicast is inherently vulnerable to the transmission failures caused by wireless channel errors. To overcome this deficiency, application-layer packet-level FEC (AL-FEC) has been proposed widely [30, 31, 50]. In AL-FEC, the FEC encoding and decoding are performed in the application layer, which can help the receiver recover the erased data packets by exploiting the additional parity packets that are generated from data packets by FEC encoder. AL-FEC is helpful, especially in multicast scenarios, since the additional parity packets can compensate the unreliable nature of multicast. Moreover, in most cases, although the lost packets of different users could be different, by utilizing AL-FEC, all such different lost packets can be recovered by the same parity packets.

Most of existing research on video multicast using AL-FEC considers the single AP environment. By extending the single AP environment to a multi-AP environment, we propose more reliable video multicast schemes, in which a video multicast user can be served by multiple coordinated neighboring APs. In hot-spot or enterprise networks where multiple APs are scattered and each AP transmits a large number of video packets to serve its associated users, the users located at boundaries might receive a very poor video streaming service even if AL-FEC is adopted. In order to enhance the performance of video streaming for users, especially those at cell edges, the users are made to (over)hear the packets from neighboring APs.

With the help of AL-FEC and the coordination of multiple APs, each AP can transmit (1) entirely different or (2) partially different FEC-encoded packets. As a result, the users will receive more FEC-encoded packets, thus increasing the probability of successfully decoding the video packets. We also propose a resource-allocation algorithm for the FEC-code rate adaptation. Video multicast with a robust FEC code rate

can enhance the AP's coverage, while requiring more resource since the AP transmits more parity packets for the same video packets. Since the wireless resource for video multicast is limited, decreasing the FEC-code rate of one AP will increase other APs' FEC code rates. For example, by letting a specific AP that covers more users transmit more parity packets and by reducing the resource of the AP that serves fewer users, we can serve more users with satisfactory video quality. In this chapter, we propose an FEC code rate adaptation algorithm to enhance the overall multicast service coverage. In addition, we propose a method for estimating the delivery ratio after FEC decoding. The proposed FEC code rate adaptation algorithm increases the number of users satisfied with the video multicast service by adjusting each AP's FEC code rate. By utilizing the remaining resources, it also tries to improve the users' perceived video quality further beyond the satisfaction level.

The contributions of this work are summarized as follows:

- To our best knowledge, this is the first work to extend AL-FEC based reliable video multicast to multiple AP environments, thus exploiting spatial and time diversities.
- By coordinating multiple APs' transmissions of FEC-encoded packets, we further enhance the diversity gain.
- We propose an FEC code rate adaptation algorithm, by which more multicast users are served with satisfactory video quality.
- An estimation method of video packet delivery ratio after FEC decoding is developed.
- The performance of the proposed multicast schemes is extensively investigated via both simulation and experimentation.



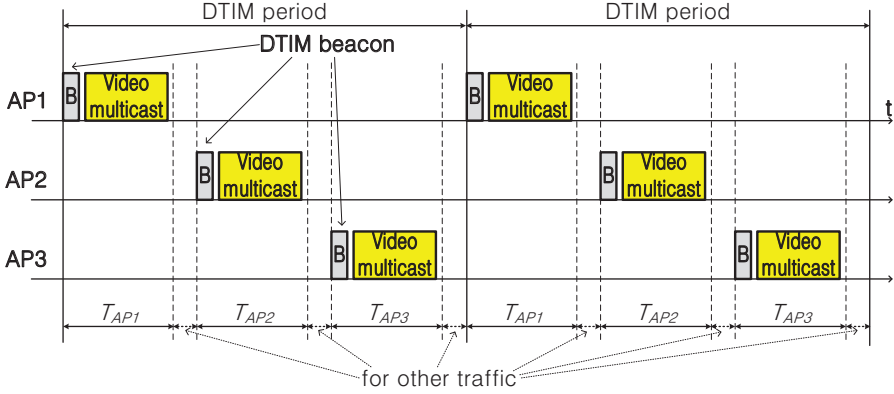


Figure 3.1: Illustration of time-slotted video multicast by multiple APs.

The rest of this chapter is organized as follows. Section 3.2 describes the system environment under consideration. Section 3.3 presents a new reliable video multicast protocol with coordinated multiple APs, and introduces its detailed procedure with AL-FEC. An FEC code rate adaptation algorithm is proposed in Section 3.4. Section 3.5 evaluates the performance of the proposed video multicast protocol, finally, the chapter concludes with Section 3.6.

## 3.2 System Environments

### 3.2.1 Time-Slotted Multicast

We first assume that users receive packets from all neighboring APs. This can be made possible by enabling the users to overhear or forcing all APs to use the same Basic Service Set Identification (BSSID) (as implemented by [33]) so that users can communicate with multiple APs with a single association.

Coordinated multiple APs then multicast their packets in a time slotted manner as illustrated in Fig. 3.1, where there APs operate on the same channel. Such time slotted

multicast avoids collision among multicast packets from different APs, and users at the intersection of neighboring cells can receive packets from multiple neighboring APs so that the multicast receivers can benefit from both spatial and time diversities. In order to implement multicast packet transmissions by these multiple APs in different time slots, we can control the transmission time of Delivery Traffic Indication Map (DTIM) beacons. In the IEEE 802.11 specification, periodically transmitted DTIM beacons are followed by broadcast or multicast downlink transmissions when there is at least one power-saving user in the network. By controlling the transmission time slots of the DTIM beacons, we can exclusively allocate multiple time slots to multiple surrounding APs for video multicast.

If multiple APs have to work on different frequency channels, their multicast transmissions can be made non-overlapping in time domain as shown in Fig. 3.1, and video multicast users can hop to each AP's operating channel at a predefined time slot to receive multiple APs' video multicast packets. Utilizing multiple network interfaces is another possible solution, when users are equipped with multiple network interface cards. That is, in order to listen to the packets of neighboring APs working on different channels, the multiple network interfaces working on different channels can be exploited. In such a case, the maximum number of simultaneously accessible channels is limited by the number of network interfaces.

In this chapter, we assume that multiple APs operate on the same channel in a time slotted manner, as shown in Fig. 3.1. Each AP periodically transmits the multicast packets within its allocated time duration, and the remaining time is used for other traffic. Since an AP can transmit video multicast packets with higher priority than non-AP STAs using the prioritized channel access of Enhanced Distributed Channel Access (EDCA) in IEEE 802.11, the transmissions of multicast packets are rarely interfered with.

### **3.2.2 FEC Coding Schemes**

There are two most popular FEC codes, Raptor code [34] and RS code [35], for AL-FEC. Raptor code is introduced as a rateless fountain erasure correction code, capable of producing an unlimited sequence of parity symbols from a block of data symbols — typically non-binary symbols. It is designed and optimized as an erasure-correction code and provides a large degree of freedom in parameter choices. The encoded symbols are generated by a combinatorial sum of data symbols.

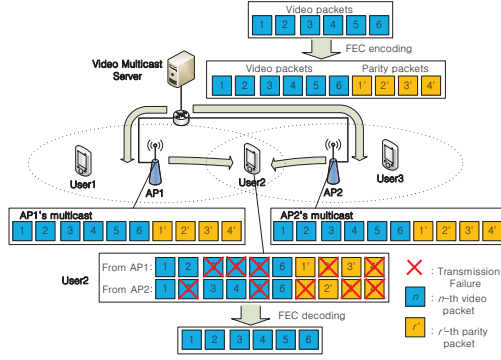
On the other hand, RS code is another powerful linear block erasure correction code. In general, RS code is more powerful than Raptor code in recovering lost symbols. However, when used in layers above the MAC layer, its efficiency tends to decrease faster than the Raptor code, due to its decoding complexity. Moreover, there are limitations in the RS code design, as there are constraints on the size of symbols and original source blocks.

For the above reasons and for utilizing the characteristics of rateless Raptor FEC code, we adopt Raptor code for the AL-FEC in this chapter. We also use the systematic Raptor code, which includes the original data symbols in the encoded symbols because the systematic Raptor codes generally perform better than the non-systematic counterpart.

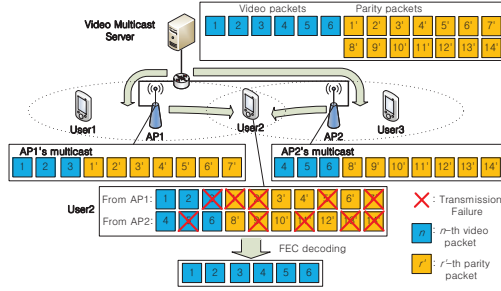
## **3.3 Reliable Video Multicast with Coordinated Multiple APs**

### **3.3.1 Proposed Video Multicast**

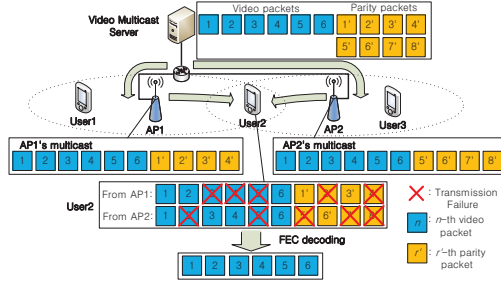
We propose reliable video multicast by exploiting both AL-FEC and coordination of multiple APs. Fig. 3.2 illustrates the proposed video multicast schemes. The video streaming server packetizes the video data and generates parity packets using the FEC encoder. Both video and parity packets are delivered to all the APs that provide video



(a) Totally overlapped video multicast



(b) Non-overlapped video multicast



(c) Partially overlapped video multicast

Figure 3.2: Illustration of the proposed reliable video multicast schemes.

multicast service, and each AP then multicasts video and parity packets using the proposed schemes. Here, we assume that an identical amount of time is allocated to all APs to simplify the description. A resource-allocation algorithm for FEC-code rate

adaptation will be presented in the next section.

Fig. 3.2(a) illustrates a proposed multicast scheme, called the *totally overlapped* video multicast. In this scheme, the APs multicast the same set of packets given that they are allocated the same amount of time. When a user (i.e., User2) is being served by multiple APs, he can receive part of video and parity packets from both AP1 and AP2. Even when his link to one AP becomes bad due to deep fading, User2 can still receive packets from the other AP, thus exploiting spatial diversity. However, the user might receive same packets multiple times from multiple APs.

Figs. 3.2(b) and 3.2(c) illustrate the other two proposed coordinated multi-AP multicast schemes. As mentioned above, thanks to the characteristic of rateless Raptor FEC coding, the video server can generate as many parity packets as needed. With the help of the coordination of multiple APs, each AP can transmit (1) entirely different or (2) partially different FEC encoded packets as shown in Figs. 3.2(b) and 3.2(c), respectively.

With *non-overlapped* video multicast in Fig. 3.2(b), each AP transmits entirely different video and parity packets based on the allocated amount of time. Compared to Fig. 3.2(a), each AP transmits fewer video packets while transmitting more parity packets in return. If the users served by a single AP, i.e., User1 and User3, receive a large enough number of video and parity packets sent by its serving AP, they can recover the unsent video packets by utilizing the received parity packets. On the other hand, the user served by multiple APs, i.e., User2, can receive more packets compared with the case of Fig. 3.2(a), as a result of non-overlapped transmissions of multiple APs. Therefore, it can recover all the video packets with a higher probability. However, the users in this scheme are likely to receive relatively fewer video packets because the total video packets are divided to multiple APs for non-overlapped transmissions. In a systematic Raptor FEC, a successful reception of a video packet can be more useful

than that of a parity packet in terms of packet recovery, and hence, the reduction of the received video packets could decrease the probability of successful FEC decoding. Consequently, in the cases of User1 and User3, more parity packets are required for successful decoding. Similarly, when FEC decoding fails, the user will encounter more video packet losses.

To overcome the deficiency of the non-overlapped multicast scheme, a hybrid scheme called *partially overlapped* video multicast, is proposed as shown in Fig. 3.2(c). Unlike the previous cases, each AP transmits all the video packets identically and is allocated entirely different parity packets to transmit. Because the AP transmits all the video packets, the users served by only one AP can receive more video packets than non-overlapped scheme, and can also recover missing video packets by FEC decoding. In addition, the users which can be served by multiple APs, i.e., User2, can receive more video packets, while fewer parity packets are likely to be utilized in FEC decoding compared with non-overlapped scheme. The partially overlapped scheme is supposed to provide more balanced video quality compared with the non-overlapped scheme, because the effectiveness of the video packet and that of the parity packet are properly utilized.

### 3.3.2 Video Multicast Procedure

Fig. 3.3 shows the procedure of the proposed video multicast schemes. This procedure is repeated every fixed interval, i.e., Group of Pictures (GoP) interval. Each step as numbered in the figure works as follows.

- 1) First, the video server conducts packetization that divides the video data (corresponding to GoP) into video symbols, which are the input to the FEC encoder. We assume that the video data is generated as Constant Bit Rate (CBR) traffic and the length of the video data per GoP is fixed to  $L_D$ . Besides, the video data are divided

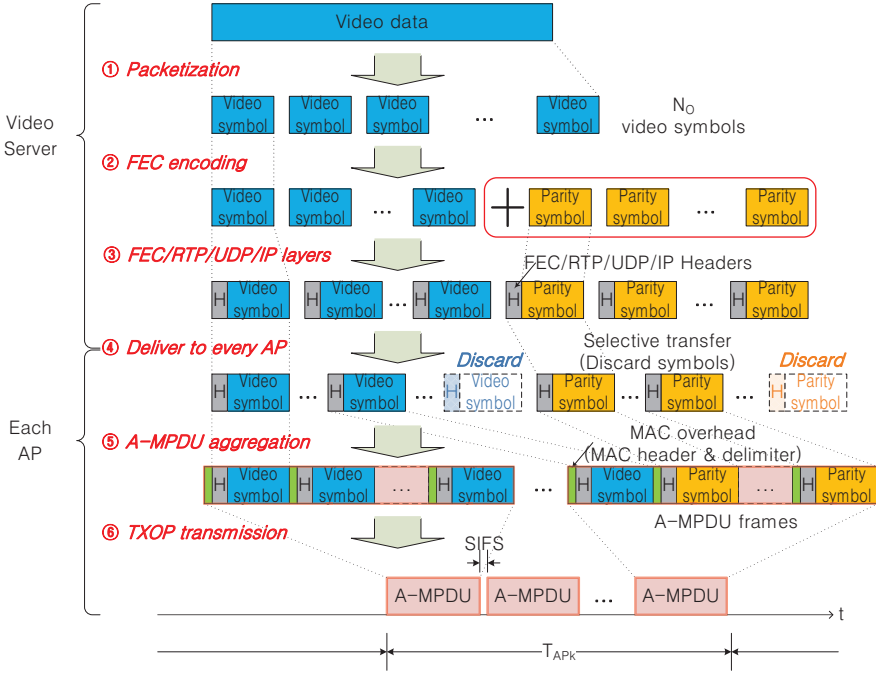


Figure 3.3: The procedure of proposed video multicast with application-layer FEC.

into  $N_O$  video symbols, where the length of each symbol is  $L_s (= L_D/N_O)$ .

2) In the application layer, FEC encoder generates as many parity symbols (with the length of  $L_s$ ) as needed from these  $N_O$  video symbols, where the number of generated parity symbols is determined by the adopted video multicast scheme.

3) These video symbols and parity symbols are then appended by some protocol headers, i.e., FEC, RTP, UDP, IP, MAC and PHY headers. However, these appended protocol headers contain some redundant information, and the header compression technique can be used to reduce the overheads of these protocols. Now, these video symbols and parity symbols appended by compressed protocol headers become video packets and parity packets, respectively.

4) Afterwards, these video packets and parity packets are delivered to multiple

APs over the wired network and the number of video multicast packets transmitted by each AP is determined by a coordinator, which is responsible for letting each AP know when to start the transmission and which packets to be transmitted over the wireless medium based on the proposed video multicast schemes.

5) Accordingly, each AP discards some video packets and/or some parity packets which do not need to be transmitted over the air as informed by the coordinator. The remaining packets are aggregated using Aggregation MAC protocol Data Unit (A-MPDU) of 802.11n [28] to reduce the overheads of the MAC layer. The encoded packets might be aggregated to multiple A-MPDU frames since the length and duration of an A-MPDU frame cannot exceed the maximum A-MPDU length (64 kbytes) and duration (10 msec), respectively.

6) Each AP transmits A-MPDU frame(s) during the allocated time slot after a DTIM beacon.<sup>1</sup> To reduce the overheads on the channel access, Transmission Opportunity (TXOP) of 802.11e [28] which allows consecutive transmissions of multiple frames is used for the efficient video multicast.

The size of allocated time slot for each AP is also decided by the coordinator, considering the number of APs, the minimum time of transmitting  $N_O$  video packets, and the airtime for the other traffic, etc. as presented in Section 3.4.2. Accordingly, the number of packets transmitted by AP  $k$ , i.e.,  $N^{(k)}$ , which is informed to each AP in Step 4, is also decided by the coordinator considering the size of allocated time slot of AP  $k$ , i.e.,  $T_{AP_k}$ ,  $L_s$ ,  $N_O$ , and other protocol overheads.

The total time for transmitting  $N^{(k)}$  packets, i.e.,  $T(N^{(k)})$ , should be smaller than  $T_{AP_k}$ . Since all the A-MPDUs are transmitted in a bursty manner according to the TXOP operation,  $T(N^{(k)})$  is equal to the sum of transmission times of A-MPDUs as

---

<sup>1</sup>DTIM period is set to GoP period.



follows:

$$T(N^{(k)}) = T_{AMPDU_1} + T_{SIFS} + T_{AMPDU_2} + T_{SIFS} + \dots + T_{SIFS} + T_{AMPDU_{n_m}}, \quad (3.1)$$

where  $T_{AMPDU_m}$ ,  $n_m$ , and  $T_{SIFS}$  are the transmission time of the  $m$ -th A-MPDU, the number of A-MPDUs, and the interval of Short Interframe Space (SIFS), respectively.  $T_{AMPDU_m}$  is determined by the number of aggregated packets in the  $m$ -th A-MPDU and the Modulation and Coding Scheme (MCS).

Therefore, determining the maximum number of parity packets, i.e.,  $N_R^{(k)}$  ( $= N^{(k)} - N_O$ ), at the appropriate MCS is important while satisfying  $T_{AP_k} \geq T(N^{(k)})$ . Of course, reducing the number of parity packets when the wireless channel condition is good could be a possible solution to save the resource for other types of traffic. Finally, each video multicast user tries to recover the video symbols from the received video and parity packets through FEC decoding.

### 3.4 FEC Code Rate Adaptation

Video multicast with the robust FEC code rate can enlarge an AP's coverage, while requiring more resource since the AP transmits more parity packets for the same video packets. Since the wireless resource for video multicast is limited, decreasing the FEC code rate of one AP will increase other APs' FEC code rate. Properly adapting the FEC code rate of APs can eliminate service coverage holes. For example, if an AP is located relatively far from the other APs, decreasing the FEC code rate of this AP is likely to enlarge the video multicast region. Meanwhile, the FEC code rate of the AP, whose coverage is largely overlapped with other neighboring APs', might not affect the size of the overall multicast service region. Moreover, by making a specific AP, which serves many users, transmit more parity packets while sacrificing the video multicast service of other APs (by increasing their FEC code rate) which serve fewer

users, it is possible to satisfy a larger number of users in the system. Accordingly, we here propose an FEC code rate adaptation algorithm for enlarging the video multicast service region.

Here we limit our scope to *partially overlapped* video multicast scheme, which is found to perform the best overall as shown in Section 3.5. We assume that a number of APs are deployed and their locations are fixed. To determine the FEC code rate of each AP, we utilize the offline channel measurement results made at multiple measurement locations. At each measurement location, a user collects the channel information (e.g., SNR value and packet error probability) from all the deployed APs, and feeds back the information to the central coordinator, which decides the FEC code rate of each AP. The measurement locations should be determined by considering the locations, where many users are likely to be. Since the locations of the APs are rarely changed, the collected information can be used for a long period. In addition, online measurements and reports to the coordinator might be also feasible while the details are beyond the scope of this chapter.

As mentioned above, the aggregate transmission time of all the APs for the video multicast is limited, i.e.,  $T_{sum\_limit} \geq \sum_k T_{AP_k}$ , where  $T_{sum\_limit}$  is the maximum transmission time for the video multicast per a given interval (e.g., DTIM period). Since the APs transmit different numbers of packets, i.e.,  $N^{(k)} (\geq N_O)$  for AP  $k$ , the sum transmission time of AP  $k$  to transmit  $N^{(k)}$  packets, i.e.,  $T(N^{(k)})$  in Equation (3.1), cannot exceed  $T_{AP_k}$ . In this section, for the efficient adaptation, we assume that the size of the allocated time slot to AP  $k$ , i.e.,  $T_{AP_k}$ , is set to  $T(N^{(k)})$ .

### 3.4.1 Estimation of Delivery Ratio

We here present the method for estimating the video packet delivery ratio, which is used by the FEC code rate adaptation algorithm later. In a systematic Raptor code,

the successful reception of the video packets can be more effective for the decoding than the reception of the parity packets. Therefore, we need to consider the reception probability of the video packets and the reception probability of the parity packets separately. For this estimation, we assume that the coordinator has all the required channel information in terms of the packet error probabilities. That is, for each measurement location  $i$  and AP  $k$ , the probability  $p_{i,k}$  that a packet from AP  $k$  is erroneously received should be known.

When AP  $k$  transmits  $N^{(k)}$  packets, the number of parity packets out of  $N^{(k)}$  is determined by  $N_R^{(k)} = N^{(k)} - N_O$ . Since all the APs multicast the same video packets in *partially overlapped* multicast scheme, the probability  $\Pr(n_i = n)$  that the number of received video packets is equal to  $n$  ( $0 \leq n \leq N_O$ ) is derived as follows.

$$\Pr(n_i = n) = f \left( n, N_O, \prod_{k=1}^{N_{ap}} p_{i,k} \right), \quad (3.2)$$

where  $n_i$  and  $N_{ap}$  are the number of received video packets and the number of APs in the network, respectively, and the function  $f(a, b, e)$  is the probability mass function of the binomial distribution representing the probability to have  $a$  successes out of  $b$  trials with the failure probability of  $e$ :

$$f(a, b, e) = \binom{b}{a} (e)^{b-a} (1-e)^a. \quad (3.3)$$

Meanwhile, the probability  $\Pr(r_i = r)$  that the number  $r_i$  of received parity packets is equal to  $r$  ( $0 \leq r \leq \sum_{k=1}^{N_{ap}} N_R^{(k)}$ ) is derived in Equation (3.4).

$$\begin{aligned} \Pr(r_i = r) = & \sum_{a_1=0}^r (f(a_1, N_R^{(1)}, p_{i,1}) \sum_{a_2=0}^{r-a_1} (f(a_2, N_R^{(2)}, p_{i,2}) \dots ( \sum_{a_{N_{ap}-1}=0}^{r-a_1-\dots-a_{N_{ap}-2}} f(a_{N_{ap}-1}, N_R^{(N_{ap}-1)}, p_{i,N_{ap}-1}) \\ & f(r - \sum_{j=1}^{N_{ap}-1} a_j, N_R^{(N_{ap})}, p_{i,N_{ap}}) \dots )). \end{aligned} \quad (3.4)$$

Because each AP transmits entirely different parity packets, the number of received parity packets is the sum of the numbers of received parity packets from all the APs.

For the estimation of the delivery ratio, we define a function of  $n$  and  $r$ ,  $P(n, r)$ , which represents the delivery ratio after Raptor decoding when the number of received video packets and the number of received parity packets are equal to  $n$  and  $r$ , respectively. The function  $P(n, r)$  can be derived by the simulation as explained in Section 3.5.1 and shown in Fig. 3.4. Therefore, the estimated delivery ratio  $P_i(N^{(1)}, \dots, N^{(k)}, \dots, N^{(N_{ap})})$  at the measurement location  $i$ , when AP  $k$  transmits  $N^{(k)}$  packets, is derived as follows.

$$\begin{aligned} P_i(N^{(1)}, \dots, N^{(N_{ap})}) \\ = \sum_n \sum_r (\Pr(n_i = n) \cdot \Pr(r_i = r) \cdot P(n, r)). \end{aligned} \quad (3.5)$$

### 3.4.2 Greedy FEC Code Rate Adaptation

The goal of the FEC code rate adaptation is to maximize the number of satisfied measurement locations. By definition, at a *satisfied* measurement location, the estimated video packet delivery ratio  $P_i(\cdot)$  should be above a given *satisfaction threshold*. Since finding the best combination of the FEC code rates for all the APs is too complicated, we propose a greedy algorithm which incrementally decreases the FEC code rate of the AP, which can additionally satisfy the most measurement locations by decreasing its code rate. If no more measurement locations can be satisfied, the proposed algorithm utilizes the remaining resource to enhance the reliability at the already satisfied measurement locations by increasing the satisfaction threshold.

Algorithm I shows the pseudo code of the proposed greedy algorithm for the FEC code rate adaptation, where (1)  $\Delta n_r$  is the number of additionally allocated parity packets, (2)  $p_{\text{thrs}}$  is the current satisfaction threshold, (3)  $p_{\text{thrs}_{\text{init}}}$  is the initial (mini-

---

**Algorithm 1** FEC code rate adaptation
 

---

**Initialization**

```

 $\Delta n_r \leftarrow 1$ 
 $S_{\text{unsat}} \leftarrow \{s_1, s_2, \dots, s_{N_{\text{MP}}}\}$ 
 $S_{\text{fail}} \leftarrow \emptyset$ 
 $p_{\text{thrs}} \leftarrow p_{\text{thrs}_{\text{init}}}$ 
for  $k \in S_{AP}$  do
   $N^{(k)} \leftarrow N_O$ 
end for
 $S_{\text{unsat}} \leftarrow S_{\text{unsat}} - \text{satisfy}(0, 0, S_{\text{unsat}}, p_{\text{thrs}})$ 

```

**Greedy algorithm**

```

while  $T_{\text{sum\_limit}} \geq \sum_k T(N^{(k)})$  do
  // Select the best AP
   $k' := \arg \max_{k \in S_{AP}} \left( \frac{|\text{satisfy}(k, \Delta n_r, S_{\text{unsat}}, p_{\text{thrs}})|}{T(N^{(k)} + \Delta n_r) - T(N^{(k)})} \right)$ 
  if  $T_{\text{sum\_limit}} \geq T(N^{(k')} + \Delta n_r) + \sum_{k \neq k'} T(N^{(k)})$  then
    if  $\text{satisfy}(k', \Delta n_r, S_{\text{unsat}}, p_{\text{thrs}}) \neq \emptyset$  then
      // Allocate more parity packets to AP  $k'$ 
       $N^{(k')} \leftarrow N^{(k')} + \Delta n_r$ 
       $S_{\text{unsat}} \leftarrow S_{\text{unsat}} - \text{satisfy}(k', \Delta n_r, S_{\text{unsat}}, p_{\text{thrs}})$ 
       $\Delta n_r \leftarrow 1$ 
    else
       $\Delta n_r \leftarrow \Delta n_r + 1$ 
    end if
  end if
else
  if  $p_{\text{thrs}} \neq p_{\text{thrs}_{\text{max}}}$  then
    // Increase the satisfaction threshold
     $p_{\text{thrs}} \leftarrow p_{\text{thrs}_{\text{next}}}$ 
     $\Delta n_r \leftarrow 1$ 
     $S_{\text{fail}} \leftarrow S_{\text{fail}} \cup S_{\text{unsat}}$ 
     $S_{\text{unsat}} \leftarrow \{s_1, s_2, \dots, s_{N_{\text{MP}}}\} - S_{\text{fail}}$ 
  else
    break
  end if
end if
end while

```

---

**proc**  $\text{satisfy}(k, n, S, p)$ 

```

 $S_{\text{sat}} \leftarrow \emptyset$ 
for  $s_i \in S$  do
  if  $P_i(N^{(1)}, \dots, N^{(k)} + n, \dots, N^{(Nap)}) \geq p$  then
     $S_{\text{sat}} \leftarrow S_{\text{sat}} \cup \{s_i\}$ 
  end if
end for
return  $S_{\text{sat}}$ 
end proc

```

---

mum) satisfaction threshold, (4)  $p_{\text{thrS}_{\text{next}}}$  is the next satisfaction threshold, (5)  $p_{\text{thrS}_{\text{max}}}$  is the maximum satisfaction threshold, (6)  $S_{AP}$  is the set of APs in the network, (7)  $S_{\text{unsat}}$  is the set of unsatisfied measurement locations which might become satisfied by the algorithm, (8)  $S_{\text{fail}}$  is the set of measurement locations which can not be satisfied with the current satisfaction threshold, (9)  $N_{\text{MP}}$  is the total number of measurement locations in the network, and (10)  $\text{satisfy}(k, n, S, p)$  is the function which returns the set of the satisfied measurement locations out of the set of measurement locations,  $S$ , when the number of multicast packets of AP  $k$ ,  $N^{(k)}$ , is changed to  $N^{(k)} + n$  and the satisfaction threshold is  $p$ , respectively.

In this algorithm, AP  $k'$ , which can satisfy more measurement locations with fewer additional parity packets, i.e., AP  $k'$  with the maximum value of

$$\frac{|\text{satisfy}(k, \Delta n_r, S_{\text{unsat}}, p_{\text{thr}})|}{T(N^{(k)} + \Delta n_r) - T(N^{(k)})},$$

is selected to increase its  $N^{(k')}$  preferentially. This procedure is repeated until the total transmission time of all the APs reaches the limit,  $T_{\text{sum.limit}}$ . If no newly satisfied measurement location is found for all APs with large  $\Delta n_r$ , satisfying more measurement locations is given up, and the satisfaction threshold value is updated to the next-higher threshold value to enhance the video quality at the already satisfied measurement locations further.

### 3.5 Performance Evaluation

In this section, we comparatively evaluate the performance of the proposed reliable video multicast protocol. An H.264 CBR video clip of 500 kbps is used for the evaluation. The number of video packets,  $N_O$ , per GoP (corresponding to 0.5 seconds) is assumed to be 44. We use the delivery ratio of video packets and Peak Signal-to-Ratio (PSNR), which is a widely-accepted measure of video quality, for our evaluation.

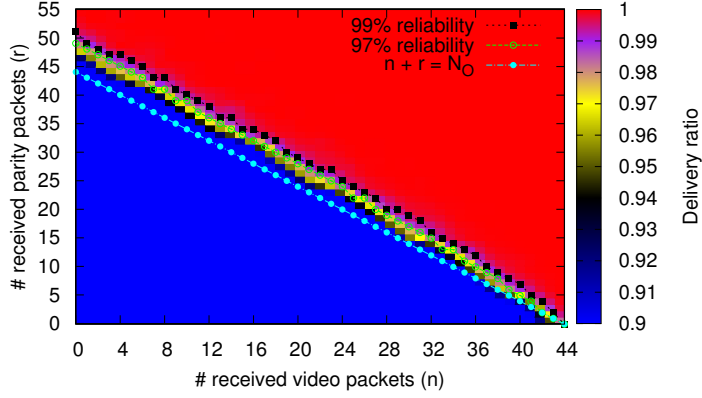
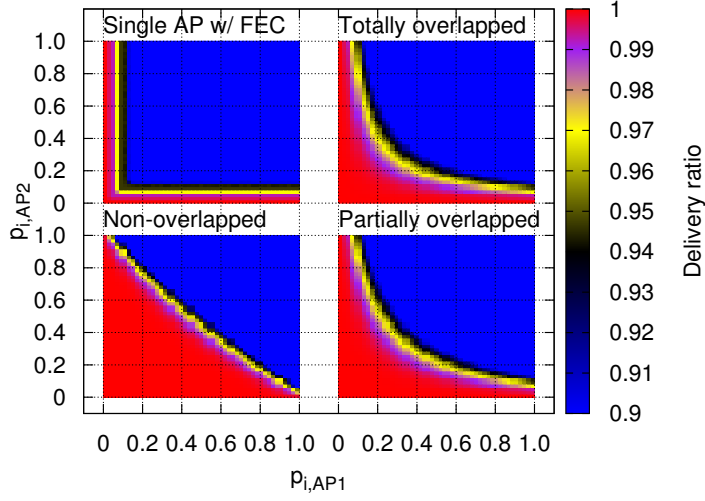


Figure 3.4: Video packet delivery ratio  $P(n, r)$  with Raptor code ( $N_O = 44$ ).

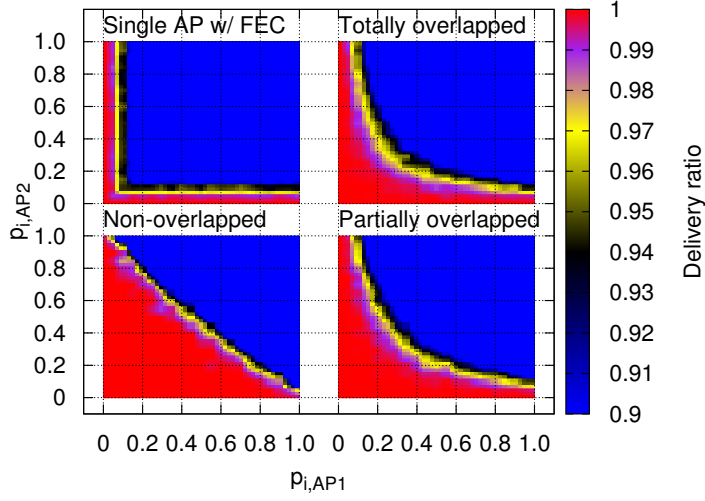
The simulations are done using NS-3 network simulator [36] integrated with real Raptor encoder and decoder. IEEE 802.11n PHY and MAC models are used, and Jake's fading model with pathloss exponent of 3.5 and Doppler speed of 1.0 m/s is used unless specified otherwise. All the multicast packets are transmitted via MCS 0 of 802.11n, i.e., 6.5 Mbps, using A-MPDU.

### 3.5.1 Raptor Code Performance

We first evaluate the performance of the employed Raptor code. Fig. 3.4 shows the average video packet delivery ratio,  $P(n, r)$  used in Equation (3.5), as the number  $n$  of received video packets and the number  $r$  of received parity packets vary. The delivery ratios are obtained via simulations using a software implementation of Raptor encoder and decoder. In the case of Raptor code, whether a decoding succeeds for a given  $(n, r)$  is not deterministic, but actually depends on which of video and parity packets are received. For a given  $(n, r)$ , we randomly select  $n$  video packets and  $r$  parity packets, and run the decoder to determine the number of successfully delivered video packets. If the decoding is successful, all  $N_O$  video packets are delivered, thus making



(a) Estimated delivery ratio



(b) Simulation results

Figure 3.5: Delivery ratio when there are two APs (no fading,  $N = 50$ ,  $N_O = 44$ ).

the delivery ratio one. However, if the decoding fails, only  $n$  video packets are assumed to be delivered, thus making the delivery ratio  $n/N_O$ . We obtain the average delivery ratio  $P(n, r)$  by averaging the results from 1,000 randomly-chosen combinations of  $n$



video packets and  $r$  parity packets.

From Fig. 3.4, we basically observe that the delivery ratio increases as the sum of received video packets and parity packets increases. The fig. also shows the minimum number of  $r$  received parity packets for a given  $n$  received video packets to achieve two target video packet delivery ratios, namely, 99% and 97%. A line representing  $n+r = N_O (= 44)$  is also drawn as a reference. We first observe that the required sum of  $n$  and  $r$  to achieve a target delivery ratio is obviously larger for a larger target ratio. Moreover, for the considered target values, the required sum is slightly larger than  $N_O$ , meaning that we need more than one parity packet to recover one video packet in an average sense. We also observe that the required sum of  $n$  and  $r$  to achieve a target delivery ratio decreases as  $n$  increases. This is because the number of video packets to be recovered by the decoding decreases as  $n$  increases.

### 3.5.2 Simulation Results: No Fading

In this subsection, we assume that FEC code rates of all APs are the same; the number of video packets,  $N_O$ , and the number of multicast packets including video packets and parity packets transmitted by an AP,  $N$ , are set to 44 and 50, respectively.

Fig. 3.5 shows the video packet delivery ratio of user  $i$  after Raptor decoding from both estimation using Equation (3.5) and NS-3 simulation, when there are two APs (i.e., AP1 and AP2) with varying packet error probabilities from AP1 and AP2, i.e.,  $p_{i,AP1}$  and  $p_{i,AP2}$ , respectively. In this simulation, fading channel is not assumed, and hence, the packet error probability is fixed. The estimation method of *partially overlapped* scheme presented in Section 3.4.1 is also applied to the estimation of the other schemes. With *single AP w/ FEC* scheme, the user receives the video packets from only one AP which achieves the lowest packet error probability. We easily find that the delivery ratio decreases as the packet error probability of AP1 or AP2 increases.

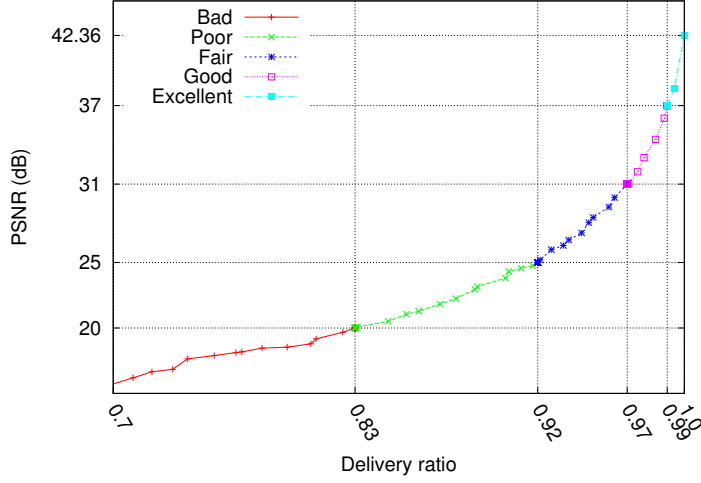


Figure 3.6: PSNR vs. delivery ratio.

Moreover, it is found that the estimated delivery ratio and simulation results are almost the same, thus verifying the validity of the estimation.

It is observed that *non-overlapped* scheme performs the best in most cases except when the gap between  $p_{i,AP1}$  and  $p_{i,AP2}$  is large. Note that when a user is served mostly by a single AP, e.g.,  $p_{i,AP1}$  is around 0.9 and  $p_{i,AP2}$  is almost 0, *non-overlapped* scheme achieves the worst performance. In this case, multi-AP diversity can not be exploited, and hence, *non-overlapped* scheme, in which each AP does not multicast all the video packets, performs poorly. As observed in Fig. 3.4, more than  $e$  parity packets are needed to recover  $e$  video packets. It is found that *partially overlapped* scheme outperforms *totally overlapped* scheme, thus making it a good compromise between *non-overlapped* and *totally overlapped* schemes.

Apparently, video quality and packet losses are tightly coupled. In video streaming, the packet loss probability over 0.01 generally results in poor video quality [37]. However, the actual quality might be different depending on the streamed video format

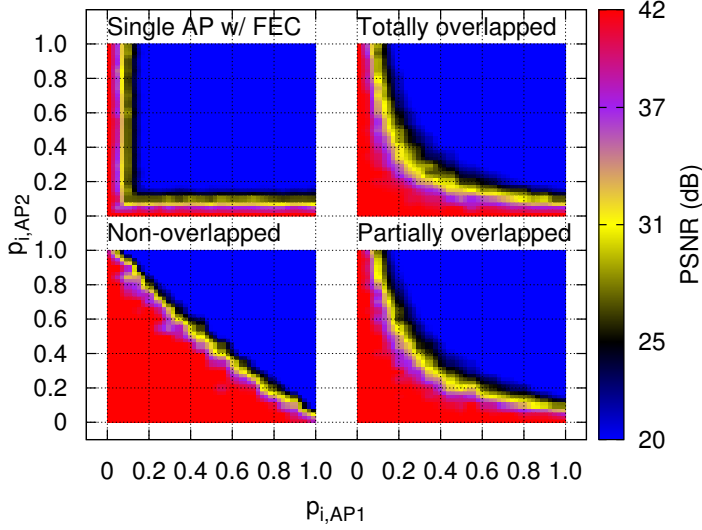


Figure 3.7: PSNR when there are two APs (no fading,  $N = 50$ ,  $N_O = 44$ ).

such as video codec. In this evaluation, H.264 video encoder and decoder are used. The encoded video clip is damaged according to the delivery ratio, and the PSNR is calculated by comparing the original video clip with the damaged video clip after H.264 decoding. Fig. 3.6 shows the relationship between the average PSNR and the video packet delivery ratio. It is shown that the PSNR value of video clip without damage is about 42 dB, and the PSNR value rapidly decreases as the delivery ratio decreases in large delivery ratio region. Based on the relationship between PSNR and Mean Opinion Score (MOS) [38], and assuming MOS of 4 (i.e., Good) as the satisfactory video quality, the delivery ratio over 0.97 is acceptable for the good video quality of this video clip.

In Fig. 3.7, the PSNR values obtained from the simulation are shown when there are two APs in the static channel environment. It is shown that the proposed video multicast schemes outperform the legacy single AP scheme.

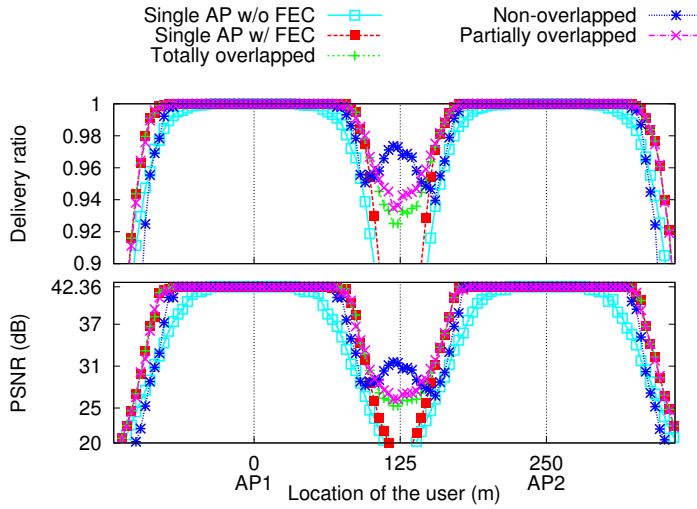


Figure 3.8: Performance when there are two APs.

### 3.5.3 Simulation Results: Fading Channel

Fig. 3.8 shows the delivery ratio and PSNR in a fading channel environment where two APs are located 250 m apart and all the users are located on the straight line connecting these two APs. It is shown that AL-FEC enlarges the satisfactory video multicast region, and *partially overlapped* scheme performs the best overall. As observed in no fading environment already, *non-overlapped* scheme performs basically the worst when a user is served by only a single AP, e.g., left side of AP1 or right side of AP2, while it outperforms the other schemes in the middle of two APs.

Fig. 3.9 shows the PSNR distribution when there are four equally apart APs and 2,000 users are randomly spread in  $360 \text{ m} \times 360 \text{ m}$  area. Fig. 3.9(a) shows the PSNR depending on the positions of the users and Fig. 3.9(b) shows empirical Cumulative Distribution Function (CDF) of PSNR observed by 2,000 users. Table 3.1 shows the ratio of satisfied users and the average PSNR based on Fig. 3.9(b). We observe that *partially overlapped* scheme achieves the best performance in terms of both metrics.

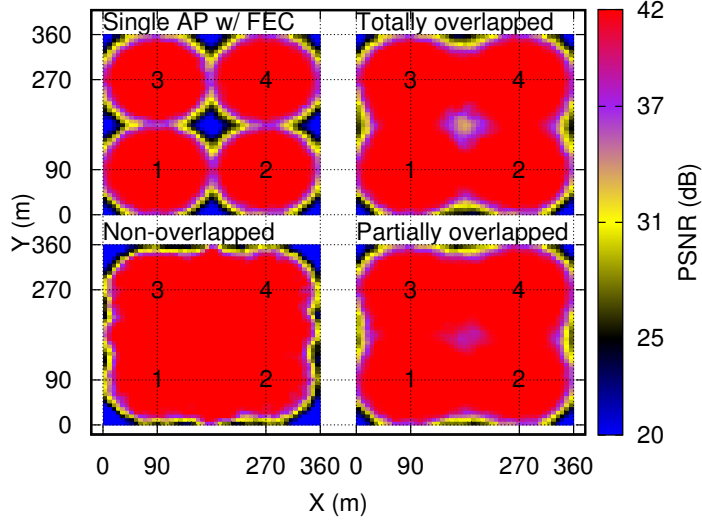
Table 3.1: Satisfied users and average PSNR

	Results in Fig. 3.9(b)		Results in Fig. 3.11	
	Satisfied users (%)	Average PSNR (dB)	Satisfied users (%)	Average PSNR (dB)
Single AP w/o FEC	68.25	34.5	67.86	33.89
Single AP w/ FEC	84.1	38.19	78.52	36.86
Totally overlapped	92.4	39.91	85.26	38.51
Non-overlapped	86.5	39.00	83.66	38.02
Partially overlapped	93.6	40.23	86.42	38.82
Partially w/ FEC adaptation			88.02	39.15

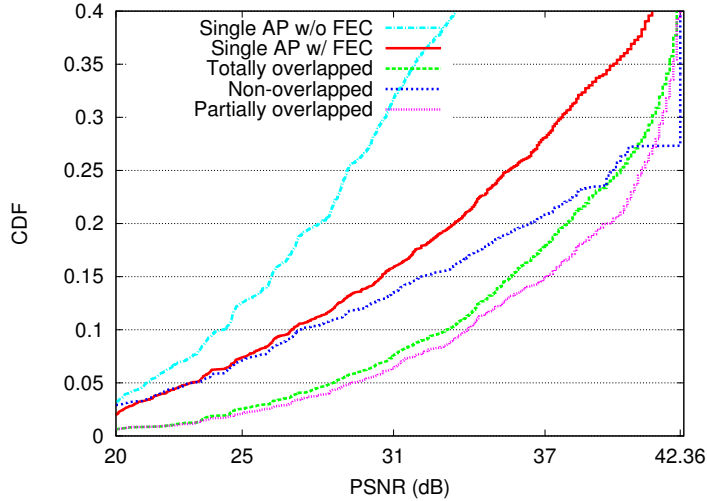
Compared with *single AP* w/o and w/ FEC, *partially overlapped* scheme enhances the satisfied user ratio by 37.1% and 11.3%, respectively. *Non-overlapped* scheme can reduce the size of coverage hole in the middle of APs the best. However, since the users served by only one AP in the area's boundary experience the worst performance, the overall performance of *non-overlapped* scheme turns out to be worse than the other proposed schemes. Based on these observations, we conclude that *partially overlapped* video multicast is the best approach for the reliable video multicast service.

### 3.5.4 Simulation Results: Code Rate Adaptation

Fig. 3.10 shows PSNR values of 500 randomly placed users when four APs are randomly located. Note that the proposed FEC code rate adaptation is expected to be effective when the APs and/or users are unevenly distributed. In this evaluation, we assume that each user is located at a measurement location so that the channel information of all the users is available at the coordinator to maximize the performance of the proposed FEC code rate adaptation algorithm. The distances between APs are not fixed, and the number of serving APs for a user can vary depending on the location of the user. For the proposed FEC adaptation algorithm, the initial satisfaction threshold,



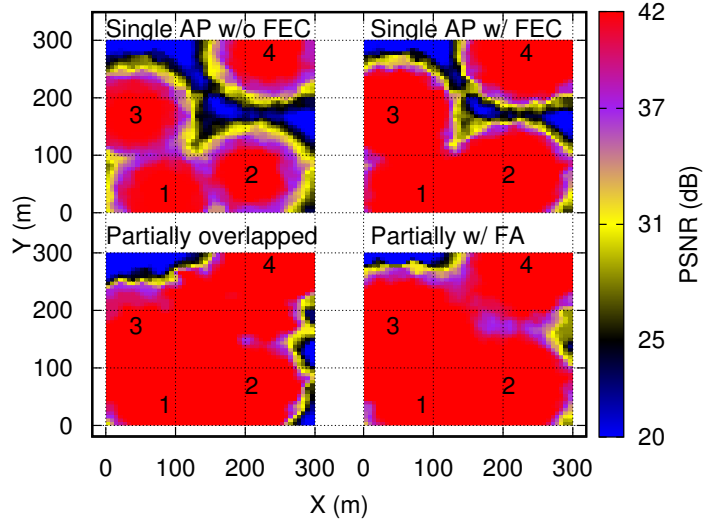
(a) PSNR



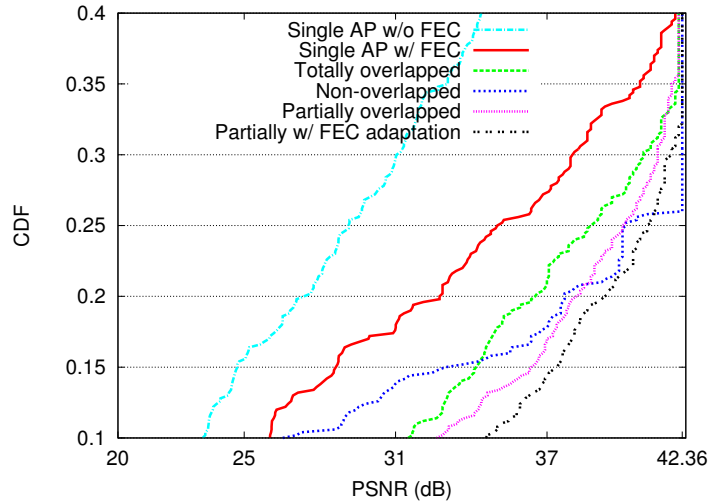
(b) CDF of PSNR

Figure 3.9: Four APs at (90,90), (270,90), (90,270), (270,270), and 2,000 users.

i.e.,  $p_{\text{thr}_{\text{init}}}$ , is set to 0.97 for the satisfactory video quality. In Fig. 3.10(a), based on the proposed FEC rate adaptation algorithm, AP1, whose coverage is relatively overlapped with neighboring APs' coverage, increases its code rate (i.e., decreases  $N^{(1)}$ )



(a) PSNR



(b) CDF of PSNR

Figure 3.10: Four APs at random locations and 500 users.

so that other APs (AP2 and AP3) can transmit more parity packets, i.e.,

$$(N^{(1)}, N^{(2)}, N^{(3)}, N^{(4)}, N_O) = (46, 52, 56, 49, 44).$$

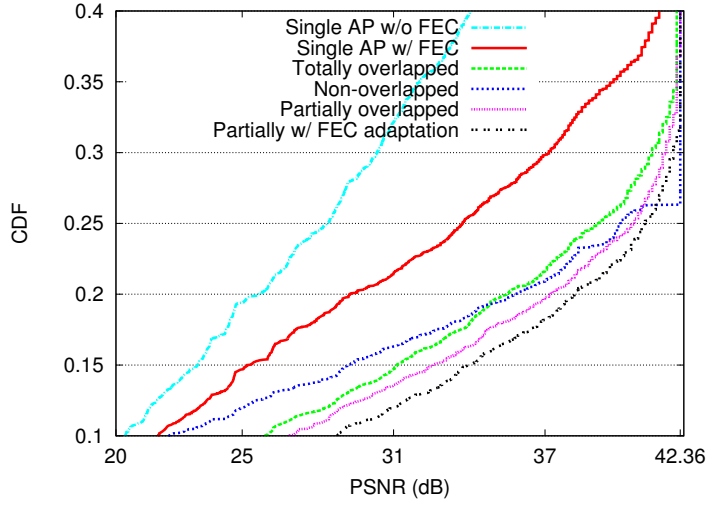


Figure 3.11: Four APs and 500 users at the random locations in  $300 \text{ m} \times 300 \text{ m}$  area.

From the empirical CDF in Fig. 3.10(b), it is found that the proposed FEC adaptation satisfies more users and enhances the overall video quality.

Fig. 3.11 shows the empirical CDF of PSNR values of 500 users when four APs and 500 users are placed at random locations. 10 simulations with different topologies are conducted and averaged for the evaluation. Table 3.1 also shows the ratio of satisfied users and the average PSNR based on Fig. 3.11. Since many users are served by only one AP, *non-overlapped* video multicast performs quite bad, while *partially overlapped* video multicast achieves the best performance. Moreover, using the proposed FEC adaptation algorithm, the overall video quality is further enhanced and more users are satisfied with good video quality. Compared with *single AP w/o* and *w/ FEC*, *partially overlapped w/ FEC* adaptation enhances the satisfied user ratio by 29.7% and 12.1%, respectively.



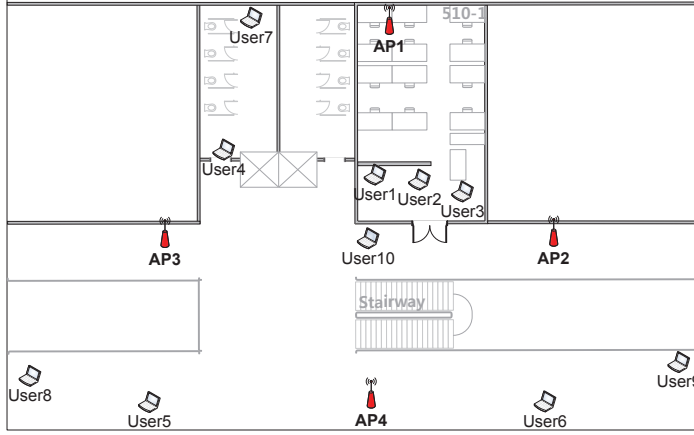


Figure 3.12: Experimental environment.

### 3.5.5 Experimental Results

Fig. 3.12 shows the experimental environment in our building, where there are four APs performing video multicast service on the same channel. All the APs are connected to a video streaming server via Ethernet. Each AP periodically transmits  $N$  FEC-encoded packets, which are generated by the video server, by taking turns in a round robin fashion. Each user records the trace of packet receptions from the APs. The trace results indicate which packets are correctly received and which are lost. Raptor decoder is used to recover the lost packets, and then, the portions of the video clip corresponding to the unrecovered lost packets are eliminated. Finally, the PSNR is determined by comparing the original and decoded video clips.

In this evaluation, FEC code rate is set to  $44/50$ , i.e.,  $N_O = 44$  and  $N = 50$ , for fixed rate schemes. For partially overlapped scheme with FEC code rate adaptation, the values of  $N^{(k)}$  for AP  $k$  as follows:

$$(N^{(1)}, N^{(2)}, N^{(3)}, N^{(4)}, N_O) = (51, 49, 56, 47, 44)$$

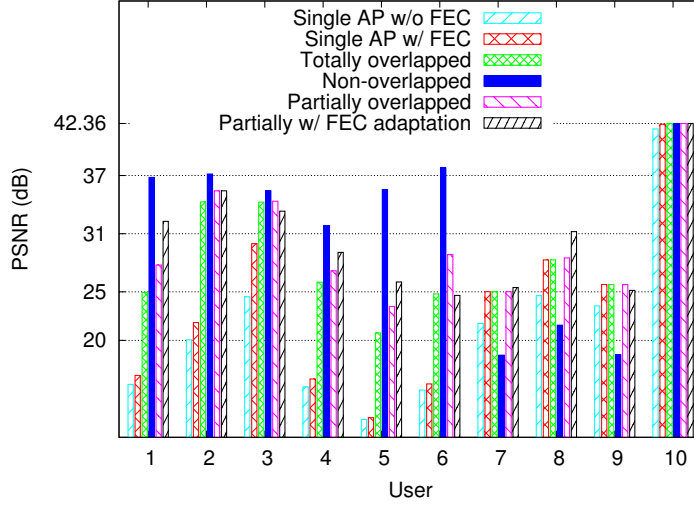


Figure 3.13: Experimental results ( $N_O = 44$ ).

by allocating the most parity packets to AP3 with most associated users. The experiments are done at a 5 GHz channel with virtually no interference and all the packets are transmitted using 6 Mbps PHY rate of 802.11a.

Fig. 3.13 shows the video multicast performance at various locations. In the case of users 1, 2, 3, and 10, they can receive the packets from four APs with some errors. On the other hand, users 4, 5, and 6 can receive the packets from only two APs among four APs, while users 7, 8, and 9 can receive the packets from only one closest AP. Therefore, in the case of the users who can receive the packets from multiple APs, utilizing the proposed multi-AP video multicast schemes, especially, *non-overlapped* scheme, the users can achieve better video performance. However, if the user can be served by only one AP, *non-overlapped* scheme performs the worst, while the other schemes with AL-FEC perform almost the same. It should be noted that with partially overlapped scheme with code rate adaptation, we have five satisfied users (i.e., PSNR over 31 dB) while there are only three satisfied users without code rate adaptation,

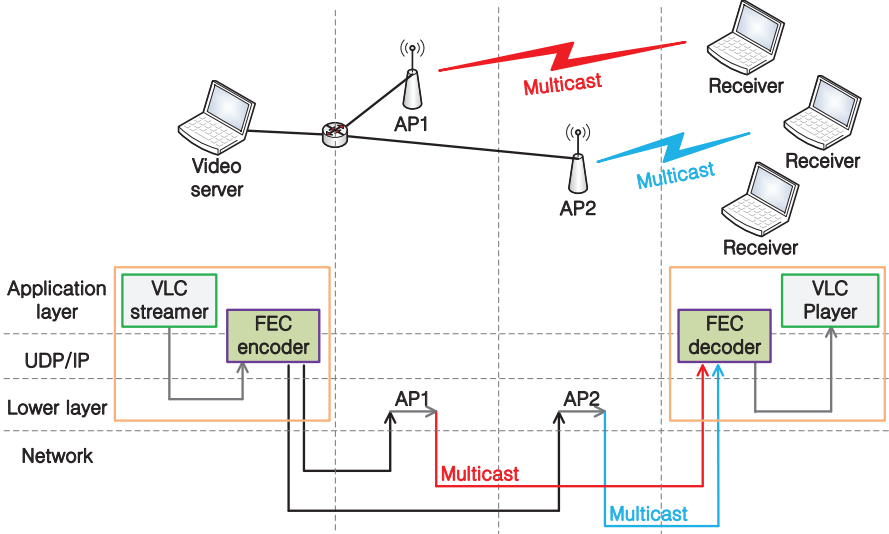


Figure 3.14: Implementation of demonstrable video multicast.

thus empirically demonstrating the utility of the code rate adaptation algorithm. It is also shown that our proposed multi-AP video multicast schemes outperform the conventional single AP schemes overall.

### 3.5.6 Prototype Implementation

We have also prototyped the proposed video multicast protocols in real video streaming environments. Fig. 3.14 shows the testbed environment. There are one video server, multiple receivers, and multiple APs for the video multicast. We use VLC media player [45], which is a popular open-source media player supporting video streaming over networks. UDP/RTP-based video streaming, H.264 video codec, and 500 kbps CBR video streaming is set for the video multicast. In general, the VLC streamer sends video stream to a specific destination IP address with a specific port number, and the VLC player in the receiver waits for the video stream with the specific port number.



Figure 3.15: A snapshot of the demonstration.

However, since the legacy VLC does not support AL-FEC, video multicast over Wi-Fi which does not support ARQ is vulnerable to the packet transmission failure. Our implementation is based on the socket programming and software-based Raptor FEC en/decoder. The FEC encoder and decoder work at the application layer of the video server and receivers, respectively. The VLC streamer, instead of sending the video stream to the destination, sends the video stream to the FEC encoder process running in the same video server machine. The FEC encoder, after generating  $N$  FEC-encoded packets from the  $N_O$  video packets, sends encoded packets to APs for multicast. The code rate is set to 10/15, i.e.,  $N_O = 10$  and  $N = 15$ , for fixed rate schemes. These FEC-encoded packets are transmitted with the destination port number equal to the port number of FEC decoder, not the VLC player's. Upon reception of the multicast packets from one or multiple APs, the FEC decoder process decodes and forwards the

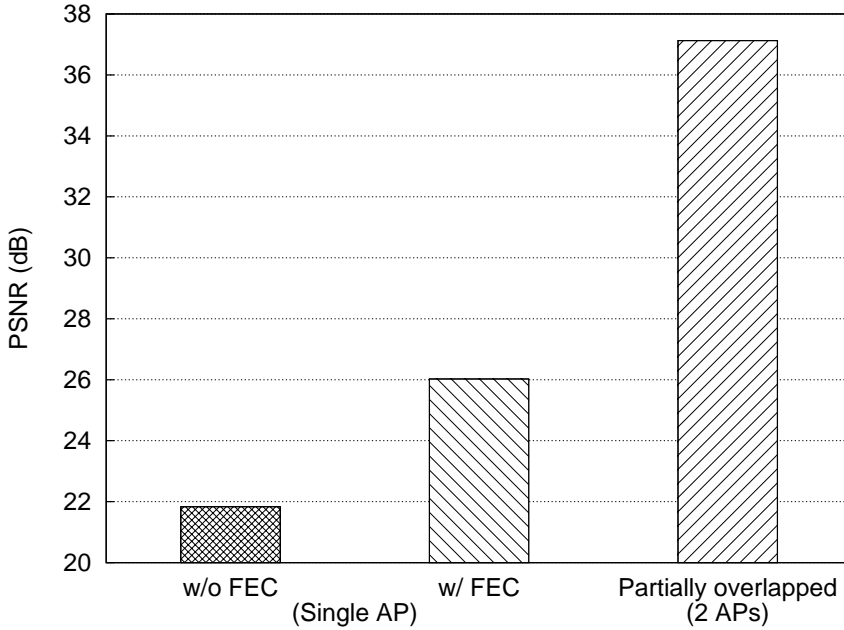


Figure 3.16: Average PSNR.

decoded video packets to the VLC player. The advantage of this structure is that it does not require any change of the legacy video streaming software for the FEC en/decoding because the communication between streamer (player) and encoder (decoder) is done via the conventional socket interface. Moreover, it can be applicable in any other video streaming software if it knows the pattern of video traffic (e.g., video source rate and GoP).

Fig. 3.15 shows a snapshot of the video multicast demonstration. Three tablet PCs work as the receivers. In this experiment, the receivers are away from the APs inso-much as the channel error occurs frequently. The first receives video packets without FEC from one AP (i.e., *w/o FEC*), the second receives and decodes FEC-encoded packets from one AP (i.e., *w/ FEC*), and the third receives FEC-encoded packets from

2 APs based on the proposed *partially overlapped* video multicast protocol. All the receivers have an embedded Wi-Fi Network Interface Card (WNIC), and an additional WNIC is used for receiving packets from 2 APs. As shown in Fig. 3.16, the average PSNR values of *w/o FEC*, *w/ FEC*, and *Partially overlapped* are 21.83 dB, 26.04 dB, and 37.12 dB during 5 minutes long video clip streaming, respectively. As shown in the snapshot, *partially overlapped* scheme achieves the best video quality and *w/ FEC* achieves the better video quality than *w/o FEC*.

### 3.6 Summary

In this chapter, we have proposed new reliable video multicast schemes in which with the help of AL-FEC and the coordination between multiple APs, each AP transmits (1) entirely different or (2) partially different FEC-encoded packets for reliable video multicast delivery. The proposed schemes extend the video multicast coverage by improving the video quality of cell-edge users. In addition, we have proposed a resource-allocation algorithm for the FEC-code rate adaptation of each AP to the limited wireless resource. The proposed FEC-code rate adaptation satisfies more users and enhances the video quality of the satisfied users. We also introduced a method for estimating the delivery ratio after FEC decoding. Our extensive evaluation using simulation and experimentation has demonstrated that the proposed schemes can enhance overall video quality for video multicast systems.

In future, we would like to expand the video multicast service area to larger areas and explore ways of utilizing spatial reuse for video multicast. We will also study combined cross-layer FEC-code rate adaptation and PHY-rate adaptation to improve resource efficiency and video quality further. We believe the proposed video multicast schemes are applicable to any wireless systems. For example, they can be used for

more reliable video streaming in smartphones with connection to both cellular and Wi-Fi networks.

## **Chapter 4**

# **Reliable Video Multicast with Efficient Feedback over Wi-Fi**

### **4.1 Introduction**

Today, the interest in Wi-Fi system, based on IEEE 802.11 standard [28], is increasing rapidly due mainly to the prevalence of smartphones. As the data rate of Wi-Fi increases, the video streaming service is becoming one of main applications over Wi-Fis today. Regarding the video streaming service, multicast transmission which transmits data simultaneously to a group of users is more bandwidth-efficient than the unicast transmission which sends data to one user at a time. IEEE 802.11 [28] standard supports multicast transmission.

However, error control with Automatic Repeat reQuest (ARQ) is not provided for the multicast transmission in legacy IEEE 802.11 standard, since there is no acknowledgement of requesting packet-retransmission. Therefore, multicast is inherently vulnerable to the transmission failures caused by wireless channel errors.

To overcome the unreliability of multicast transmission, two emerging standards



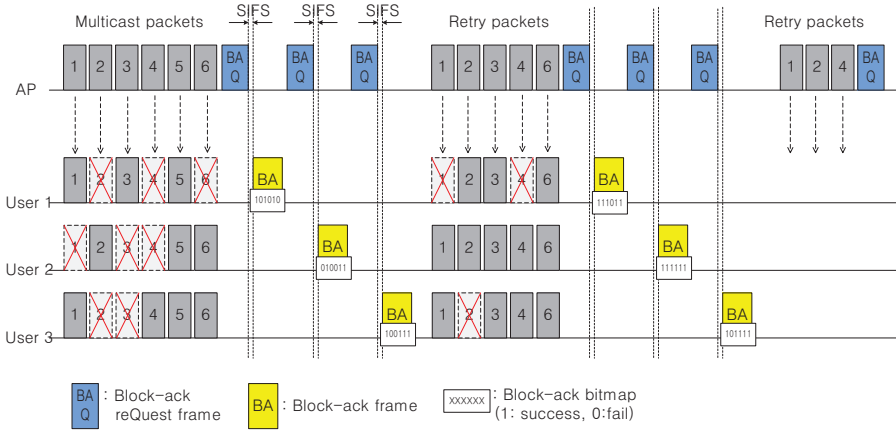


Figure 4.1: An example of GCR procedure.

define new features for the reliable video multicast service, i.e., Directed Multicast Service (DMS) in 802.11v [46], and GroupCast with Retries (GCR) in 802.11aa [47].

DMS allows a multicast user to request its serving AP to transmit multicast frames destined to itself as unicast frames. This conversion from multicast to unicast may have advantages in terms of reliability and efficiency, in that unicast transmission can utilize MAC-layer ARQ, RTS/CTS exchange, and higher PHY rate. However, the same multicast frame is transmitted multiple times with different destination addresses whenever DMS service is requested by multiple users. This reduces the benefit of the multicast transmission.

On the other hand, in order to provide reliable multicast service, GCR defines two additional retransmission schemes, namely, GCR unsolicited retry (GCR-UR) and GCR Block Ack (GCR-BA). GCR-UR makes the AP retransmit multicast frames without receiving any retry request from receivers. In order to utilize the time diversity gain, original frames and its retransmitted frames should be transmitted in different transmit opportunities (TXOPs). However, GCR-UR might make the meaningless retransmis-

sion of the multicast frames even though all the multicast users already receive the multicast frames.

GCR-BA enables multicast receivers to use the block acknowledgement (Block Ack) for multicast frames. Fig. 4.1 shows an example scenario of the GCR-BA operation. After sending a number of multicast frames, the AP regularly requests a user to transmit the Block Ack frame by sending an individual Block Ack reQuest (BAQ) frame, then the receiving user sends a Block Ack (BA) frame to indicate which MAC protocol data units (MPDUs) are correctly received. After gathering the Block Acks from one or more of GCR group members, the AP decides which MPDUs should be retransmitted. The choice of users to whom the AP requests the Block Ack is implementation-dependent. However, GCR-BA cannot guarantee the reliability of the multicast transmission as long as all the users do not send BA frames. On the contrary, collecting all the users' information of the received frames makes a huge overhead. To guarantee the reliability of the multicast users which send BA frames, the AP retransmits the MPDUs which are not received by all the users.

Meanwhile, packet-level Forward Error Correction (FEC) is a well-known approach for reliable video multicast. By generating parity packets, the sender enables the receivers to recover lost packets using those parity packets. The advantage of packet-level FEC is in that different receivers can recover different lost packets by utilizing the same parity packets. In most cases, although the lost packets of different users could be different, by utilizing FEC, such different lost packets can be recovered by the same parity packets. Various erasure correction coding schemes such as Reed-Solomon (RS) code and Raptor code can be used for this approach.

In this chapter, in order to provide the reliable high-quality video streaming over Wi-Fi, we propose the reliable multicast protocols based on both ARQ and packet-level FEC together. In addition, to reduce the overheads of feedback messages while

providing the reliable multicast service, we propose efficient feedback protocols for the reliable multicast. When both packet-level FEC and ARQ are used for the multicast, sending the information about the number of required parity frames for the successful recovery of the lost packets as the feedback message is more proper for the multicast users. In addition, the AP needs to know only the feedback value, i.e., the number of required parity frames, of the worst user(s) among the multicast users for the ARQ, not all the users' feedback values. Therefore, we propose efficient feedback protocols which can dramatically reduce the feedback overheads by intending the concurrent transmissions of multicast users' feedback, while let the AP learn easily the number of required parity frames of the worst user(s).

Moreover, the adaptive PHY rate selection for the multicast is proposed. In IEEE 802.11n [28] standard, the closed-loop Modulation and Coding Scheme (MCS) feedback mechanism is supported using HT-control field of MAC header. However, this MCS feedback mechanism is useful for only unicast transmissions. To extend it for the multicast transmission, the sender has to send MCS feedback request messages to the multiple multicast receivers and receive MCS feedback messages from the multiple multicast users individually. Utilizing the proposed efficient feedback protocols, which has the strength that it can easily collect the worst information from the multiple multicast users, the protocol for the adaptive PHY rate selection for the multicast transmission is proposed.

The rest of this chapter is organized as follows. Section 4.2 describes the motivation of the proposed reliable multicast protocols. Section 4.3 presents new feedback protocols for the reliable multicast. The PHY rate adaptation utilizing the efficient feedback protocols is proposed in Section 4.4. Section 4.5 evaluates the performance of the proposed multicast protocols, and finally, the chapter concludes with Section 4.6.

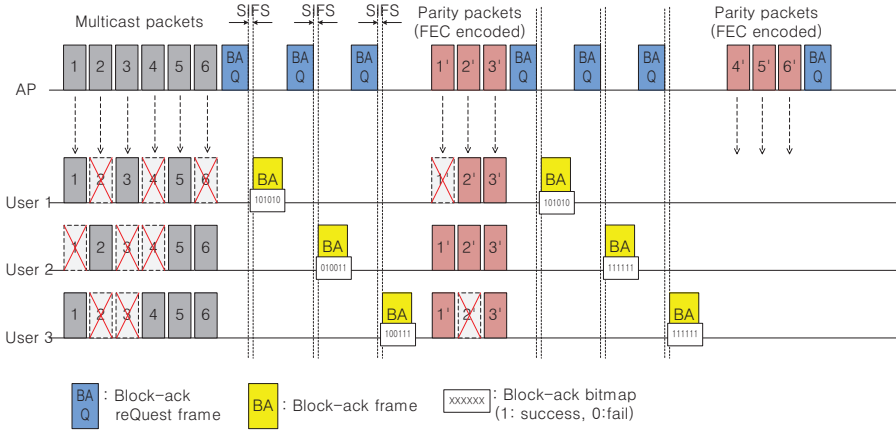


Figure 4.2: An example of GCR w/ FEC.

## 4.2 Motivation

Fig. 4.2 shows an example scenario of GCR-BA operation when the FEC is used. After receiving the BA frames, the AP sends FEC-encoded parity packets instead of original multicast packets for the retransmission. In the case of packet-level FEC, each multicast user can recover the missing frames by the additional transmissions of the parity packets. Therefore, for recovering the missing frames utilizing FEC, the number of received frames is more important than the indication which frames are correctly received, since the different receivers can recover different lost packets using the same parity packets. However, since the multicast receiver sends the BA frame to indicate which multicast packets are correctly received, the user repeatedly sends the BA frames until it recovers the lost packets. In addition, since the AP cannot guarantee the receptions of the transmitted parity packets on each user, the AP selects the number of parity packets to be transmitted based on the BA bitmaps of BA frames.

In order to provide reliable multicast service, when packet-level FEC is used, send-

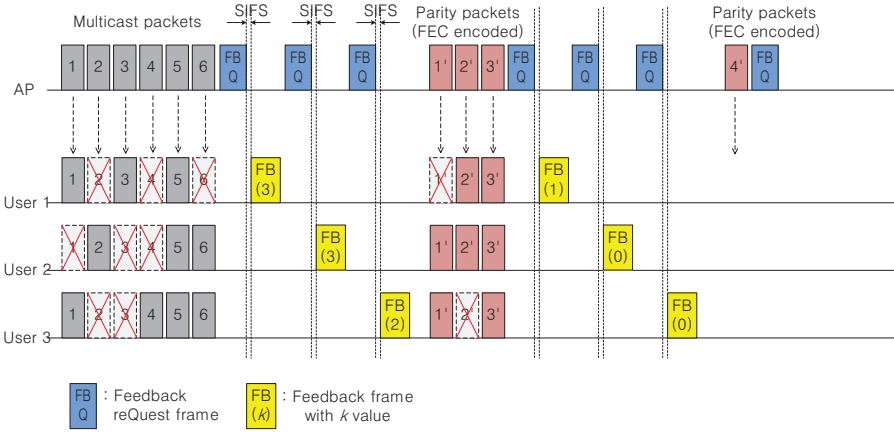


Figure 4.3: An example of ARQ w/ FEC procedure.

ing the information about the number of required parity frames for the successful recovery of the lost packets is more proper, instead of sending the BA frames which contain Bitmap field for indicating the received frames such as GCR-BA. Fig. 4.3 shows an example scenario of ARQ operation for multicast users when the FEC is used. The AP sends Feedback reQuest (FBQ) frame instead of BA reQuest (BAQ) frame, and then the multicast user sends Feedback (FB) frame instead of BA frame. This can slightly reduce the overhead of the feedback procedure for ARQ by including a single number of required parity frames instead of the BA bitmap of the multicast frames in the BA frame. The expected number of required parity frames is almost the same as the number of lost frames in the ideal FEC coding scheme. For the realistic FEC coding scheme, each user requests one or two more parity frames than the number of lost packets considering the coding performance of the given FEC coding scheme.

In addition, considering all the users' reliability, the sender identification of the feedback message is not important for the retransmission. In the case of GCR-BA, to receive the BA frame, the sender individually requests BA frame to each user. To

reduce this overhead, the sender can send a group feedback request frame. The user which receives this group feedback request frame responds via the feedback message which carries the number of required parity frames. Of course, the user which do not require the reliable multicast service does not need to send feedback message. The sender, after receiving the feedback messages from the multiple multicast users, transmits parity frames considering the largest number of required parity frames. Since the Raptor FEC has the characteristic of the rateless coding, it can generate unlimitedly many parity frames. In this sense, the Raptor FEC is proper for the reliable multicast protocols with ARQ and FEC.

### **4.3 Proposed Feedback Protocols for Reliable Multicast**

In this section, to reduce the overheads of feedback messages while providing the reliable multicast service, we propose efficient feedback protocols for the reliable multicast utilizing both ARQ and FEC together. The proposed feedback protocols are summarized as follows:

- 1. Idle-time-based feedback**
- 2. Slot-based feedback**
- 3. Flash-based feedback**
- 4. Busy-time-based feedback**

All the proposed feedback protocols utilize the simultaneous transmissions by the multiple users in view of the collision. By utilizing the simultaneous transmissions, in the proposed feedback protocols, unlike the GCR-BA, the feedback overheads do not increase as the number of multicast users increases.

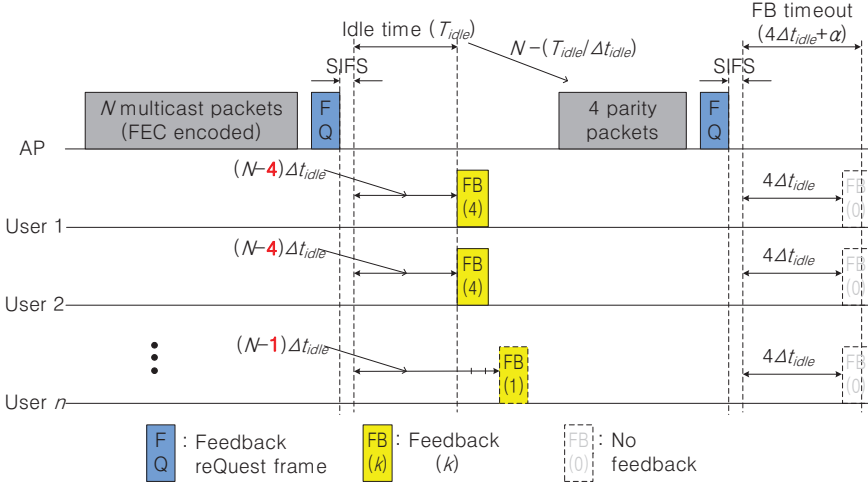


Figure 4.4: An example of reliable multicast with idle-time-based feedback.

#### 4.3.1 Idle-time-based Feedback

Fig. 4.4 shows an example procedure of the reliable multicast with idle-time-based feedback. After the AP sends  $N$  multicast packets after FEC encoding, where  $N$  is the number of multicast packets to be transmitted, it sends Feedback reQuest (FQ) frame to check the number of required parity packets of the users for the recovery of the lost packets. Each user, upon receiving the FQ frame, sends feedback (FB) frame after waiting for the corresponding waiting time to the feedback value and Short Interframe Space (SIFS) interval, similar to the backoff procedure of IEEE 802.11. The corresponding waiting time of user  $i$ , i.e.,  $T_{idle,i}$ , is equal to  $(N_{max} - k_i)\Delta t_{idle}$ , where  $N_{max}$ ,  $k_i$ , and  $\Delta t_{idle}$  are the maximum feedback value carried by FQ frame, the feedback value of user  $i$  for indicating the number of required parity packets, and the time unit for indicating the feedback value, respectively. Since the AP needs to know the worst users' feedback value for the retransmission, the user which needs more parity packets for the recovery of the lost packets waits less time. On the contrary, the user

which needs less parity packets waits more time while sensing the transmissions of other users' FB frames. Of course, the user does not need to send FB frame when it receives all the multicast packets or it senses the transmissions of other users' FB frames. In this protocol, the collisions between the FB frames of the multiple users is not important. As we have mentioned above, the AP does not need to know the sender identification of each feedback message. The AP only checks the idle time between the FQ frame and the first FB frame (or the first busy time) and can learn the largest feedback value based on the length of this idle time. After the AP collects the feedback values of the users, the AP generates as many parity packets as the largest feedback value(s). When the idle time is equal to  $T_{idle}$ , the number of generated parity packets is calculated from  $N_{max} - (T_{idle}/\Delta t_{idle})$ . Unlike the GCR-BA, the size of feedback overhead is unrelated to the number of multicast users, and hence, the proposed protocol is advantageous when the number of multicast users is relatively large. This procedure is repeatedly done until all the STAs recover the multicast packets correctly or the number of retransmissions reaches the maximum retransmission limit. Meanwhile, the protocol has a weakness in that the AP should wait as much as the maximum idle time, i.e., FB timeout ( $= N_{max}\Delta t_{idle}$ ), after sending FQ frame, even though all the users do not need any additional parity packet.

### 4.3.2 Slot-based Feedback

Fig. 4.5 shows an example procedure of the reliable multicast with slot-based feedback. After the AP sends  $N$  multicast packets, it sends Feedback reQuest (FQ) frame to check the number of required parity packets of the users. Each user sends feedback (FB) frame on the corresponding time slot to indicate its feedback value without considering the collision after receiving the FQ frame. For the efficiency, the slot for the larger feedback value is located earlier, so that the AP can learn the largest feedback



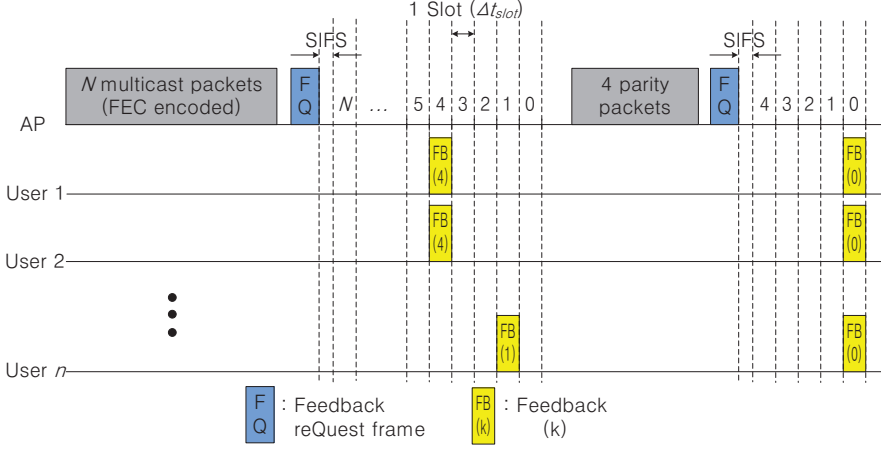


Figure 4.5: An example of reliable multicast with slot-based feedback.

value earlier. The number of slots is equal to  $N_{max}$ , which is announced by FQ frame. Due to the collision, the AP can not receive the FB frame correctly, however, the AP can sense the channel status, i.e, whether the channel is busy or idle in a specific time slot. Therefore, the AP can learn that some user(s) send FB frame in that slot. The retransmission procedure is the same as the protocol of idle-time-based feedback. The length of each time slot, i.e.,  $\Delta t_{slot}$  might be very short insomuch as the user transmits very short tone signal which only can indicate the channel busy status. However, to send a very short tone signal, some additional efforts for the modification on the current Wi-Fi device are required. Meanwhile, every feedback procedure has the fixed overhead as much as the length of all the slots, even though all the users do not need to require the additional parity packets.

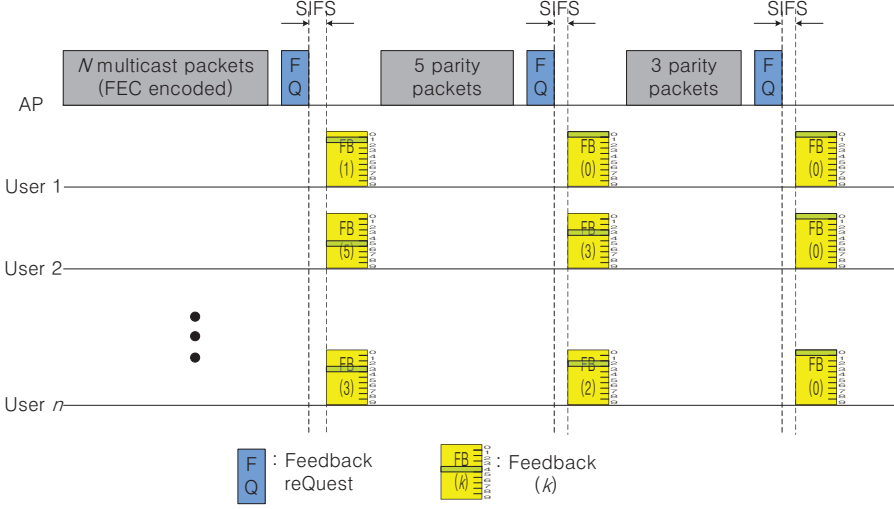


Figure 4.6: An example of reliable multicast with flash-based feedback.

### 4.3.3 Flash-based Feedback

Fig. 4.6 shows an example procedure of the reliable multicast with flash-based feedback. In the case of slot-based feedback, the length of all the slots might be the big overhead. IEEE 802.11 uses Orthogonal Frequency Division Multiplexing (OFDM) system. In [48], utilizing OFDM system, the proposed system provides that a device sends a flash signal, which is the high powered single subcarrier signal, on a specific subcarrier frequency in particular time slot for sending the control message concurrently with the other device's transmission. To reduce the overhead, utilizing this flash signal in [48], each user sends feedback (FB) frame which carries a flash signal on only the corresponding frequency subcarrier of the feedback value, similarly to the uplink channel access of Orthogonal Frequency Division Multiple Access (OFDMA). By checking the carried flash signal on each subcarrier, the AP can learn the largest feedback value. In this protocol, the collision between the flash signals is not a mat-

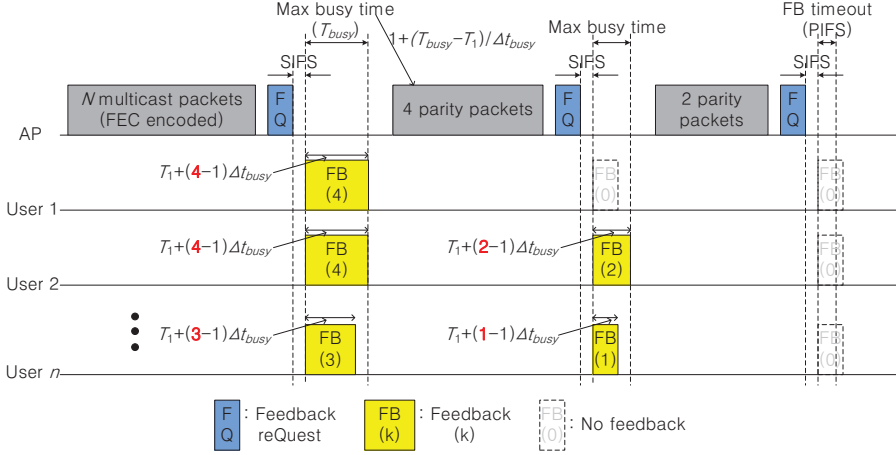


Figure 4.7: An example of reliable multicast with busy-time-based feedback.

ter, since the AP wants to know only the corresponding feedback value sent by some user(s). The proposed protocol can reduce the feedback overhead dramatically, however, there are implementation issues to modify the existing Wi-Fi system for sending the flash signal on only the corresponding frequency subcarrier.

#### 4.3.4 Busy-time-based Feedback

Fig. 4.7 shows an example procedure of the reliable multicast with busy-time-based feedback. Unlike the idle-time-based feedback, all the users send FB frame right after receiving Feedback reQuest (FQ) frame of the AP with the SIFS interval. In this protocol, the transmission time of the FB frame for user  $i$ , i.e.,  $T_{busy,i}$ , indicates the corresponding feedback value  $k$  of user  $i$ . Therefore, the user which has a smaller feedback value sends a shorter FB frame, while the user which has a larger feedback value sends a longer FB frame.  $T_{busy,i}$  is equal to  $T_1 + (k - 1)\Delta t_{busy}$ , where  $T_1$  and  $t_{busy}$  are the transmission time of the FB frame for indicating the feedback value as 1 and the time

unit for indicating the feedback value, respectively. For controlling the transmission time of the FB frame to indicate the corresponding feedback value, the FB frame additionally carries meaningless payload for increasing the transmission time of FB frame, and thus, it is easily implementable in the existing Wi-Fi system. The concurrent transmissions of multiple FB frames make collision, however, the AP needs to know only the busy time during the transmissions of the FB frames because only the largest feedback value is used for selecting the number of parity packets to be transmitted. The AP can learn the largest feedback value from the maximum busy time after sending a FQ frame, i.e.,  $T_{busy}$ , by calculating  $1 + (T_{busy} - T_1) / \Delta t_{busy}$ . A user does not need to send the FB frame when its feedback value is equal to zero, that is, when the user correctly receives all the multicast packets. Therefore, when all the users do not need any additional parity packet, the AP can detect the end of retransmission within the short FB timeout, e.g., Priority Interframe Space (PIFS) interval, because the idle channel during FB timeout after sending the FQ frame indicates all the users' successful receptions of the multicast packets. Accordingly, busy-time-based feedback protocol is expected to achieve the better performance than the idle-time-based feedback and slot-based feedback protocols. Even if flash-based feedback protocol can achieve the better performance than the other feedback protocols, due to the complexity and implementation issues, we conclude that busy-time-based feedback protocol is the most proper protocol for the reliable multicast, considering both the complexity and the efficiency of FB protocols. The detailed comparison is presented in Section 4.5.

#### 4.4 PHY Rate Adaptation in Multicast Transmission

The proposed feedback protocols can dramatically reduce the feedback overheads compared with the existing reliable multicast protocols, i.e., GCR-BA and DMS. Uti-

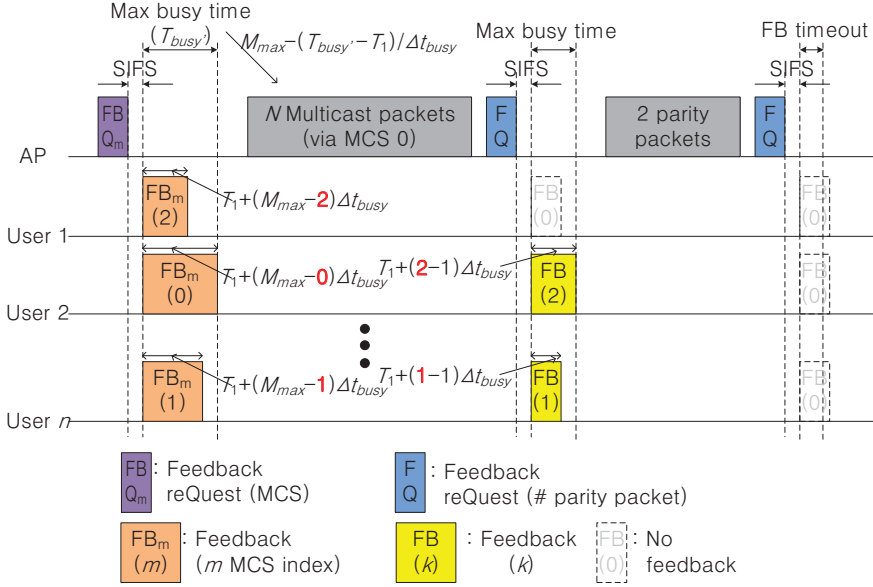


Figure 4.8: An example of reliable multicast with busy-time-based feedback and PHY rate adaptation.

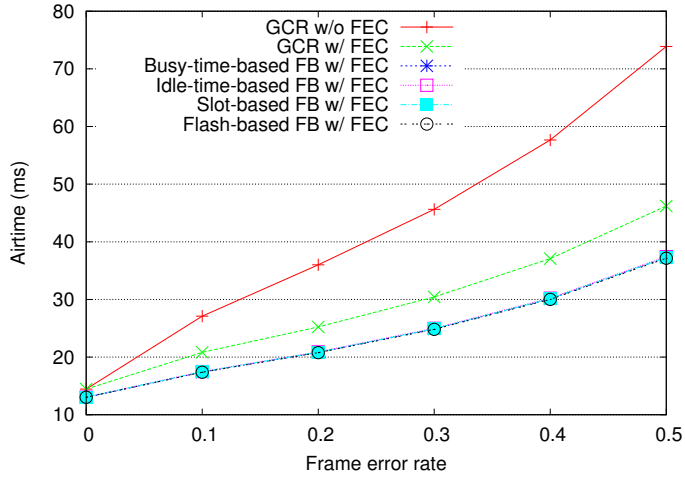
lizing the proposed feedback protocols, which has the strength that it can easily collect the largest feedback value from multiple multicast users, the AP can adaptively select the PHY rate based on the feedback information.

The closed-loop Modulation and Coding Scheme (MCS) feedback mechanism is supported using HT-control field of MAC header in IEEE 802.11n [28]. However, this MCS feedback mechanism is useful only for the unicast transmission. To extend it for the multicast transmission, the sender has to send MCS feedback request messages to the multiple multicast receivers and receive MCS feedback messages from the multiple multicast users individually. To overcome this huge overhead, we propose a closed-loop MCS feedback mechanism for the multicast transmission. In general, the multicast transmission is performed with the robust MCS since the sender cannot know

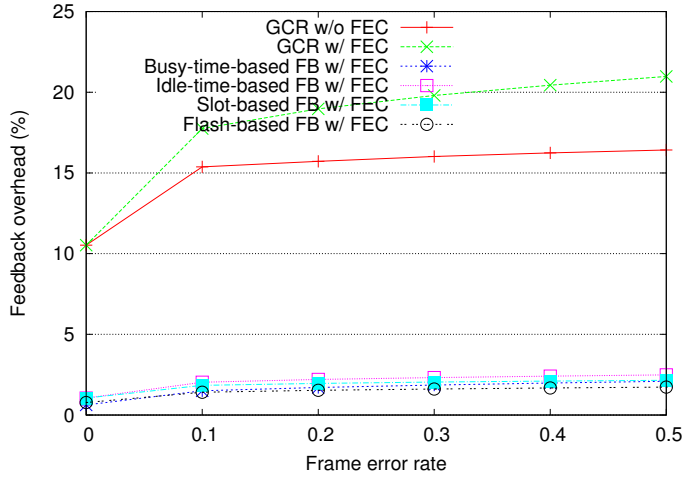
the channel status to the multicast receivers. By using this MCS feedback mechanism, the multicast transmission with the higher MCS is possible.

Fig. 4.8 shows an example procedure of the reliable multicast with busy-time-based feedback and PHY rate adaptation. Before sending multicast packets, the AP sends MCS Feedback reQuest (FBQ<sub>m</sub>) frame. Similarly to the closed-loop MCS feedback in 802.11n, each user, which receives the FBQ<sub>m</sub> frame, checks the signal strength of FBQ<sub>m</sub> frame for selecting the preferred MCS for the transmissions of multicast packets. When the signal strength is high, the user requests high MCS transmission of multicast packets. The feedback value of the MCS index  $m$  is represented by the transmission time of the MCS feedback (FB<sub>m</sub>) frame when busy-time-based feedback protocol is used. The FB<sub>m</sub> frame with the more robust MCS has the longer transmission time for letting the AP know the most robust MCS among the feedback messages. The transmission time of FB<sub>m</sub> frame which indicates feedback value as  $m$  is equal to  $T_1 + (M_{max} - m)\Delta t_{busy}$ , where  $M_{max}$  is the number of possible MCSs. For selecting the feedback value of MCS index of the user, the user needs to know which MCS index is the best for the multicast transmission even in the case when the user has the worst channel among the multicast users.

Actually, utilizing the proposed feedback mechanism, FEC code rate adaptation is also possible. However, sending the parity packets in advance before receiving the feedback messages for the retransmission might be the overhead when the channel error rarely happens or the wireless channel status is varying over time. Besides, since the proposed feedback protocol can have relatively small overhead considering the transmission time for the multicast packets, transmitting parity packets after receiving feedback message is more efficient than the transmission of parity packets in advance. The performance when FEC coding before receiving the feedback messages is used is evaluated in Section 4.5.



(a) Average airtime



(b) Feedback overhead

Figure 4.9: Performance comparison for the different frame error rate (MCS: 6.5 Mbps, # multicast users= 10).

## 4.5 Performance Evaluation

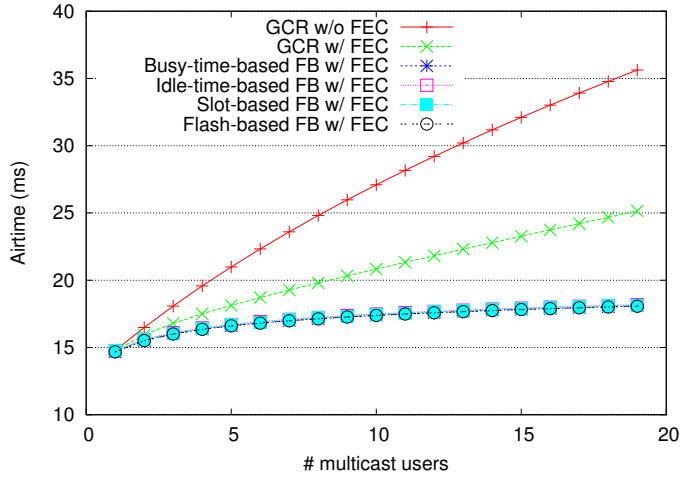
In this section, we comparatively evaluate the performance of the proposed reliable multicast protocols. An H.264 CBR video clip of 500 kbps is used for the evaluation.

The number of multicast packets to be transmitted at one time, i.e.,  $N$ , is assumed to be 10. We evaluate both the average airtime for transmitting  $N$  multicast packets correctly and Peak Signal-to-Ratio (PSNR), which is a widely-accepted measure of video quality. The average airtime indicates the delay performance from the AP to the worst multicast user(s).

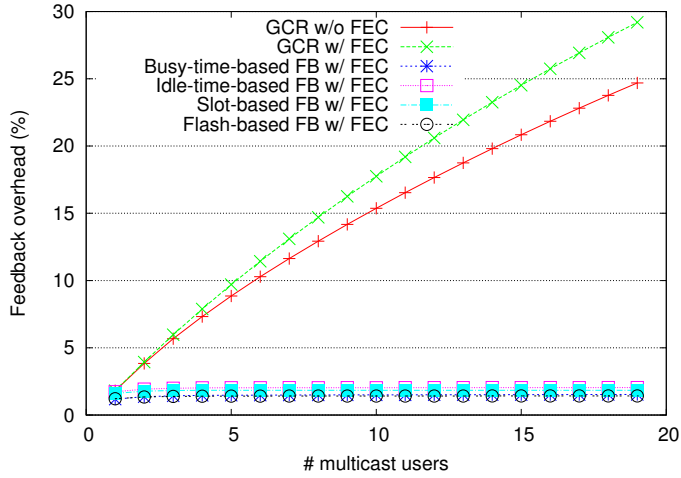
IEEE 802.11n PHY and MAC models are used, and the static wireless channel without the channel fading is assumed unless specified otherwise. All the multicast packets are transmitted via MCS 0 of 802.11n, i.e., 6.5 Mbps, using A-MPDU unless specified otherwise. The size of  $\Delta t_{busy}$ ,  $\Delta t_{idle}$ ,  $\Delta t_{slot}$  are set to the length of one OFDM symbol, i.e., 4  $\mu$ s.  $T_1$  in Busy-time-based feedback is equal to the length of Null Data Packet (NDP) frame which does not carry any MAC payload.

Fig. 4.9 shows the performance of GCR-BA and the proposed feedback protocols for the different frame error rate when the number of multicast users is 10. As the frame error rate increases, the average airtime increases, because the AP transmits more multicast packets for recovering the lost packets. It is found that GCR w/o FEC consumes much more airtime for successfully transmitting  $N$  multicast packets than GCR w/ FEC scheme and the proposed multicast protocols consumes much less airtime than GCR schemes. Fig. 4.9(b) shows the feedback overhead, which is the ratio of the airtime for the feedback exchanges to the total airtime. In the case of GCR w/o FEC and GCR w/ FEC, relatively higher feedback overheads are required for the reliable multicast than the proposed feedback protocols. On the other hand, the feedback overheads of the proposed feedback protocols are less than 3 %, and hence the proposed feedback protocols are very efficient protocols for reliable multicast. Flash-based FB achieves the best performance among the proposed feedback protocols and Busy-time-based FB outperforms Idle-time-based FB and Slot-time-based FB, since Busy-time-based FB especially requires less waiting time when all the multicast users





(a) Average airtime



(b) Feedback overhead

Figure 4.10: Performance comparison for the different number of multicast users (MCS: 6.5 Mbps, frame error rate= 0.1).

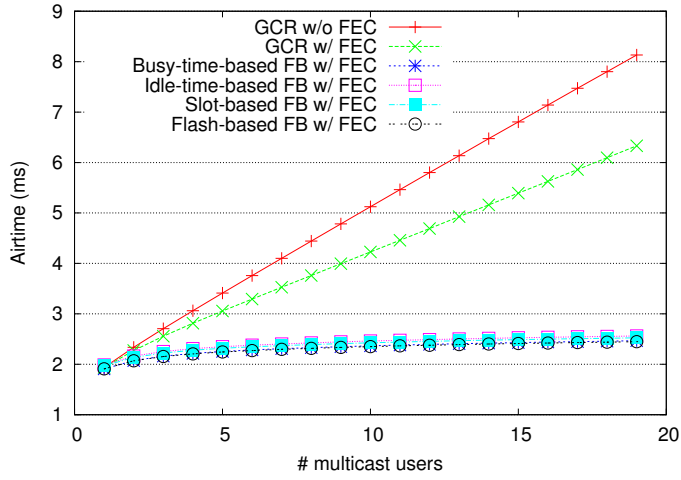
successfully recovery all the multicast packets.

Fig. 4.10 shows the performance comparisons between GCR-BA and the proposed

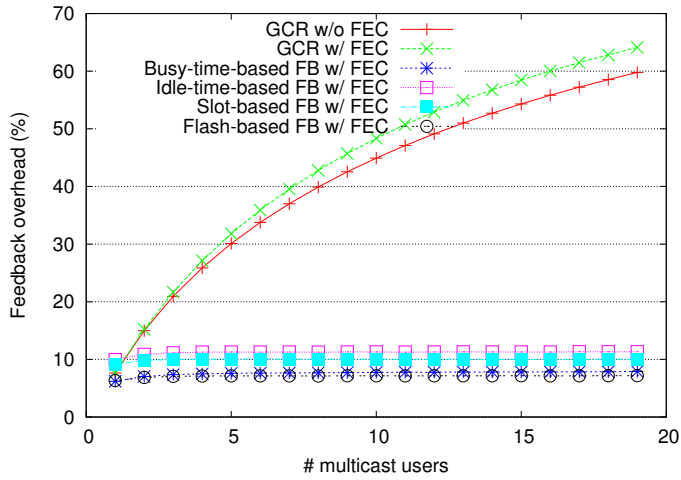
feedback protocols depending on the number of multicast users when the frame error rate is fixed to 0.1. As the number of multicast users increases, more feedback overheads are required. However, compared with the proposed feedback protocols, GCR w/o FEC and GCR w/ FEC schemes consume more airtime for successfully transmitting  $N$  multicast packets, and the feedback overhead increases as the number of multicast users increases. Meanwhile, in the cases of the proposed feedback protocols, the feedback overheads are almost fixed regardless of the number of multicast users, since the proposed feedback protocols utilize the collisions among feedback messages of multicast users.

Fig. 4.11 shows the performance depending on the number of multicast users when the frame error rate is fixed to 0.1 and all the multicast packets are transmitted via MCS 7 of 802.11n, i.e., 65 Mbps. Since the multicast packets are transmitted via the high rate, the feedback overheads relatively increase. In the cases of GCR w/o FEC and GCR w/ FEC schemes, the airtime for the feedback exchanges is even larger than the airtime for the transmission of multicast packets when the number of multicast users is larger than 12.

Fig. 4.12 shows the performance comparisons between FEC w/o ARQ and FEC w/ ARQ schemes. The average airtime of GCR w/ ARQ and Busy-time-based FB w/ ARQ increases as the frame error rate increases, since the AP transmits more parity packets to recover the lost packets in the high frame error environments. Meanwhile, since FEC w/o ARQ schemes do not provide any retransmission procedure, the airtime is always the same regardless of frame error rate.  $N_{enc}$  indicates the number of transmitted FEC-encoded multicast packets including the original multicast packets and parity packets. As  $N_{enc}$  increases, more airtime is required. However, since FEC w/o ARQ schemes do not guarantee the reliable transmissions, PSNR is severely reduced in high frame error rate environments. GCR w/ ARQ and Busy-time-based FB



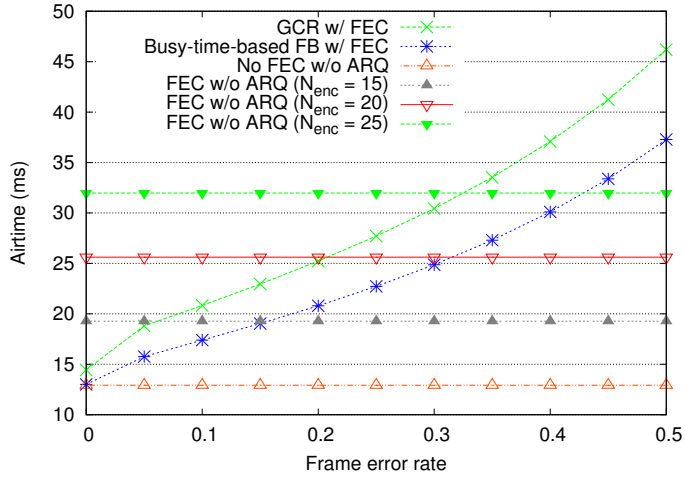
(a) Average airtime



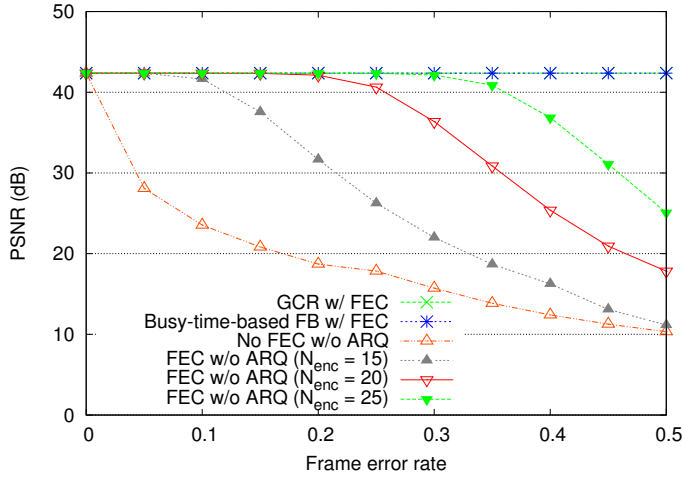
(b) Feedback overhead

Figure 4.11: Performance comparison for the different number of multicast users (MCS: 65.0 Mbps, frame error rate= 0.1).

w/ ARQ always provide the best video quality even though more airtime is required for high frame error rate.



(a) Average airtime



(b) PSNR

Figure 4.12: Performance comparison between w/ ARQ and w/o ARQ (MCS: 6.5 Mbps, # multicast users= 10).

Fig. 4.13 shows the performance of the MCS adaptation in the multicast transmission when Busy-time-based FB is used. As the Signal-to-Noise Ratio (SNR) increases,

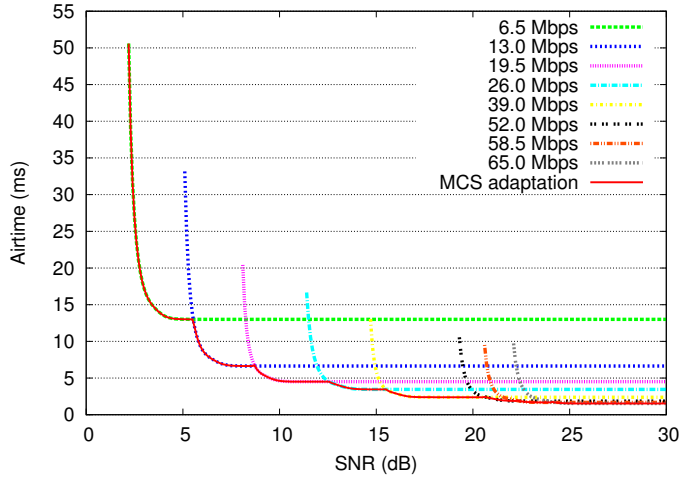
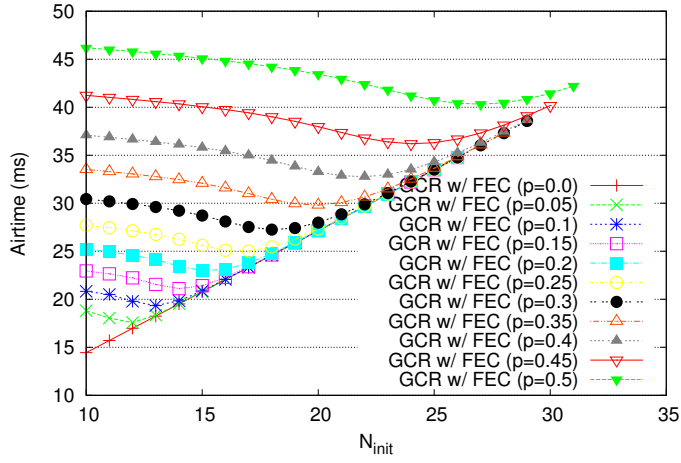


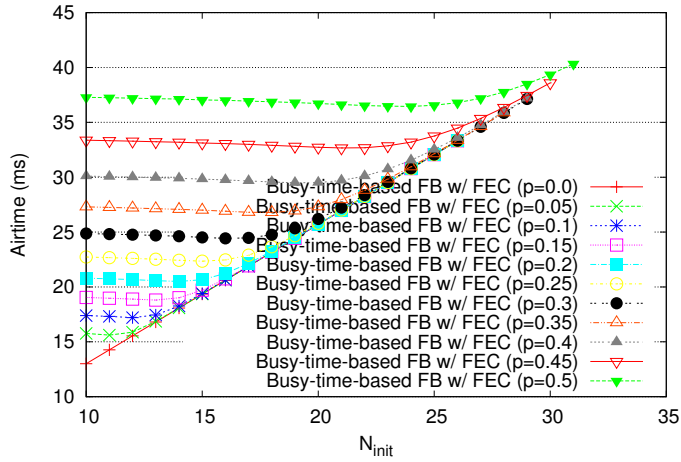
Figure 4.13: The average airtime for the various MCSs (Busy-time-based FB, # multi-cast users= 10).

the average airtime decreases since the frame error rate decreases for all the MCSs. The high rate MCS can reduce the transmission time of the multicast packets, however, the frame error rate might increase. Therefore, the selection of proper MCS in a given wireless channel environment (e.g., SNR) is important. The proposed MCS adaptation provides the best MCS selection for the minimum airtime as shown in the figure.

Fig. 4.14 shows the average airtime depending on  $p$  and  $N_{init}$ , where  $p$  and  $N_{init}$  are the frame error rates and the number of transmitted multicast packets including original packets and the parity packets which are transmitted in advance before any feedback exchange, respectively. In the case of GCR w/ FEC in Fig. 4.14(a), there is the best  $N_{init}$  value at a given frame error rate for reducing the airtime, since the overhead of feedback exchanges is relatively large. That means, the transmissions of the FEC-encoded parity packets before the feedback exchange considering the frame error rate might be efficient when the feedback overhead is considerable. Meanwhile,



(a) GCR w/ FEC



(b) Busy-time-based FB

Figure 4.14: The average airtime for the different frame error rates and  $N_{init}$  (MCS: 6.5 Mbps, # multicast users= 10).

in the case of Busy-time-based FB w/ FEC in Fig. 4.14(b), sending the parity packets in advance before receiving the feedback messages might be the overhead when the

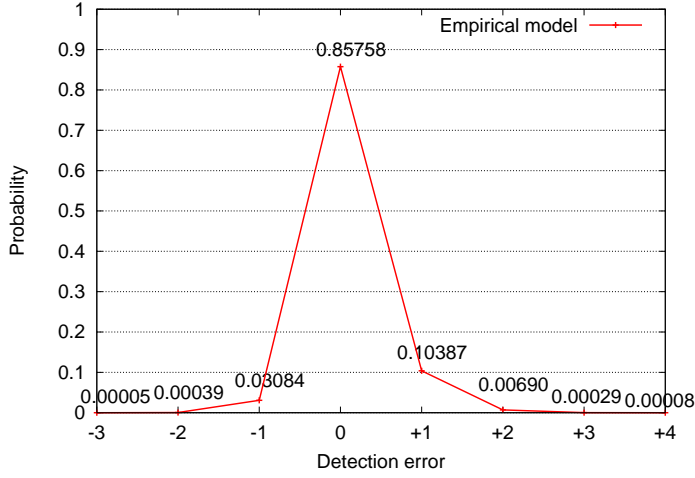


Figure 4.15: Empirical model based on the experiments.

channel error rarely happens or the wireless channel status varies over time. That is, the additionally transmitted parity packets might be the meaningless overhead when the lost packets can be recovered without the additional parity packets.

#### 4.5.1 Performance evaluation considering feedback error

In Busy-time-based feedback, the AP can learn the largest feedback value from the maximum busy time after sending a FQ frame, i.e.,  $T_{busy}$ , by calculating  $1 + (T_{busy} - T_1)/\Delta t_{busy}$ . However, sometimes actual Wi-Fi devices cannot exactly measure the length of channel-busy time. We verify the accuracy of commercial Wi-Fi device' measurement of channel-busy time. In the experiments, Qualcomm Atheros AR9380 Wi-Fi chipset [55] is used and we modify the existing Wi-Fi device driver (Compat-drivers-3.8.3-2 [56]) to measure channel-busy and channel-idle time. In this chapter, since we assume  $\Delta t_{busy}$  is equal to the length of one OFDM symbol (i.e., 4 us), the measured busy time is translated to the number of OFDM symbols, and we compare the number

of actual OFDM symbols and the number of measured OFDM symbols. Therefore, considering the error of measurement of channel-busy time, the largest feedback value is calculated by  $1 + \lfloor (T_{busy} - T_1) / \Delta t_{busy} + 0.5 \rfloor$ .

In the experiment, four transmitters simultaneously transmit feedback signals with the different (or same) feedback values (i.e., the number of OFDM symbols) and the receiver measures the channel-busy time of the simultaneous feedback, and we measure the busy time in the environments of the various combinations of feedback values. When only one transmitter transmit feedback signals with various feedback values without any simultaneous transmission, the receiver almost exactly measure the number of OFDM symbols with very high probability (= 0.9996). However, when four transmitters simultaneously transmit feedback signals, the receiver measures the number of OFDM symbols with 85.758 % probability among 50,000 samples, due to the simultaneous transmissions from multiple transmitters.

Fig. 4.15 shows the empirical model based on the experiments. The detection error indicates the value of (the number of sensed OFDM symbols - the number of actual OFDM symbols). That is, 'O' indicates the case of the accurate measurement, and '+1' and '-1' indicate the cases that the receiver measures one symbol more and less than the number of actual OFDM symbols, respectively. Even though the accuracy is lower than 90 %, the case that the gap between the number of sensed OFDM symbols and the number of actual OFDM symbols is larger than 2 occurs with very lower probability (= 0.00771). The detection error makes unnecessary additional parity packets' transmissions or additional feedback exchange procedures when the receiver overestimates the busy time or underestimates the busy time, respectively. However, in our proposed Busy-time-based feedback protocol, when all the users correctly all the multicast packets, that is, the maximum feedback value is equal to 0, the detection error will not occur, since no signal is transmitted after FQ frame.



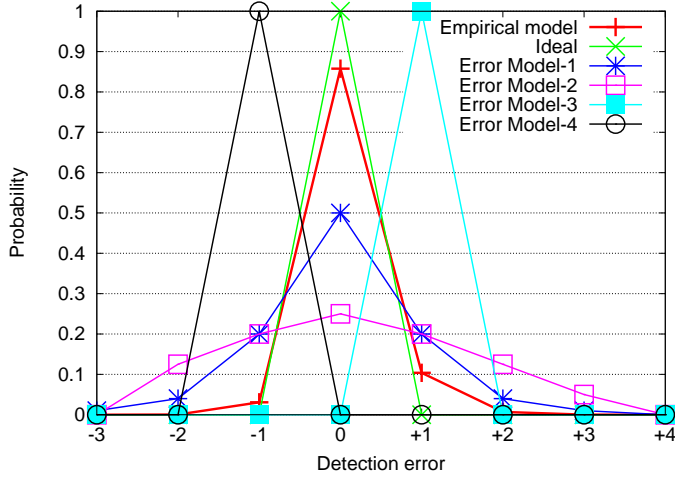
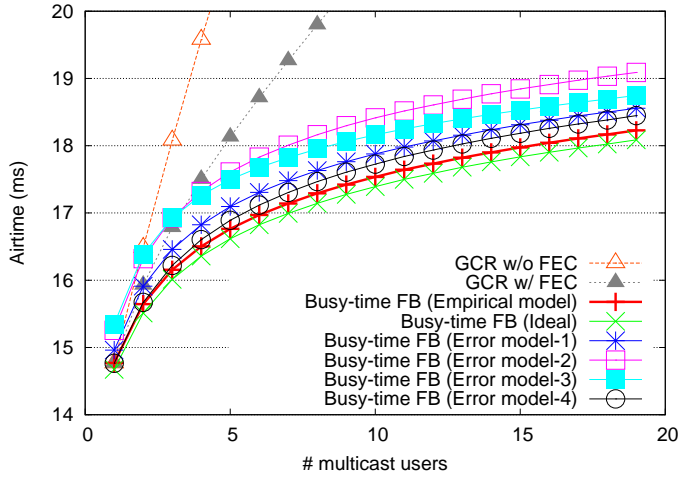


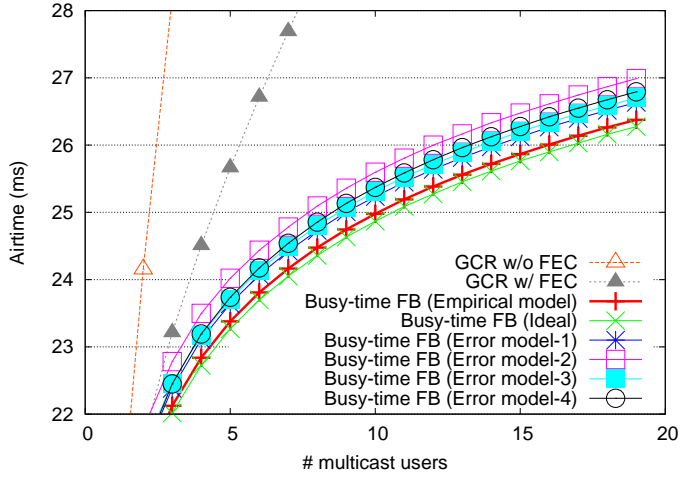
Figure 4.16: Assumed feedback error model.

Using this empirical error model in Fig. 4.15, we evaluate the performance of proposed Busy-time-based feedback protocol. As shown in Fig. 4.16, we assume some additional feedback error models for the comparison. *Ideal* indicates the case that the detection error never happen. *Error model-1* and *Error model-2* are the cases that each accuracy is equal to 0.5 and 0.25, respectively. *Error model-3* and *Error model-4* are the extreme cases that the number of sensed OFDM symbols is always one symbol larger and smaller than the number of actual OFDM symbols, respectively. These error models are used for verifying the performance degradation due to the detection error.

Figs. 4.17 and 4.18 shows the average airtime for the the different detection error models. *Ideal* achieve the best performance since there is no detection error. In *Empirical model* which accuracy is 85.758 %, the average airtime is slightly larger than *Ideal* case since the detection error makes unnecessary additional parity packets' transmissions or additional feedback exchange procedures. We find that the average airtime increases as the accuracy decreases from the results of *Ideal*, *Empirical model*,



(a) Frame error rate= 0.1



(b) Frame error rate= 0.3

Figure 4.17: Performance comparison for the different detection error models (MCS: 6.5 Mbps).

*Error model-1*, and *Error model-2*. As shown in Figs. 4.17(a), 4.17(b), and 4.18, *Error model-4* achieves the better performance than *Error model-3* in low frame error rate

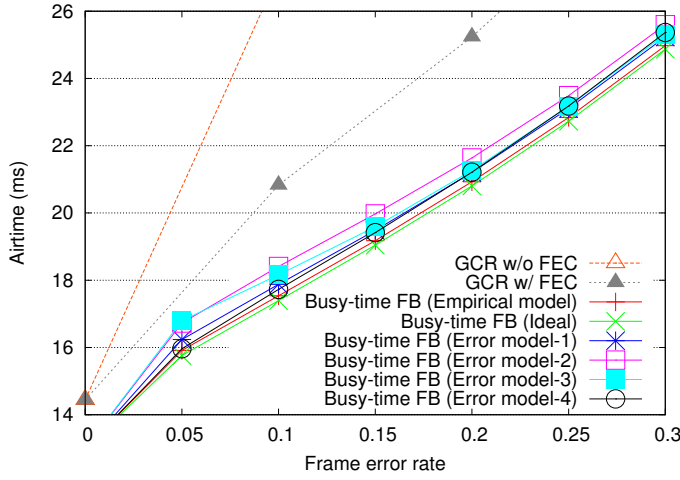


Figure 4.18: Performance comparison for the different detection error models (MCS: 6.5 Mbps, # multicast users= 10).

environment, and *Error model-3* achieves the better performance than *Error model-4* in high frame error rate environment. The additional parity packet's transmission makes unnecessary overhead in low frame error rate environment, however, in high frame error rate environment, the additional parity packet's transmission helps the recovery of lost multicast packets because the parity packets can also be lost. From the results, we find that the performance does not seriously decrease even in low accuracy cases. Considering the transmitted parity packets' possible transmission failures and the very low overhead of the proposed feedback exchange protocol, the serious performance degradation due to the detection error rarely happens. Therefore, even if the detection error sometimes occurs, the proposed Busy-time-based feedback protocol works well, and the video multicast with this Busy-time-based feedback protocol provides the near-perfect reliability with relatively low overhead.

## 4.6 Summary

In this chapter, we propose the reliable multicast protocol considering both ARQ and packet-level FEC together. For the proposed reliable multicast protocol, the multiple feedback protocols, i.e., Idle-time-based feedback, Slot-based feedback, Flash-based feedback, and Busy-time-based feedback, are also proposed for reducing the feedback overheads. The proposed feedback protocols let the AP know easily the number of required parity frames of the worst user(s) by reducing the feedback transmissions or intending the concurrent transmissions, which makes the collisions, between feedback messages for reducing the feedback overheads. In addition, utilizing the proposed efficient feedback protocols, we propose the PHY rate adaptation based on the close-loop MCS feedback in multicast transmissions. From the evaluations, the proposed protocols can reduce the feedback overheads, while the reliable multicast transmissions are guaranteed.

For the future work, we would like to extend the proposed reliable multicast protocols to the environments of multiple APs. By adjusting the number of transmitted parity packets of each AP, more efficient recovery of the lost packets is expected. In addition, we expect that the proposed feedback protocols can be available for FEC code rate adaptation. The combined cross-layer FEC-code rate adaptation and PHY-rate adaptation are an good solution for high-quality video streaming while providing the resource efficiency.

## **Chapter 5**

### **Conclusion and Future Work**

#### **5.1 Research Contributions**

In this dissertation, we addressed the high-quality reliable video streaming considering the resource efficiency over wireless networks. The main contributions of the dissertations are as follows.

In Chapter 2, we propose new link adaptation policies for high-quality uncompressed video streaming at 60 GHz band. For the better link adaptation, we adopt UEP schemes and develop a new parameter, i.e., ePSNR. ePSNR estimates the video quality in the error-prone wireless channel environments, and the proposed link adaptation policies select the appropriate MCSs using this ePSNR value. Through the proposed link adaptation policies, we can provide high video quality and efficient resource allocation at the same time.

In Chapter 3, we have proposed new reliable video multicast schemes in which with the help of AL-FEC and the coordination between multiple APs, each AP transmits (1) entirely different or (2) partially different FEC-encoded packets for reliable video multicast delivery. The proposed schemes extend the video multicast coverage

by improving the video quality of cell-edge users. In addition, we have proposed a resource-allocation algorithm for the FEC-code rate adaptation of each AP to the limited wireless resource. The proposed FEC-code rate adaptation satisfies more users and enhances the video quality of the satisfied users. We also introduced a method for estimating the delivery ratio after FEC decoding. Our extensive evaluation using simulation and experimentation has demonstrated that the proposed schemes can enhance overall video quality for video multicast systems.

In Chapter 4, we propose the reliable multicast protocol considering both ARQ and packet-level FEC together. For the proposed reliable multicast protocol, the multiple feedback protocols, i.e., Idle-time-based feedback, Slot-based feedback, Flash-based feedback, and Busy-time-based feedback, are proposed for reducing the feedback overheads. The feedback overheads are reduced by intending the concurrent transmissions which makes the collisions between feedback messages, while the AP easily knows the number of requiring parity frames of the worst user(s) for the recovery of all the lost packets. In addition, utilizing the proposed efficient feedback protocols, we propose the PHY rate adaptation based on the close-loop MCS feedback in multicast transmissions. From the evaluations, the proposed protocols can reduce the feedback overheads, while the reliable multicast transmissions are guaranteed.

The summary of this dissertation is presented in Fig. 5.1.

## **5.2 Future Research Directions**

This section presents some additional research issues that are related to the high-quality video streaming over wireless networks, which require further investigation.

First, though we in Chapter 2 consider uncompressed video, the size of video source is still a big constraint for reliable video streaming. Adaptation of video source

Video streaming over wireless networks		
<b>Ch. 2</b> Link adaptation for uncompressed video streaming in 60 GHz wireless network	<b>Ch. 3</b> Reliable video multicast over Wi-Fi networks with coordinated multiple APs	<b>Ch. 4</b> Reliable video multicast with efficient feedback over Wi-Fi
One-to-one (Unicast)	One-to-multiple (Multicast)	
Low latency uncompressed video over 60 GHz band	Compressed video over Wi-Fi	
UEP	FEC	
ePSNR	Coordinated multiple APs (diversity gain)	ARQ with efficient feedback protocols
Link adaptation for resource efficiency	FEC code rate adaptation	PHY rate adaptation
Better reliability		Near-perfect reliability
High-Quality & reliable video streaming + Resource efficiency		

Figure 5.1: The summary of this dissertation.

format is worth considering for the future work in order to resolve this problem. By adapting both video source format and MCS, more efficient resource allocation with acceptable video quality is expected. Nowadays, the uncompressed video streaming is considered even in Wi-Fi network, via the emerging Wi-Fi system, i.e., 802.11ac [?], which can provide very high throughput (up to nearly 7 Gbps). We plan to extend our work to this emerging Wi-Fi system and other 60 GHz systems, too.

Second, in future, through extending the proposed reliable video multicast in Chapter 3, we would like to expand the video multicast service area to larger areas and explore ways of utilizing spatial reuse for video multicast. We will also study combined cross-layer FEC-code rate adaptation and PHY-rate adaptation to improve resource efficiency and video quality further. We believe the proposed video multicast schemes are applicable to any wireless systems. For example, they can be used for more reliable video streaming in smartphones with connection to both cellular and Wi-Fi networks.

Finally, in addition to the proposed reliable multicast in Chapter 4, we would like to extend the proposed reliable multicast protocols to the environments of multiple APs. By adjusting the number of transmitted parity packets of each AP, more efficient recovery of the lost packets is expected. In addition, we expect that the proposed feedback protocols can be available for FEC code rate adaptation. The combined cross-layer FEC-code rate adaptation and PHY-rate adaptation are an good solution for high-quality video streaming while providing the resource efficiency.



# Bibliography

- [1] IEEE P802.11n, Part 11: Wireless LAN Medium Access Control (MAC) and Physical Layer (PHY) Specifications: Enhancements for Higher Throughput, Oct. 2009.
- [2] Intel Wireless Display (WiDi).  
<http://www.intel.com/go/wirelessdisplay/>.
- [3] Apple Airplay.  
<http://www.apple.com/airplay/>.
- [4] Miracast.  
<http://www.wi-fi.org/wi-fi-certified-miracast/>.
- [5] Android Transporter for the Nexus 7 and the Raspberry Pi.  
<http://esrlabs.com/android-transporter-for-the-nexus-7-and-the-raspberry-pi/>.
- [6] Samsung AllShare Cast.  
<http://www.samsung.com/>.
- [7] M.-T. Sun and A. R. Reibman, *Compressed Video Over Networks, Signal Processing and Communications Series*, Marcel Dekker Inc., New York, 2001.

- [8] R. Korte and W. Simpson, "The Case for Uncompressed Video Contribution," White Paper, Level 3 Communications, Oct. 2010.
- [9] S. K. Yong and C.-C. Chong, "An Overview of Multigigabit Wireless through Millimeter Wave Technology: Potentials and Technical Challenges," *EURASIP Journal on Wireless Communications Networking*, vol. 2007, no. 1, Jan. 2007.
- [10] H. Singh, J. Oh, C. Kweon, X. Qin, H.-R. Shao, and C. Ngo, "A 60 GHz Wireless Network for Enabling Uncompressed Video Communication," *IEEE Communications Magazine*, vol. 46, no. 12, pp. 71-78, Dec. 2008.
- [11] H. Singh, H. Niu, X. Qin, H.-R. Shao, C. Y. Kwon, G. Fan, S. S. Kim, and C. Ngo, "Supporting Uncompressed HD Video Streaming without Retransmissions over 60 GHz Wireless Networks," in *Proc. IEEE WCNC 2008*, Las Vegas, Nevada, Apr. 2008.
- [12] Z. Lan, J. Wang, C.-S. Sum, T. Baykas, C. Pyo, F. Kojima, H. Harada, and S. Kato, "Unequal Error Protection for Compressed Video Streaming on 60 GHz WPAN System," in *Proc. IWCMC 2008*, Crete Island, Greece, Aug. 2008.
- [13] IEEE 802.15.3c: Wireless Medium Access Control (MAC) and Physical Layer (PHY) Specifications for High Rate Wireless Personal Area Networks (WPANs): Amendment 2: Millimeter-wave based Alternative Physical Layer Extension, Oct. 2009.
- [14] ECMA International 387, High Rate 60 GHz PHY, MAC and HDMI PAL, *Standard ECMA-387 2nd Edition*, Dec. 2010.
- [15] ECMA International 368, High Rate Ultra Wideband PHY and MAC, *Standard ECMA-368 3rd Edition*, Dec. 2008.

- [16] High-Definition Multimedia Interface (HDMI) Specification, Version 1.4, May 2009.
- [17] IEEE P802.11ad/D9.0, Part 11: Wireless LAN Medium Access Control (MAC) and Physical Layer (PHY) Specifications: Enhancements for Very High Throughput in the 60 GHz Band, Jul 2012.
- [18] Wireless High-Definition (WirelessHD).  
<http://www.wirelesshd.org/>.
- [19] Wireless Gigabit Alliance (WiGig).  
<http://wirelessgigabitalliance.org/>.
- [20] J. Klaue, B. Rathke, and A. Wolisz, "Evalvid – A Framework for Video Transmission and Quality Evaluation," in *Proc. 13th International Conference on Modeling, Techniques and Tools for Computer Performance Evaluation*, Urbana, Illinois, Sep. 2003.
- [21] P. Ferre, A. Doufexi, J. Chung-How, A. Nix, and D. Bull, "Link Adaptation for Video Transmission over COFDM based WLANs," in *Proc. IEEE 10th Symposium on Communications and Vehicular Technology in the Benelux*, Eindhoven, Holland, Nov. 2003.
- [22] H. Xu, V. Kukshya, and T. S. Rappaport, "Spatial and Temporal Characteristics of 60-GHz Indoor Channels," *IEEE Journal on Selected Areas in Communications*, vol. 20, no. 3, pp. 620-630, Apr. 2002.
- [23] D. Qiao, S. Choi, and K. G. Shin, "Goodput Analysis and Link Adaptation for IEEE 802.11a Wireless LANs," *IEEE Trans. on Mobile Computing*, vol. 1, no. 4, pp. 278-292, Oct.-Dec. 2002.

- [24] J. del Prado and S. Choi, "Link Adaptation Strategy for IEEE 802.11 WLAN via Received Signal Strength Measurement," in *Proc. IEEE ICC 2003*, Anchorage, Alaska, May 2003.
- [25] P. Ferre, J. Chung-How, D. Bull, and A. Nix, "Distortion-Based Link Adaptation for Wireless Video Transmission," *EURASIP Journal on Advances in Signal Processing*, vol. 2008, 2008.
- [26] C.-W. Hsu and C.-T. Chou, "Interference-Free Coexistence among Heterogenous Devices in the 60 GHz Band," in *Proc. QShine 2009*, Las Palmas de Gran Canaria, Spain, Nov. 2009.
- [27] X. An and R. Hekmat, "Directional MAC Protocol for Millimeter Wave based Wireless Personal Area Networks," in *Proc. VTC Spring 2008*, May 2008.
- [28] *IEEE 802.11-2012, Part 11: Wireless LAN medium access control (MAC) and physical layer (PHY) specifications*, IEEE std., Mar. 2012.
- [29] *IEEE 802.11ac/D5.0, Part 11: Wireless LAN medium access control (MAC) and physical layer (PHY) specifications: Enhancements for very high throughput for operation in bands below 6 GHz*, IEEE std., Jan. 2013.
- [30] M. Choi, M. Samokhina, K. Moklyuk, S. Choi, J. Heo, and S.-J. Oh, "VPAL: Video packet adaptation layer for reliable video multicast over IEEE 802.11n WLAN," *Computer Communications*, vol. 33, no. 18, pp. 2271–2281, 2010.
- [31] Y. Shin, M. Choi, J. Koo, and S. Choi, "Video multicast over WLANs: power saving and reliability perspectives," *IEEE Network*, vol. 27, no. 2, 2013.

- [32] A. Basalamah and T. Sato, “Adaptive FEC reliable multicast MAC protocol for WLAN,” in *Proceedings of IEEE Vehicular Technology Conference (VTC) Fall*, 2007, pp. 244–248.
- [33] Meru networks. <http://www.merunetworks.com/>.
- [34] A. Shokrollahi, “Raptor codes,” *IEEE Transactions on Information Theory*, vol. 52, no. 6, pp. 2551–2567, 2006.
- [35] I. S. Reed and G. Solomon, “Polynomial codes over certain finite fields,” *Journal of the Society for Industrial & Applied Mathematics*, vol. 8, no. 2, pp. 300–304, 1960.
- [36] The network simulator – ns-3. <http://www.nsnam.org/>.
- [37] S. Jakubczak and D. Katabi, “A cross-layer design for scalable mobile video,” in *Proceedings of ACM MobiCom*, 2011, pp. 289–300.
- [38] J. Klaue, B. Rathke, and A. Wolisz, “Evalvid—A framework for video transmission and quality evaluation,” *Computer Performance Evaluation: Modelling Techniques and Tools*, pp. 255–272, 2003.
- [39] M. van der Schaar, S. Krishnamachari, S. Choi, and X. Xu, “Adaptive cross-layer protection strategies for robust scalable video transmission over 802.11 WLANs,” *IEEE Journal on Selected Areas in Communications*, vol. 21, no. 10, pp. 1752–1763, 2003.
- [40] M. A. Santos, J. Villalon, and L. Orozco-Barbosa, “A novel QoE-aware multicast mechanism for video communications over IEEE 802.11 WLANs,” *IEEE Journal on Selected Areas in Communications*, vol. 30, no. 7, pp. 1205–1214, 2012.

- [41] R. Chandra, S. Karanth, T. Moscibroda, V. Navda, J. Padhye, R. Ramjee, and L. Ravindranath, "Dircast: A practical and efficient wi-fi multicast system," in *Proceedings of IEEE International Conference on Network Protocols (ICNP)*, 2009, pp. 161–170.
- [42] W.-S. Lim, D.-W. Kim, and Y.-J. Suh, "Design of efficient multicast protocol for IEEE 802.11n WLANs and cross-layer optimization for scalable video streaming," *IEEE Transactions on Mobile Computing*, vol. 11, no. 5, pp. 780–792, 2012.
- [43] Y. Zhu, Q. Zhang, Z. Niu, and J. Zhu, "Leveraging multi-AP diversity for transmission resilience in wireless networks: Architecture and performance analysis," *IEEE Transactions on Wireless Communications*, vol. 8, no. 10, pp. 5030–5040, 2009.
- [44] J. M. Vella and S. Zammit, "Infrastructure dependent wireless multicast—The effect of spatial diversity and error correction," in *Proceedings of ICUMT*, 2012, pp. 981–988.
- [45] VideoLan. <http://www.videolan.org/>.
- [46] IEEE 802.11v, Amendment to Part 11: Wireless Medium Access Control (MAC) and Physical layer (PHY) specifications: IEEE 802.11 Wireless Network Management, Feb. 2011.
- [47] IEEE 802.11aa, Amendment to Part 11: Wireless Medium Access Control (MAC) and Physical layer (PHY) specifications: MAC Enhancements for Robust Audio Video Streaming, May 2012.
- [48] A. Cidon, et al., "Flashback: decoupled lightweight wireless control," in *Proc. ACM SIGCOMM*, 2012.

- [49] Gupta, S. K. S., V. Shankar, and S. Lalwani, "Reliable multicast MAC protocol for wireless LANs," in *Proc. ICC 2003*, 2003.
- [50] Anas Basalamah and Takuro Sato, "Adaptive FEC reliable multicast MAC protocol for WLAN," in *Proc. VTC-2007 Fall*, 2007.
- [51] Choi, S., Choi, N., Seok, Y., Kwon, T., and Choi, Y., "Leader-based rate adaptive multicasting for wireless LANs," in *Proc. Globecom 2007*, Nov. 2007.
- [52] Kim, Byung-Seo, Sung Won Kim, and Randy L. Ekl., "OFDMA-based reliable multicasting MAC protocol for WLANs," in *IEEE Transactions on Vehicular Technology*, pp. 3136-3145, 2008.
- [53] V. Srinivas and Lu Ruan., "An efficient reliable multicast protocol for 802.11-based wireless LANs," in *Proc. WoWMoM 2009*, 2009.
- [54] N. Choi, Y. Seok, T. Kwon, and Y. Choi, "Leader-Based Multicast Service in IEEE 802.11v Networks," in *Proc. CCNC 2010*, Jan. 2010.
- [55] Qualcomm Atheros. <http://www.qca.qualcomm.com/>.
- [56] Compat-drivers. <http://wireless.kernel.org/>.

## 초 록

오늘날 무선 네트워크 통신 기술의 발달로 인해 고품질의 비디오 스트리밍 서비스에 대한 요구가 급증하고 있다. 새로운 60 GHz 광대역 고속 무선 통신 기술은 기존의 무선 통신 기술에서는 불가능했던, 고품질의 무압축 비디오 스트리밍을 가능하게 한다. 제한된 무선 자원 환경에서 고품질의 비디오 서비스를 지원하기 위해 주어진 채널 환경에서 적절한 변조 및 코딩 기술을 선택하는 효율적인 링크 적응 기법이 필요하다. 비디오 스트리밍의 품질을 수치로 평가하는 ePSNR을 정의하고, 불평등 오류 보호 기법(UEP)을 추가로 도입하여 보다 세밀한 링크 적응 기법을 가능케 한다. 정의한 ePSNR을 기반으로 (1) 주어진 무선 자원에서 비디오 품질을 최대화, 혹은 (2) 목표 비디오 품질을 만족하는 무선 자원 사용을 최소화, 하는 두가지 링크 적응 기법들을 제안한다. 다양한 시뮬레이션 결과를 통해, 정의한 ePSNR이 비디오 품질을 잘 표현하고 있음을 확인하였다. 또한, 제안한 링크 적응 기법들이 비디오 스트리밍 서비스를 위한 적절한 품질을 제공하면서, 동시에 자원 효율성을 향상시킴을 검증하였다.

한편, 순방향 오류 정정 기법(FEC)은 무선랜 환경에서 고품질의 신뢰성있는 비디오 멀티캐스트를 지원한다. 무선랜 환경에서 복수개의 액세스포인트(AP)간의 조정을 통한 신뢰성있는 비디오 멀티캐스트 기법을 제시한다. 복수개의 AP간의 조정을 통해 각각의 AP들이 (1) 완전히 서로 다른, 혹은 (2) 부분적으로 서로 다른, 인코딩된 패킷들을 전송하게 하여, 공간 및 시간적 다양성을 멀티



캐스트 유저에게 제공할 수 있다. 추가로, 제한된 무선 자원을 보다 효율적으로 사용하기 위해, 순방향 오류 정정 기법의 코딩 비율 적응 기법을 위한 자원 할당 알고리즘을 제안한다. 또한, FEC 디코딩 후의 비디오 패킷의 전송율을 예측할 수 있는 방법을 제안한다. 다양한 시뮬레이션과 실험을 통해 제안한 기법들의 우수성을 확인하였다.

멀티캐스트 전송은 기본적으로 무선 채널 오류로 인해 전송 실패가 발생할 가능성을 내포한다. 그러나 기존의 무선랜 표준에서는 멀티캐스트 환경에서 자동 반복 요청 기법(ARQ)을 통한 손실 조정 방법을 제공하지 않았다. 멀티캐스트 전송의 비신뢰성 문제를 해결하기 위해, 자동 반복 요청 기법(ARQ)과 순방향 오류 정정 기법(FEC)를 함께 고려한 신뢰성 있는 멀티캐스트 전송 기법을 제안한다. 신뢰성 있는 멀티캐스트 전송을 위한 피드백 교환의 오버헤드를 줄이기 위한 복수개의 효율적인 피드백 기법을 제시한다. 제안한 피드백 기법은 액세스 포인트(AP)가 멀티캐스트 유저들의 손실된 패킷들의 복원을 위해 필요한 패리티(parity) 패킷의 개수를 쉽게 알 수 있도록 한다. 피드백 간의 충돌을 감안한 의도적인 동시 전송을 통해 피드백 오버헤드를 감소시킬 수 있다. 추가로, 효율적인 피드백 프로토콜을 활용하여, 변조 및 코딩 기법(MCS)의 폐쇄적 피드백 기반의 물리 전송 속도 적응 기법을 제안한다. 성능 검증을 통해 제안한 기법들이 효율적으로 피드백 오버헤드를 감소시키며, 동시에 신뢰성 있는 멀티캐스트 전송을 보장함을 검증하였다.

**주요어:** 비디오 스트리밍, 링크 적응기법, 무압축 비디오, expected PSNR, 60 GHz 네트워크, 불평등 오류 보호기법(UEP), 비디오 멀티캐스트, 순방향 오류 정정 (FEC), Raptor FEC, Wi-Fi, 협력 다중 액세스포인트, 자동 반복 요청(ARQ), 효율적인 피드백

**학번:** 2007-30842